APPLICATION OF RECENT OPTIMIZATION ALGORITHMS ON SLOPE STABILITY PROBLEMS

A THESIS SUBMITTED TO
THE GRADUATE SCHOOL OF NATURAL AND APPLIED SCIENCES
OF
MIDDLE EAST TECHNICAL UNIVERSITY

BY

SADRA AZIZI

IN PARTIAL FULFILLMENT OF THE REQUIREMENTS
FOR
THE DEGREE OF MASTER OF SCIENCE
IN
CIVIL ENGINEERING

JULY 2018

Approval of the thesis:

APPLICATION OF RECENT OPTIMIZATION ALGORITHMS ON SLOPE STABILITY PROBLEMS

submitted by **SADRA AZIZI** in partial fulfillment of the requirements for the degree of **Master of Science in Civil Engineering Department, Middle East Technical University** by,

Prof. Dr. Halil Kalıpçılar
Dean, Graduate School of **Natural and Applied Sciences** ———————

Prof. Dr. İsmail Özgür Yaman
Head of Department, **Civil Engineering** ———————

Asst. Prof. Dr. Onur Pekcan
Supervisor, **Civil Engineering Dept., METU** ———————

Examining Committee Members:

Prof. Dr. Bahadır Sadık Bakır
Civil Engineering Dept., METU ———————

Asst. Prof. Dr. Onur Pekcan
Civil Engineering Dept., METU ———————

Prof. Dr. Oğuzhan Hasançebi
Civil Engineering Dept., METU ———————

Assoc. Prof. Dr. Zeynep Gülerce
Civil Engineering Dept., METU ———————

Asst. Prof. Dr. Salih Tileylioğlu
Civil Engineering Dept., Çankaya University ———————

Date: 18.07.2018

I hereby declare that all information in this document has been obtained and presented in accordance with academic rules and ethical conduct. I also declare that, as required by these rules and conduct, I have fully cited and referenced all material and results that are not original to this work.

Name, Last Name: Sadra Azizi

Signature:

ABSTRACT

APPLICATION OF RECENT OPTIMIZATION ALGORITHMS ON SLOPE STABILITY PROBLEMS

Azizi, Sadra
M.Sc., Department of Civil Engineering
Supervisor: Assist. Prof. Dr. Onur Pekcan

July 2018, 107 pages

Stability analysis of earth slopes in general involves determining the minimum factor of safety (FS) associated with the most critical failure surface. This objective is too challenging to accomplish considering the broad diversity of slope problems in geometry, geotechnical parameters of the soil, location of the groundwater table, and condition of the external loadings. Robust optimization techniques, however, have recently performed well in determining safety factors of various man-made and natural slopes of different complexities simultaneous with fast and confidently locating the corresponding slip surfaces.

In this study, three recently developed optimization methods, Hybrid Artificial Bee Colony algorithm with Differential Evolution (HABCDE), Grasshopper Optimization Algorithm (GOA) and improved harmony search algorithm (LHS), are combined with a non-circular surface generation scheme to identify location of the slip surface. To evaluate the safety factor along each slip surface, a concise algorithm of the Morgenstern-Price method is employed in the analyses. Results obtained through application of the proposed methods into three case studies including different layers and geometries indicates that HABCDE outperforms the two other methods both on fast convergence and accuracy in the minimization

procedure which makes it comparable to the best methods implemented in slope stability analysis to date.

Keywords: Geotechnical Engineering, Slope Stability, Critical Slip Surface, Metaheuristic Methods, Factor of Safety

ÖZ

ŞEV STABILITE ANALIZLERININ OPTIMIZASYON TEKNIKLERI KULLANILARAK DEĞERLENDIRILMESI

Azizi, Sadra
Yüksek Lisans, İnşaat Mühendisliği Bölümü
Tez Yöneticisi: Dr. Öğr. Üyesi Onur Pekcan

Temmuz 2018, 107 sayfa

Şevlerin duraylılık analizi, en kritik kayma yüzeyi ile en düşük güvenlik faktörünün (GF) belirlenmesini içerir. Bu amaçla yapılan çalışmalar, geometrik eğim çeşitliliği, toprağın geoteknik parametreleri, yeraltı suyu seviyesinin yeri ve harici yüklerin durumu göz önünde bulundurulduğunda oldukça zor bir problem haline gelmektedir. Bununla birlikte son zamanlarda, güçlü optimizasyon teknikleri farklı kayma yüzeylerinin çeşitli insan yapımı ve doğal eğimlerin güvenlik faktörlerinin belirlenmesinde, hızlı ve güvenli bir şekilde belirlenmesinde iyi bir performans sergilemiştir.

Bu çalışmada, şev kayma yüzeyi ve güvenlik faktörünü belirlemek için Ayırıcı Evrimli Hibrit Yapay Arı Kolonisi algoritması (AEHYAKA), Çekirge Optimizasyon Algoritması (ÇOA) ve Geliştirilmiş Uyum Arama Algoritmasını (GUAA) içeren üç yeni optimizasyon yöntemi dairesel olmayan bir yüzey oluşturma algoritması ile birleştirilmiştir. Her bir kayma yüzeyi boyunca güvenlik faktörünü değerlendirmek için yapılan analizlerde Morgenstern-Price metodu algoritması kullanılmıştır. Önerilen metotların, farklı katmanlar ve geometri içeren 3 örnek çalışma ile uygulanması sonucu elde edilen sonuçlar, AEHYAKA 'nin, hem hızlı yakınsama hem de doğruluk açısından diğer iki yöntemi geride bıraktığını ve

bu durumun şev stabilitesi analizinde bugüne kadar uygulanan en iyi yöntemlerle karşılaştırılabilir olduğunu göstermektedir.

Anahtar Kelimeler: Geoteknik mühendisliği, Şev Stabilitesi, Kritik Kayma Yüzeyi, Sezgi Ötesi Yöntemler, Güvenlik Faktörü

To My Family

ACKNOWLEDGMENTS

This thesis was written with the help and assistance of various people and I would like to take this opportunity to acknowledge the tremendous help they have given me while I was completing my thesis.

First and foremost, I would like to express my sincere appreciation and gratitude to my advisor, Dr. Onur Pekcan, whose enlightening remarks, encouraging feedback and friendly attitude all year long, made this dissertation possible. Dr. Pekcan has been both my dissertation adviser and my mentor, providing me with endless encouragement and helping me go through all the difficulties I came across as a student and a researcher. He was very generous in sharing his experiences in academic life and beyond which made the biggest positive difference in my life.

I would also like to thank the examining committee members Dr. Bahadır Sadık Bakır, Dr. Oğuzhan Hasançebi, Dr. Zeynep Gülerce and Dr. Salih Tileylioğlu for spending their valuable time on reviewing my thesis and providing feedback.

I would like to express my sincere and special gratitude to my family for their constant care and understanding, encouragement and endless love throughout my life. I have always felt their supports even if I had been away from them. Without their unconditional trust, timely encouragement, and endless patience throughout my life, I could not be who I am now.

I owe special thanks to my wonderful cousin Hamed Ahmadzadeh for his invaluable assistance and encouragements, his thoughts, phone calls and visits throughout my study. He has always been like a brother to me and one of the greatest supporters in my life. I also want to express my great appreciation to Taher Ghalandary, Navid Alamati, Majid Jarrah and Mohammad Reza Kolahi for their valuable friendship, endless support and being there whenever I needed a friend.

I would also like to acknowledge my colleagues, Reza Salatin, Farshad Kamran, Ali Farshkaran, Armin Taghipour, Rasoul Tariverdilou and my fellow AI2LAB members for their valuable friendship and support during my thesis journey

TABLE OF CONTENTS

ABSTRACT v
ÖZ vii
ACKNOWLEDGMENTS x
TABLE OF CONTENTS xiii
LIST OF TABLES xv
LIST OF FIGURES xvi
LIST OF ABBREVIATIONS xix
CHAPTERS
1. INTRODUCTION 1
1.1. Background 1
1.2. Research Objective 5
1.3. Scope 6
1.4. Thesis Outline 7
2. LITERATURE WORK 9
2.1 Slope Stability Analysis Methods 9
2.1.1 Limit Equilibrium Methods 10
2.1.2 Numerical Methods 16
2.2 Current Challenges 18
2.3 Determination of the Critical Failure Surface 19
2.3.1 Differential evolution 21
2.3.2 Harmony Search 24
2.3.3 Artificial Bee Colony 26
3. MAIN WORK 29
3.1 Trial Slip Surface Generation Method 29
3.2 Calculation of Factor of Safety 31
3.3 Optimization Methods 37

3.3.1 Improved harmony search algorithm 38
3.3.2 Grasshopper optimization algorithm 44
3.3.3 Hybrid Artificial Bee Colony with Differential Evolution 47
4. CASE STUDIES 53
4.1 Case study 1 54
4.2 Case study 2 59
4.3 Case study 3 65
4.4 Case Study 4 74
5. SUMMARY AND CONCLUSION 89
5.1 Summary 89
5.2 Findings of the Study 90
5.3 Future Works 91
REFERENCES 93
APPENDIX
A: CONVERGENCE RATE COMPARISON 99

LIST OF TABLES

TABLES

Table 1 - Summary of Limit equilibrium methods 16
Table 2 - Result Comparison – Example 1 55
Table 3 - Results of this study—Example 1..... 56
Table 4 - Soil Parameters – Example 2..... 60
Table 5 - Result comparison—Example 2 61
Table 6 - Results of this study—Example 2..... 62
Table 7 - Soil parameters—Example 3 66
Table 8 - Result comparison—Example 3 67
Table 9 - Results of this study—Example 3, Case (1) 68
Table 10 - Results of this study—Example 3, Case (2) 72
Table 11 - Soil Parameters – Example 4..... 75
Table 12 - Result Comparison – Example 4 76
Table 13 - Results of this study—Example 4..... 77

LIST OF FIGURES

FIGURES

Figure 1 - Taiwan freeway landslide 2
Figure 2 - Banjarnegara, Indonesia landslide 3
Figure 3 - Forces applied on the sample slice 12
Figure 4 – Forces applied on the sample slice 13
Figure 5 - Forces applied on the sample slice 13
Figure 6 - Forces applied on the sample slice 14
Figure 7 - Forces applied on the sample slice 15
Figure 8- Geometric Description of the Surface Generation Method 31
Figure 9 - (a) Slope Geometry and General Failure Surface, (b) Inter-Slice Forces in Slice Number (i) 33
Figure 10 - Flowchart of FS Algorithm 36
Figure 11 - Two main branches about the improvisation process 42
Figure 12 - LHS Algorithm 43
Figure 13 - GOA Algorithm 47
Figure 14 - HABCDE Algorithm 51
Figure 15 - Flowchart for HABCDE Algorithm 52
Figure 16 - Slope geometry—Example 1 54
Figure 17 - Comparison of the convergence rates -- Example 1 (a) all the methods (b) proposed methods 58
Figure 18 - Critical Slip Surfaces -- Example 1 59
Figure 19 - Geometry of Slope – Example 2 60
Figure 20 - Comparison of the convergence rates -- Example 2 (a) all the methods (b) proposed methods 64
Figure 21 - Critical Slip Surfaces -- Example 2 65
Figure 22 - Geometry of Slope—Example 3 66

Figure 23 - Comparison of the convergence rates -- Example 3, Case (1) (a) all the methods (b) proposed methods 70
Figure 24 - Critical Slip Surfaces —Example 3, Case (1) 71
Figure 25 - Comparison of the convergence rates -- Example 3, Case (2) (a) all the methods (b) proposed methods 73
Figure 26 - Critical Slip Surfaces —Example 3, Case (2) 74
Figure 27 - Geometry of the slope – Example 4 75
Figure 28 Comparison of the convergence rates -- Example 4, Case (1) (a) all the methods (b) proposed methods 81
Figure 29 - Comparison of the convergence rates -- Example 4, Case (2) (a) all the methods (b) proposed methods 82
Figure 30 - Comparison of the convergence rates -- Example 4, Case (3) (a) all the methods (b) proposed methods 84
Figure 31 - Comparison of the convergence rates -- Example 4, Case (4) (a) all the methods (b) proposed methods 85
Figure 32 – Critical Slip Surfaces – Example 4 87
Figure 33- Convergence Rate Comparison – Example 1 100
Figure 34 - Convergence Rate Comparison – Example 2 101
Figure 35 - Convergence Rate Comparison – Example 3, Case (1) 102
Figure 36 - Convergence Rate Comparison – Example 3, Case (2) 103
Figure 37 - Convergence Rate Comparison – Example 4, Case (1) 104
Figure 38 - Convergence Rate Comparison – Example 4, Case (2) 105
Figure 39 - Convergence Rate Comparison – Example 4, Case (3) 106
Figure 40 - Convergence Rate Comparison – Example 4, Case (4) 107

LIST OF ABBREVIATIONS

ABBREVIATION	
ABC	Artificial Bee Colony
ACO	Ant Colony Optimization
DE	Differential Evolution
DEM	Distinct Element Method
DFP	Davidon-Fletcher-Powell
FDM	Finite Difference Method
FEM	Finite Element Method
FS	Factor of Safety
GA	Genetic Algorithms
GOA	Grasshopper Optimization Algorithm
GSA	Gravitational Search Algorithm
HABCDE	Hybrid Artificial Bee Colony Algorithm with Differential Evolution
HM	Harmony Memory
HMCR	Harmony Memory Consideration Rate
HMS	Harmony Memory Size
HS	Harmony Search
ICA	Imperialistic Competitive Algorithm
LEM	Limit Equilibrium Method

LHS	Improved Harmony Search Algorithm
M-P	Morgenstern-Price Method
MHM	Modified Harmony Search Algorithm
PAR	Pitch Adjusting Rate
PPACO	Premium-Penalty Ant Colony Optimization
PSO	Particle Swarm Optimization
SA	Simulated Annealing
SHM	Simple Harmony Search Algorithm
SRM	Strength Reduction Method

CHAPTER 1

INTRODUCTION

1.1. Background

Recent growth in human population has led to an increasing demand on major infrastructure projects such as constructions of roads and railways or buildings, which generally involve ground disturbance in the area of construction. In many cases, large-scale earthwork activities require forming engineered cut and fill slopes prior to any further developments. Therefore, the stability of slopes needs to be assessed in advance to construction to gain insights about the site conditions as well as to decrease the risk of having potential property damages and more importantly human losses.

Slope failures are commonly investigated type of geo-hazards, triggered by different major causes including intense rainfalls, inadequate drainage, sudden ground vibrations, loss of vegetation, etc., which eventually result in either an increase in the stress applied, or cause a reduction in the shear strength of the soil in situ. The incidence of slope failures may potentially lead to considerable environmental, financial and human losses, most notably in populated urban areas. Such ground instabilities may also hinder further progress in the construction activities and challenge the engineers in charge of the construction.

Two examples of catastrophic landslides, which were responsible for major economic loss as well as serious injuries and fatalities, are illustrated in Figures 1 and 2. Figure 1 corresponds to a slope failure, which occurred on April 25, 2010, in Taiwan (Chen et al., 2015). As a result of this ground failure, the National Freeway No.3 was blocked for one month due to a massive debris flow that had covered the road section at the downstream. A comprehensive investigation of the

area demonstrated that weathering had occurred at the upper layers which had increased the water infiltration into the soil and consequently had led to water accumulation between the layers. As a result, the decline in interface friction resulted in slope instability in this area (Chen et al., 2015).

Figure 1 - Taiwan freeway landslide (Taiwan National Freeway Bureau)

Figure 2 represents another devastating landslide occurred on December 13, 2014, in Indonesia. As a result of this disaster, a large number of houses in the area were heavily damaged and the total number of fatalities and injuries was considerable. Comprehensive site investigations revealed that heavy rainfall in a short period of time (11 days) in addition to the steep configuration of the slope were the major causes and the triggering factors of the ground failure (Nur, 2014).

Considering the possible outcomes, in regions of high failure risks, large amounts of money are yearly invested in the proper maintenance of major geotechnical structures such as embankments or dams and in the design of man-made facilities adjacent to slopes. Therefore, studies related to better understanding of the stability of slopes play a crucial role especially from economy and sustainability point of view.

Figure 2 - Banjarnegara, Indonesia landslide (Nur, 2014)

To date, considerable efforts have been made to evaluate the stability of earth slopes of different configurations under various loading conditions prior to major constructions adjacent to slopes, and to take necessary actions to improve the stability of slopes in areas of high failure risk. For this purpose, different numerical and analytical methods including, limit analysis method, limit equilibrium method (LEM), finite difference method or finite element method, have been so far developed by the researchers in order to properly assess the stability of slopes. However, studies indicate that LEM is as yet the most popular approach among the researchers for stability analyses. Over the past few years, a set of LEM based techniques that vary in their underlying assumptions has been widely utilized in different stability assessment problems.

Stability of slopes in LEM is precisely quantified using a term so-called “Factor of Safety” (“FS”), which indicates the ratio between the existing shear strength and the shear stress acting on the sliding body. However, an accurate safety assessment by using LEMs requires a number of trial slip surfaces to be initially generated

followed by calculation of the value of factor of safety corresponding to each slip surface and finally indicating the surface with the lowest FS value as the surface of highest failure probability for the entire slope. However, indicating the most critical slip surface would remain challenging for engineers, as far as the accuracy of the approximations along with the time required for the completion of the computations are concerned.

This objective can be achieved following a trial and error approach. Although useful, this method lacks precision particularly in the case of nonhomogeneous soil slopes. The incompetency in this method is however associated with its dependency on the adequacy of the preliminarily generated trial failure surfaces within the slope profile. Considering the fact that the critical slip surface identified by using the approach is not necessarily the most vulnerable surface, inappropriate values are therefore likely to be obtained in the analyses.

Alternatively, available evidence from published case studies, have demonstrated the capability of optimization techniques in the reliable assessment of the stability of slopes. To date, different classical optimization methods have been implemented in the analyses. These techniques, considering their inherent limitations, are also proved to be dependent on the proper selection of trial solutions and thus might also overestimate the value of safety factor and consequently fail to acquire a precise measure in the analyses. However, recent advances in computing science have paved the way for the development of enhanced computing schemes such as metaheuristics, which have proved successful in solving various real problems. Successful application of such optimization techniques has recently, gained significant attention by geotechnical researchers worldwide (Yung Ming Cheng et al., 2012). To date, a broad range of novel optimization methods has been used in the literature to explore the most vulnerable failure surface as well as to determine the factor of safety against instabilities in the case of study. Review of the results obtained for these methods testify their competence in better evaluating the stability of earth slopes given the improvements made in the obtained results. Particularly when applied to a multi-layered slope with a complex geometry, the optimization

technique is required to accurately locate the geological slip surface, over a short period with relatively less computational efforts. Consequently, this objective necessitates the use of alternative optimization techniques in order to obtain superior results, especially for complex case studies.

In this study, an effective analysis framework is developed implementing three recently developed metaheuristic methods, combined with a simplified Morgenstern-Price approach so as to determine the minimum factor of safety pertaining to the most critical slip surface within the soil profile. Subsequently, the proposed framework is utilized in stability analysis of four slope problems with various complexities and its performance is benchmarked against its conventional competitors.

1.2. Research Objective

This study primarily intends to develop a functional analysis framework to assess the factor of safety of earth slopes on the basis of limit equilibrium methods. However, the formulation derived for the factor of safety in an advanced LEM, such as Morgenstern-Price method, suffers from specific drawbacks, i.e. discontinuity and the existence of several local minima (Chen et al. 1988, Cheng et al. 2007) that make slope stability analysis a challenging problem to solve. To successfully deal with this problem, limit equilibrium methods coupled with various metaheuristic optimization techniques are employed in the analyses. In this regard, the factor of safety equation is generally considered as the objective function of the optimization problem and a thorough minimization process is performed to explore the optimum solution in the search space. An overall evaluation regarding the safety of the case of study can be reached after the analyses are completed.

Another major objective of this study is the fast and accurate localization of the critical slip surface that yields the minimum factor of safety of the entire slope. Having determined the zone with high failure risk, necessary actions need to be taken to reinforce the vulnerable surface with its surroundings.

1.3. Scope

Studies thus far have firmly indicated the significance of the meticulous geometrical modeling of the soil in situ, on the validity of the slope stability assessments. A number of major factors found to be influencing the analyses include: the geometry of the slope, consideration of the existence of water table along with the external loadings in the analyses, and above all the validity of the values assumed for the soil parameters. Accordingly, these aspects are required to be considered in the calculations for more realistic results to be acquired.

Investigations have established the direct role undesirable conditions within the soil profile, e.g., the presence of a weak layer, play in activating the failure mechanism of the slopes. In this study, various case of studies from simple homogeneous to multi-layered heterogeneous earth slopes with varied geometries and stratifications are considered, in order to better investigate the impact of variation in ground conditions on the overall stability of slopes. Furthermore, a deterministic approach is adopted for the analyses considering constant values for the key parameters of the soil medium, namely coefficient of cohesion, unit weight, friction angle, and pore water pressure ratio within each of the layers.

Available evidence of ground failures in areas with high precipitation rate has indicated the adverse influence of the pore water pressure on the soil strength. In this study, the destabilizing effects of external loadings and ground water table as well as the combined effects of these parameters on the stability condition of two case studies, are efficiently investigated.

Other slope stability evaluation techniques including finite element method (FEM) are kept out of the scope of this study. Although powerful, FEM is generally not adopted for the analysis of typical geotechnical problems owing to the difficulties involved in an accurate modeling of the problem along with a large number of parameters required to be initialized in the analysis.

1.4. Thesis Outline

This study consists of five themed chapters, starting with this introductory chapter. Subsequent chapters are organized as follows: The second chapter is devoted to literature work associated with slope stability analysis methods, current challenges, and optimization techniques. In the third chapter, the main work of the study, including the method used for generating trial slip surfaces and the adopted optimization algorithms are explained in details. In the fourth chapter, the application of the proposed method on benchmark case studies have been exemplified and the last chapter includes the conclusions of this study and identifies areas for the future work.

CHAPTER 2

LITERATURE WORK

This chapter provides an overview of the practical methods introduced thus far for the stability analysis of earth slopes in a two-dimensional space. In this regard, formulation of a number of widely-known techniques that are developed on the basis of limit equilibrium methods (LEM) or finite element methods (FEM) is detailed. Furthermore, recent challenges and essential considerations in an exhaustive slope stability assessment are briefly addressed in this chapter. Finally, a summary of the techniques used in the literature for tackling the difficulties in identifying the most vulnerable failure surface within the slope is provided.

2.1 Slope Stability Analysis Methods

To date, considerable efforts have been made to evaluate the stability of earth slopes of different configuration under various loading conditions prior to major constructions adjacent to slopes, and to take necessary actions to improve the stability of slopes in areas of high failure risk. For this purpose, different numerical and analytical methods including, limit analysis method, limit equilibrium method (LEM), finite difference method or finite element method, have been so far developed by the researchers in order to properly assess the stability of slopes. However, studies indicate that LEM is as yet the most popular approach among the researchers for stability analyses. Over the past few years, a set of LEM based techniques that vary in their underlying assumptions. In the following subsection, a number of most commonly used techniques pertaining to limit equilibrium methods are described in detail.

2.1.1 Limit Equilibrium Methods (LEM)

Despite the potential drawbacks in each of the methods, LEM is as yet the most adopted approach since it can be confidently applied to slopes of diverse geometric shapes comprising different soil characteristics and water content, subjected to external loading conditions of different kinds. Besides, overall attitude toward LEM has become favorable due to its relatively straightforward implementation. Limit equilibrium methods are, for the most part, formed on the basis of the methods of slices which enjoys the following features as in the study by (D. Y. Zhu et al., 2003):

1. The sliding mass of the soil is ordinarily divided into multiple vertical, inclined or horizontal slices; however, vertical slices approach is the most commonly employed technique in the research works to date.
2. The sliding mass above the failure surface is brought into the limiting state, by evenly mobilizing the strength along the entire surface.
3. Simplifying assumptions concerning inter-slice forces need to be made in order to solve this statically indeterminate problem.
4. The safety factor is calculated according to the moment and/or force equilibrium equations.

In order to properly quantify the chance of failure in slopes, an index which is referred to as factor of safety (FS) is introduced. Factor of safety, in general, is identified by evaluating the ratio between sum of the forces which resist the slippage of the soil mass over the failure surface ($F_{resisting}$)−friction between soil particles for instance−and the forces driving the soil mass down the slope ($F_{driving}$)−such as gravitational forces and external forces, as presented in Equation (1).

$$F = \frac{sum\,of\ the\,resisting\ \ forces\,(F_{resisting})}{sum\,of\ the\,driving\ \ forces\,(F_{driving})} \qquad (1)$$

Safety of the earth slopes is determined by comparing the calculated FS values with a target value which equals unity when the forces acting on the soil mass are balanced and the slope is in the state of equilibrium. However, a FS value less than unity indicates a state in which the failure is likely to occur (driving forces > resisting forces), and in contrast, a value greater than unity for factor of safety, corresponds to a slope in which the resisting forces outperform the driving forces and thus, the slope remains stable under the given loading conditions (Duncan et al., 2014).

As mentioned previously, in limit equilibrium analysis, sliding mass of the soil is ordinarily divided into multiple vertical slices, so as to specify the forces applied on each of the slices, i.e., internal and external forces, which are then utilized in evaluating the safety factor of the case of study. Furthermore, in limit equilibrium method the value of safety factor is considered to be constant along the failure surface according to the study by (Y. M Cheng & Lau, 2008); thus, factor of safety for a single slice represents the safety factor of the whole slope.

Further to the features outlined earlier, limit equilibrium method is regarded as a statically indeterminate problem and thus far several methods that vary depending on the simplifying assumptions that are made in modeling the inter-slice forces are introduced. Among the methods developed for the slope stability analysis, a number of relatively rigorous ones that has found widespread application in the literature are briefly outlined below.

2.1.1.1 Ordinary method of slices

The ordinary method of slices which is also known as, Swedish method of slices, is the primary method of slices introduced for slope stability analysis. The inter-slice normal and forces in this method are neglected and a surface of circular geometry is considered for the expected failure surface. Additionally, moment equilibrium condition is merely met for the body of soil above the slip surface, and the factor of safety is obtained summing all moments about the center point of the circle corresponding to the slip surface. This method, while simple, is not precise

owing to the conservative values obtained for the factor of safety. Figure 3 represents a schematic view of the forces considered in the ordinary method of slices:

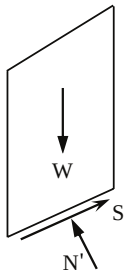

Figure 3 - Forces applied on the sample slice

2.1.1.2 Simplified Bishop Method

The simplified Bishop method is commonly used for slope stability analysis in the literature. Inter-slice normal forces are considered in this method, whereas the inter-slice shear forces are ignored (Abramson et al., 2002). Furthermore, for any individual slice of the body of the soil, the vertical force equilibrium condition is met. In this method also, a circular shape is considered for the expected failure surface and, moment equilibrium condition is satisfied for the mass of soil above the slip surface. Besides, in order for the factor of safety to be calculated an iterative procedure needs to be followed since the equation derived for the safety factor- by summing moments about the center point of the slip surface- has the FS on both sides. Although not all static equilibrium conditions are satisfied in this method, the factor of safety values evaluated through following this procedure are relatively accurate and are comparable with those obtained using much thorough LEM techniques as will be discussed in the following. A schematic view of the forces considered in simplified Bishop method is represented in Figure 4:

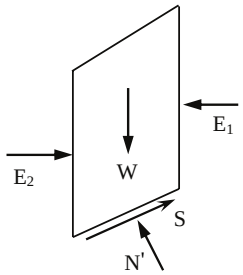

Figure 4 – Forces applied on the sample slice

2.1.1.3 Janbu's Simplified Method

In the Janbu's Simplified method, similar to the Bishop's Simplified method, while the normal inter-slice forces are considered, inter-slice shear forces are neglected. However, in this method, unlike Bishop's simplified method, moment equilibrium condition is not satisfied and instead, the factor of safety equation is derived from the horizontal force equilibrium of an individual slice. In addition, a non-circular geometry is considered for the expected failure surface in this method. In order to include the influence of inter-slice shear forces on the factor of safety, a correction factor is introduced which is dependent on the friction angle, the shape of the slip surface and the cohesion (Janbu, 1975). A schematic view of the forces considered in simplified Bishop method is represented in Figure 5:

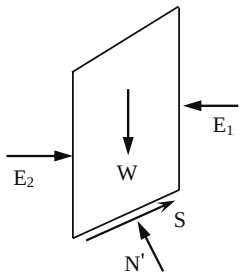

Figure 5 - Forces applied on the sample slice

2.1.1.4 Morgenstern-Price Method

In the Morgenstern-Price method (M-P) both the inter-slice normal and shear forces, as presented in Figure 6, are considered. Besides, a slip surface of non-circular shape is considered and for each individual slice of the entire mass of the soil above the slip surface, two conditions of equilibrium, namely moment as well as the force equilibrium are satisfied. An inter-slice force function which represents the ratio of normal forces over shear inter-slice forces is proposed in the M-P method. This ratio, however, is dependent on a scaling factor λ and, a prescribed function f(x) that may be assumed of any form such as constant, trapezoidal, half-sine or a user-defined function.

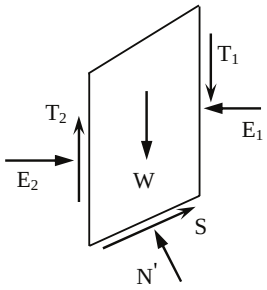

Figure 6 - Forces applied on the sample slice

Due to nonlinearity and complexity of the equilibrium equations, the original M-P method is highly nonlinear and sophisticated. An alternative formulation which is easier to implement is developed by (Fredlund & Krahn, 1977). In this regard, two equations for factor of safety one principally based on the force equilibrium and another based on the moment equilibrium conditions are derived. Following an iterative procedure, the corresponding factor of safety can be evaluated. In this study, a concise and reformulated form of Morgenstern-Price method is adopted for the slope stability analyses which will be outlined in detail in what follows.

2.1.1.5 Spencer's Method

Spencer's method also, as presented in Figure 7, considers both normal and inter-slice shear forces during the analysis. Besides, fulfilling the two necessary conditions for static equilibrium helps this method to rigorously assess the overall stability of slopes. Key assumptions made in Spencer's method are similar to those of M-P method and the difference lies in the type of inter-slice force function, where a constant ratio is considered in Spencer's method.

As in the M-P method, two equations for factor of safety, principally based on the overall force and the overall moment equilibrium, are derived. Following an iterative procedure, the corresponding factor of safety can be evaluated.

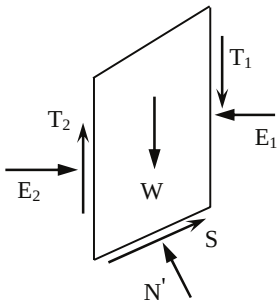

Figure 7 - Forces applied on the sample slice

2.1.1.6 Sarma's Method

This advanced method of slope stability analysis considers both inter-slice shear and normal forces acting on non-vertical slices of the sliding body and, fulfills the force and moment equilibrium conditions necessary to the static equilibrium of the entire mass of soil (Abramson et al., 2002; Sarma, 1973). Besides, in this method, a non-circular geometry is considered for the slip surfaces. These specific features make the Sarma's method an ideal technique for analyzing soils slopes of different geometries.

The procedure followed in the Sarma's method is different from that of other methods in that a value is initially assumed for the factor of safety and, efforts are made to assess the magnitude of a horizontal acceleration which is applied to the mass of soil above the slip surface to bring it to the point of failure. Consequently, a relationship between the acceleration and the presumed factor of safety is developed using which, the static FOS corresponding to a horizontal acceleration of zero magnitude, is determined (Abramson et al., 2002). Table 1 below, represents an overview of the limit equilibrium methods that are developed to date.

Table 1 - Summary of Limit equilibrium methods (Pockoski & Duncan, 2000)

Method	Slip surface shape	$\sum M_{overall}$	$\sum M_{individual\text{-}slice}$	$\sum H$	$\sum V$
Swedish Circle	Circular	Yes	No	No	No
Ordinary Method of Slices (Fellenius 1927)	Circular	Yes	No	No	No
Bishop's Modified Method (Bishop 1955)	Circular	Yes	No	No	Yes
Morgenstren and Price's Method (Morgenstren and Price 1965)	Any shape	Yes	Yes	Yes	Yes
Spencer's Method (Spencer 1967)	Any shape	Yes	Yes	Yes	Yes
Corps of Eng. Modified Swedish (1970)	Any shape	No	No	Yes	Yes
Lowe and Karafiath (1960)	Any shape	No	No	Yes	Yes
Janbu Simplified (Janbu 1954)	Any shape	No	No	Yes	Yes

Where; $\sum M_{overall}$ is overall moment equilibrium, $\sum M_{individual\text{-}slice}$ is moment equilibrium for individual slice, $\sum H$ is horizontal force equilibrium, $\sum V$ is vertical force equilibrium.

2.1.2 Numerical Methods

Despite the extensive use of limit equilibrium methods in slope stability analysis in practice, many efforts have been made to find alternative schemes which mostly

eliminate the need for initial assumptions prior to evaluations, such as the consideration of probable location and shape for the slip surface in LEM. Another drawback of these methods, however, is the type of inter-slice forces considered for each slice within the soil mass (Griffiths & Lane, 1999).

Successful application of numerical in solving various problems in different fields of engineering has recently drawn increasing attention from geotechnical engineers worldwide. In the following sections, three numerical approaches that are widely adopted in the literature, particularly for analyzing complex engineering problems, are detailed:

2.1.2.1 Finite Element Method (FEM)

Traditional limit equilibrium methods, according to Stead et al. (2001), might fail to adequately evaluate the slope instabilities, particularly in the case of complex failure mechanisms, such as internal deformations, brittle fractures, and progressive failure phenomenon, etc. The reason for this inadequacy lies in the fact that the stress-strain relationship within the soil medium is not considered in the limit equilibrium analysis. Adoption of the finite element method, in contrast, provides important insights into the stress distribution and strain conditions within the soil, and thus anticipates the deformations in the slope. The soil medium in the FEM analysis is discretized into small elements that are connected together by nodal points. The overall distribution of the stresses within the soil can then be completely determined by calculation of the stresses and strains in these elements, followed by application of the superposition theorem. Factor of safety in a slope stability analysis with FEM is commonly calculated by using strength reduction method (SRM), in which soil strength parameters, namely friction angle (φ) and cohesion (c), are reduced concurrently until the sliding occurs.

2.1.2.2 Finite Difference Method (FDM)

In this approach, like in the finite element method, the soil medium is initially discretized into various small zones which are connected by the points called

Gridpoints. However, stress and deformations in finite difference method can be merely determined at these gridpoints, while these results are available for any point within the medium in the finite element method. To date, FDM methods have been widely implemented in the design process of various geotechnical engineering infrastructures, as an adequate alternative to traditional limit equilibrium methods, however, FEM methods are preferred when high accuracy is demanded.

2.1.2.3 Distinct Element Method (DEM)

This numerical method provides geotechnical engineers with important insights into the mechanism of failure by simulating the stepwise movements of the sliding body over the course of analysis. In this method, the model used for the soil medium consists of a large number of arbitrarily shaped discrete particles in which both the interparticle interactions and the finite movements of the elements are efficiently considered (Hart, 1995), However, as noted by Cheng et al.(2014), slope stability analysis using DEM requires much computation time and its sensitivity to parameters involved in the analysis might hinder its broad application in typical engineering problems.

2.2 Current Challenges

The appropriate method for analyzing the stability of slopes is, in general, adopted on the basis of the geometry and classification of the soil mass within the earth slope, as well as on the basis of the shape expected for the failure surface (Abramson et al., 2002). Available evidence in the literature reveals that adoption of different limit equilibrium analysis techniques might result in slight differences in the value of factor of safety, owing to the variations in the simplifying assumptions made in each method. Also, in their study of the application of finite element methods in analyzing a special case of slope problem, Cheng et al. (2014) demonstrated the deficiency of this method in a reliable assessment of the factor of safety. Consequently, for a better stability evaluation in challenging construction projects the use of various analysis methods is recommended.

One of the main challenges involved in a reliable slope stability analysis is the assumption of a realistic mechanism of failure for the slope. As noted by Cheng et al. (2014), all slope instabilities in nature occur three-dimensionally. Consequently, adoption of two-dimensional models can affect the reliability of slope stability analyses and therefore, degrade the accuracy of the factor of safety. However, the two-dimensional analysis is usually conducted for typical slope stability problems, considering the drawbacks of the three-dimensional slope modeling which includes the requirement of huge computational efforts and difficulties in identifying the slope sliding direction and etc. (Y Cheng & Lau, 2014).

2.3 Determination of the Critical Failure Surface

The most challenging step in a complete slope stability analysis is the fast and accurate localization of the critical geological slip surface in order to estimate the corresponding factor of safety in an earth slope of high failure probability. Although the accurate determination of the failure surface in case of homogeneous soil conditions may not be essential, high sensitivity of the safety factor to even slight changes in the location of the failure surface has been proven (Y Cheng & Lau, 2014). To achieve this purpose, formerly, several trial slip surfaces based on the personal judgment of the researchers were initially generated and the associated factors of safety were subsequently calculated through the implementation of the limit equilibrium methods. Thus, the critical slip surface of the problem was the surface with the lowest FS value. Although useful, this approach lacks the ability to determine the most critical failure surface (minimum safety factor), particularly in the case of multi-layered nonhomogeneous slope problems.

Specific features of the FS function, i.e. discontinuity and the existence of several local minima (Z. Chen & Shao, 1988; Y. M. Cheng, Li, Chi, et al., 2007) have made slope stability analysis a challenging problem to solve. To successfully deal with this problem, limit equilibrium methods coupled with various optimization techniques are employed in the analyses including conventional optimization methods such as calculus of variation by Baker and Gaber (1978), dynamic

programming by Baker (1980) and Yamagami and Jiang (1997), alternating variable methods by Celestino and Duncan (1981) and Li and White (1987), simplex method together with steepest descent method and the Davidson-Fletcher-Powekk method by Chen and Shao (1988), simplex method by Nguyen (1985), conjugate-gradient method by Arai and Tagyo (1985). Furthermore, Yamagami and Ueta (1988) used simplex, Powell, Broyden-Fletcher-Goldfarb-Shanno (BFGS) and Davidon-Fletcher-Powell (DFP) algorithms in slope stability analysis. Greco (1996) solved this problem by adopting Monte Carlo and pattern search methods. later, Malkawi et al. (2001) applied Monte Carlo simulation to several slope stability problems.

Considering these problem-specific difficulties, using such classical methods which are proved to be dependent on the preliminarily selected trial solutions, might fail to obtain a reliable measure of the safety factor. However, recent advances in computing science have enabled the development of advanced computing schemes such as metaheuristics, which have found their way into solving various real problems. These methods are generally developed by imitating the creatures' behavior and by studying nature as the source of inspiration.

Successful application of such optimization techniques has recently, gained significant attention by geotechnical researchers worldwide. The applicability of numerous recently developed metaheuristics, for the slope stability assessment, have been studied thus far such as the implementation of Genetic Algorithms (GA) in the studies conducted in different years by Goh (2000), McCombie and Wilkinson (2002), Das (2005), Zolfaghari et al. (2005), Sun et al. (2008), Sengupta and Upadhyay (2009) and Li et al. (2010). Particle Swarm Optimization (PSO) which is well implemented in the study of different problems, has been employed by Cheng et al. (2007), and Khajehzadeh et al. (2012) in locating critical slip surfaces. Other optimization methods adopted in slope stability analysis include Simulated Annealing (SA) and Tabu Search methods by Cheng et al. (2007), Harmony Search (HS) algorithm by Cheng et al. (2008), Fish Swarm Algorithm by Cheng et al. (2008), Leap Frog Optimization by Bolton et al. (2003), ACO by

Kahatadeniya et al. (2009), Gravitational Search Algorithm (GSA) by Khajehzadeh et al. (2012) and Artificial Bee Colony (ABC) by Kang et al. (2013). In recent years, various innovative optimization techniques have been utilized in order to assess the stability of different earth slopes such as chaos optimization in the study by Hu et al. (2013), swarm intelligence techniques by Gandomi et al. (2015), Immunised evolutionary programming and meeting ant colony method by Gao(2015; 2016), a modified genetic algorithm proposed by Jurado-Pi~na and Jimenez (2015), premium-penalty ant colony optimization (PPACO) by Gao (2016) and imperialistic competitive algorithm (ICA) by Kashani et al. (2016).

Considering the fact that not all the optimization algorithms are able to perform well under benchmark problems of all kind (Wolpert & Macready, 1997), the use of alternative novel techniques becomes an indispensable part of the analyses in the hope of acquiring superior results for each case study.

This study evaluates the efficacy of three recently developed metaheuristic techniques, namely hybrid artificial bee colony with differential evolution (HABCDE), improved harmony search algorithm (LHS), and Grasshopper optimization algorithm (GOA) in stability analysis of multiple slope problems. Detailed implementation procedure of each method is further explained in the following chapter. Furthermore, in order to reach a valuable conclusion, performance of the proposed techniques is benchmarked against several widely-used optimization methods. In the following section, detailed information about the optimization algorithms adopted in this study for the sake of comparison is provided.

2.3.1 Differential evolution (DE)

Differential evolution (DE) is a stochastic population-based optimization algorithm developed by storn and price (1995). Successful applications of this method on various global optimization problems have helped make DE a highly desirable method. DE is categorized as evolutionary algorithms which take advantage of using three evolutionary operations such as mutation, crossover and selection in

order to enhance the performance of multiple solutions over a predefined number of iterations. Multiple variants of DE have been introduced in the literature. The method DE/best/1/bin is employed in this study which demonstrates that (1) the best candidate solution with the minimum fitness is selected for mutation, (2) one differential vector is merely used and (3) the binomial crossover scheme is employed. DE algorithm is made up of the following steps:

2.3.1.1 Initialization

In this step, multiple individuals containing n number of control variables are generated randomly to form a population of size N. Each individual can be defined as follows:

$$X_i = \left[x_{i1}, ..., x_{ij}, ..., x_{in} \right]^T \quad (2)$$

In Equation (2), X_i corresponds to the i^{th} individual in the population and the subscripts of each element represent the current number of population and dimension, respectively.

2.3.1.2 Evaluation of the individuals

In this step, the value of objective function (factor of safety) for each of the candidates are evaluated.

2.3.1.3 Mutation

Initial position vectors are likely to need improvements before they can yield fitness values close to the global optimum. Equation (3) represents a mutation vector produced by adding the best vector - the individual with the lowest fitness – to the weighted difference of two randomly selected vectors. Presence of the best individual in the mutation vector helps the candidate solutions move towards the design vector with the minimum fitness. In Equation (3), F is an arbitrary scaling

factor between [0,1] and $r1$, $r2$ are two discrepant integer numbers selected randomly.

$$P_i = X_{best} + F(X_{r1} - X_{r2}) \tag{3}$$

2.3.1.4 Crossover

A trial vector $Ui = [u_{i1},..., u_{ij},..., u_{in}]$ is then introduced by applying the crossover operation, as presented in Equation (4), to combine the current individual's design variables with those of mutant vector.

$$u_{i,j} = \begin{cases} p_{i,j} & if\ (rand_j \le CR\ or\ j = rand_i) \\ x_{i,j} & if\ (rand_j > CR\ or\ j \ne rand_i) \end{cases} \tag{4}$$

In Equation (4), $rand_j$ is a uniformly distributed random number between [0,1], $rand_i$ represents a random number chosen from the set $[1,2,\ldots,N]$ and CR is a user-defined crossover constant within [0,1].

2.3.1.5 Selection

Applying selection operator, Equation (5), individuals with better fitness values – lower safety factor–are selected comparing the corresponding fitness values of trial and current individuals.

$$X_i^{(t+1)} = \begin{cases} U_i^{(t)} & if\ FS(U_i^{(t)}) < FS(X_i^{(t)}) \\ X_i^{(t)} & else \end{cases} \tag{5}$$

In Equation (5), $U_i^{(t)}$ and $X_i^{(t)}$ are trial and current individuals in t^{th} iteration, respectively, and $Z_i^{(t+1)}$ denotes the current individual chosen for the next iteration.

2.3.1.6 Termination

The procedure will be terminated if (1) a predefined number of iterations is reached or (2) no improvement seen in the value of the best individual over a pre-assigned number of iterations.

2.3.2 Harmony Search (HS)

Harmony Search algorithm (HS) which is introduced by Geem et al. (2001), pertains to evolutionary algorithms, an important subset of metaheuristics. HS is a stochastic population-based optimization method which is developed based on the process of improvising the most pleasing harmony by the orchestra, i.e., evaluating the optimum value of the objective function in an optimization problem. Due to the advantages of this method, including simplicity along with requiring only a few parameters to be adjusted, HS has been widely implemented in the literature to solve problems of different difficulties. The initial set of random solutions, namely harmony memory (HM), which consists of a predefined number of harmonies, so called HMS, gets improved in successive iterations through replacing a newly improvised harmony of better state with the worst harmony in the memory. To achieve this goal, three operations are utilized which includes (1) harmony memory consideration, (2) pitch adjustment and (3) randomization. The implementation procedure of the harmony search algorithm is summarized as follows:

2.3.2.1 Initialization of the optimization problem and algorithm parameters

In this step, dimension of candidate solutions D, lower and upper bounds of each solution's control variables and maximum generation number G, are determined. It is also necessary to specify the harmony memory size (HMS), harmony memory consideration rate (HMCR) and pitch adjusting rate (PAR) in this step.

2.3.2.2 Initialization of the harmony memory (HM)

An initial memory of HMS candidate solutions, $HM = [X_1, X_2, \ldots, X_{HMS}]$, is constituted wherein the variables of each solution is initialized using Equation (6), as follows:

$$x_{i,j} = l_j + rand().(u_j - l_j) \tag{6}$$

where $x_{i,j}$ denotes the j^{th} decision variable of the i^{th} individual, l_j and u_j represent the lower and upper limits for the corresponding variable, respectively. $rand()$ is a uniformly distributed random number in [0,1] interval.

2.3.2.3 Improvisation of a new harmony from the HM

Three major operations, namely memory consideration, pitch adjustment and randomization, are required to be implemented in improvising a new harmony in HS algorithm. In memory consideration operation, each decision variable in the new harmony is derived from the corresponding element in a randomly selected harmony in the memory with the probability of HMCR percent, otherwise Equation (7) is used to complete the harmony through generating a valid random value.

$$v_{i,j} = \begin{cases} x_{rnd,j} & rand() < HMCR \\ l_j + rand().(u_j - l_j) & else \end{cases} \tag{7}$$

where k is a randomly selected index which refers to the k^{th} harmony in the memory. Additionally, the variables of the new harmony which were selected from the harmony memory, need to be modified by pitch adjustment operator, as in Equation (8):

$$v_{i,j} = \begin{cases} v_{i,j} \pm rand().bw_j & rand() < PAR \\ v_{i,j} & else \end{cases} \quad (8)$$

where bw_j is a user-specified pitch bandwidth for the j^{th} component of the new candidate solution.

2.3.2.4 Update the HM

Finally, the newly improvised harmony is substituted for the worst component of the harmony memory, if it results in a lower objective function value.

2.3.2.5 Repeat

The procedure will be repeated until (1) a predefined number of iterations is reached or (2) no improvement seen in the value of the best individual over a pre-assigned number of iterations.

2.3.3 Artificial Bee Colony (ABC)

ABC is a nature-inspired population based algorithm which was introduced by Karaboga (2005) that imitates the social behavior of a swarm of bees in locating food sources. The application of ABC to various optimization problems in obtaining the optimum solution (a rich source of food) has demonstrated the flexibility and efficacy of this method. However, previous studies have shown a clear need for improvement in ABC, since it lacks an efficient exploitation of the search space which instead performs well in exploration (G. Zhu & Kwong, 2010). Bees swarm is classified into three categories: (1) Employed bees, (2) Onlooker bees and (3) Scout bees; Sharing the information acquired by exploring the food sources (initial solutions) in the neighborhood, leads the forager bees to the most promising source of food, i.e. optimum solution for the given problem. Exploration of the feasible food resources in the vicinity of the hive and collecting requisite information are thoroughly performed by employed bees, while the onlooker bees

serve the swarm in the assessment of collected information and selecting a food source of high extraction capability. Scout bees are responsible for discovering new food sources to replace with the exhausted ones. Three major phases of the ABC method are described as follows:

2.3.3.1 Initialization

First, a population of potential solutions containing SN randomly initialized individuals is generated using Equation (9). Each individual X_i $(i = 1, 2, ..., SN)$ can be initialized as follows:

$$X_{id} = X_{mind} + rand[0,1](X_{maxd} - X_{mind}) \tag{9}$$

where X_{id} is the d^{th} design parameter of the i^{th} solution in the population, X_{mind} and X_{maxd} denote the boundary limitations for the d^{th} variable of X_i, and rand [0,1] is a uniformly distributed random number between [0,1].

2.3.3.2 Employed bee phase

At this step, employed bees attempt to locate a new source of food in the vicinity of the current sources. To accomplish this objective Equation (10) is adopted, as follows:

$$V_{id} = X_{id} + \varphi_{id}(X_{id} - X_{kd}) \tag{10}$$

where, the subscript i denotes the index number of the current solution, k refers to a randomly chosen solution from the population and $i \neq k$, and j is a random index. φ_{id} is a random number between [0,1]. Finally, the solutions with better fitness values are selected, applying the greedy selection between updated solutions and the old ones.

2.3.3.3 Onlooker bee phase

Onlooker bees evaluate the information collected by employed bees to select a rich source of food in order to search for better sources in their vicinity. This selection is performed based on a probability which is proportional to the fitness value of the solution (nectar amount of food source), as shown below:

$$prob_i(G) = \frac{fitness_i}{\sum_{n=1}^{SN} fitness_n} \tag{11}$$

where $fitness_i$ is the fitness value associated with the i^{th} solution. Once an appropriate candidate is selected, Equation (10) is then used to generate a new candidate solution in the neighborhood. As in the previous phase, a greedy selection between the updated solution and the old one is applied in order to select the solution of the optimal value.

2.3.3.4 Scout bee phase

In ABC algorithm, a control parameter, namely limit, is defined in order to indicate which of the solutions is abandoned (i.e. food sources exhausted). As a result, an alternative food source is required to be located by a scout bee using Equation (9) and replaced with the exhausted one.

CHAPTER 3

MAIN WORK

In this chapter, a complete description of the framework proposed for a reliable slope stability evaluation with the application of optimization techniques is provided. This procedure embraces three major steps, which include (1) generating a number of trial slip surfaces, (2) evaluating safety factors corresponding to the generated surfaces and lastly, (3) looking for the most critical failure surface possessing the minimum safety factor. Following the procedure explained in the first step, several non-circular failure surfaces composed of a predefined number of slices can be generated. The value of safety factor is then required to be calculated for each trial surface. Finally, in the third step, the optimization technique intends to locate much critical surfaces within the slope, through making admissible changes in the initial geometry of the surfaces. Detailed information about each step is given in the following subsections.

3.1 Trial Slip Surface Generation Method

Initial trial surfaces can have either circular or non-circular geometry. A number of slope stability studies have demonstrated that circular failure surfaces can be successfully used where the case of study consists of a homogeneous soil layer; however, the stability of slopes with multi-layered soil profile can be more precisely evaluated through generating non-circular trial failure surfaces within the analysis (Zolfaghari et al., 2005). Various methods have so far been implemented in the literature for generating trial slip surfaces, and as noted by Cheng et al. (2008) the results obtained in the analysis is highly dependent on the slip surface generation method, and therefore different outcomes may be expected for the same slope in this regard.

Amongst the methods proposed for generating trial slip surfaces to date, the method recommended in the study by Cheng et al. (2008) is taken as the base for the procedure followed in this study, through which admissible slip surfaces, i.e. concave upward surface, can be formed as further outlined below. An example of the generated surfaces is represented in Figure 8. The function g(x) indicates the ground surface and h(x) marks the boundary separating different soil layers in the slope. The n-slice nonlinear slip surface T is readily formed by connecting $n+1$ vertices $(V_1, V_2, ..., V_{n+1})$ specified by the coordinates $(x_1, y_1), (x_2, y_2), ..., (x_{n+1}, y_{n+1})$. The following steps are followed to generate a valid trial slip surface:

- Initially, the x-coordinates of the start and endpoint of the surface along with the inclination of the first (β_1) and last (β_{n+1}) slices are randomly determined within their respective pre-defined ranges. Using the ground surface function g(x), corresponding vertical coordinates can then be specified. Care is required when defining the boundary limitations of the (β_1) and (β_{n+1}) in order to generate admissible surfaces.

- Two lines are drawn through two end points of the surface with the specified angles and the intersection point, i.e. V', is determined.
- Equation (12) and (13) are employed to determine the coordinates of two new vertices, i.e. second vertex V_2 and a temporary vertex V_7' .

$$x_2 = x_1 + (x'_{n+2} - x_1)(0.5 - r(-0.5, 0.5)) \quad (12)$$

$$y_2 = y_1 - (x_2 - x_1)\tan(\beta_1) \quad (13)$$

where r is a randomly generated number between -0.5 and 0.5.

- Subsequent points corresponding to the third and fourth vertices, V_3 and V_4 respectively, are placed at two neighboring line segments of the largest

horizontal lengths using equations similar to those of the previous step. This procedure is followed in order to indicate the coordinates of all vertices which simply constitute a trial surface of n slices described by the vector $V = (x_1, x_{end}, \beta_1, \beta_{end}, \delta_5, ..., \delta_{2n})$. The slip surface generation procedure is then followed by safety factor evaluation of the respective surfaces, which is further explained in the succeeding section.

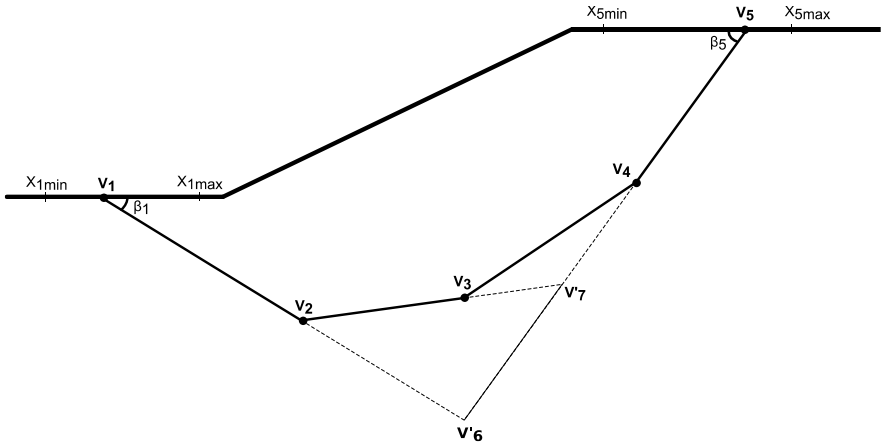

Figure 8- Geometric Description of the Surface Generation Method

3.2 Calculation of Factor of Safety

As outlined in the previous chapter, several limit equilibrium methods that vary depending on the inter-slice forces assumptions are introduced thus far, within them the M-P method (Morgenstern & Price, 1965) in which all the equilibrium conditions are perfectly met, has been exhaustively used in various studies in the literature. This method, however, suffers from the difficulty to suggest appropriate equations for the factor of safety and the scaling factor due to the non-linearity of the force and moment equilibrium equations.

To overcome these difficulties, in this study a reformulated Morgenstern-Price method is adopted for the slope stability analysis, which is developed by Zhu et al.

(2005). The changes made in this improved technique contributes to its simplicity and facilitates the implementation of this algorithm into a computer program (D. Y. Zhu et al., 2005).

As proposed in the original M-P method, the ratio of the normal forces over shear inter-slice forces is calculated as follows:

$$T = f(x).\lambda.E \tag{14}$$

where T and E refer to the inter-slice shear and normal forces, respectively. In addition, *f(x)* in this equation is a prescribed function that may be in the form of a constant, a trapezoidal, a half-sine or a user-defined function. λ is a scaling factor that is to be determined when calculating the factor of safety.

Prior to the evaluation of the safety factor, the soil mas above the failure surface, like other methods of slices, is divided into a number of slices which is then followed by determination of the forces imposed on each individual slice. Figure 9 below illustrates the geometry of a simple slope along with the inter-slice forces on a representative slice. The symbols h_i, b_i and α_i denote the slice height, slice width and inclination of the slice base, respectively. Furthermore, W_i denotes weight of the slice, K_c refers to seismic coefficient in the horizontal direction, w_i is the inclination of the external loading Q_i . Resultant pore water force is represented by U_i , while u_i denotes the mean water pressure. In addition, N'_i corresponds to the effective normal force on the slice base, c_i is the effective cohesion, φ'_i is the effective internal friction angle, F_s is the safety factor and S_i represents the slice base mobilized shear resistance. E_i and E_{i-1} are the normal inter-slice forces exerted on the slice, while Z_i and Z_{i-1} denote the distances from the bottom of the slice to the point of application of the corresponding normal inter-slice forces.

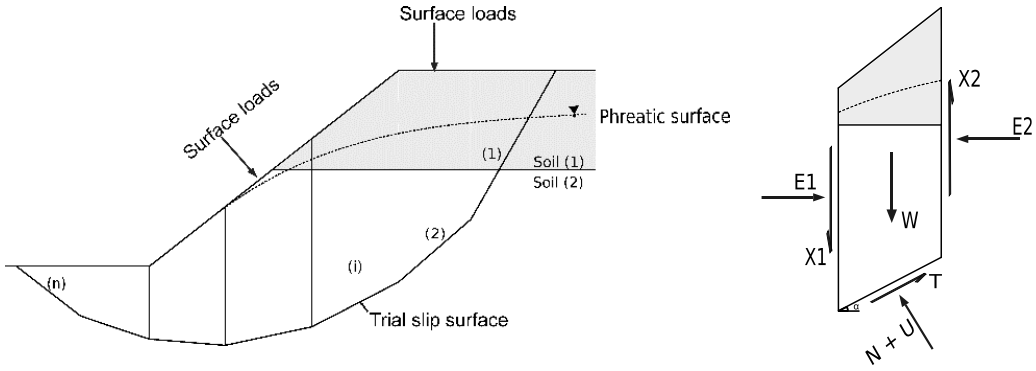

Figure 9 - (a) Slope Geometry and General Failure Surface, (b) Inter-Slice Forces in Slice Number (i)

In Figure 9 (b), N is the normal force acting on the base of the slice, W denotes the slice weight, and U represents the resultant water force at the base. In addition, T denotes the shear force on the base, α is the angle of base inclination and finally, X and E denote the inter-slice shear and normal forces, respectively.

In an effort to derive an expression for the factor of safety, Zhu et al. (2005) considered the condition of equilibrium to the forces both perpendicular and parallel to the slice base, which yielded the following Equation:

$$FS = \frac{\sum_{i=1}^{n-1}(R_i \prod_{j=1}^{n-1} \psi_j) + R_n}{\sum_{i=1}^{n-1}(T_i \prod_{j=1}^{n-1} \psi_j) + T_n} \qquad (15)$$

where, R_i represent the sum of the forces resisting the slippage, Equation (16), and T_i corresponds to the sum of the forces which may lead to failure of the slope, Equation (17).

$$R_i = [W_i \cos\alpha_i - K_h W_i \sin\alpha_i + Q_i \cos(\delta_i - \alpha_i) - U_i] \times \tan\phi_i' + c_i' l_i \qquad (16)$$

$$T_i = [W_i \sin\alpha_i + K_h W_i \cos\alpha_i - Q_i \sin(\delta_i - \alpha_i) \quad (17)$$

$$E_i \Phi_i = [\psi_{i-1} E_{i-1} \Phi_{i-1} + F_s T_i - R_i \quad (18)$$

$$\Phi_i = (\sin\alpha_i - \lambda f_i \cos\alpha_i)\tan\phi_i' + (\cos\alpha_i + \lambda f_i \sin\alpha_i) F_s \quad (19)$$

$$\psi_{i-1} = [(\sin\alpha_i - \lambda f_{i-1} \cos\alpha_i)\tan\phi_i' + (\cos\alpha_i + \lambda f_{i-1} \sin\alpha_i) F_s] / \Phi_{i-1} \quad (20)$$

where parameter E refers to the inter-slice forces on the vertical sides of slices. From the Equation (15), it can be inferred that an iterative procedure needs to be followed so as to determine the factor of safety since the equation has the FS on both sides.

Likewise, resolving moments about a point in the center of the slice, an explicit Equation is developed for the scaling factor:

$$\lambda = \frac{\sum_{i=1}^{n} [b_i (E_i + E_{i-1}) \tan\alpha_i + K_h W_i h_i + 2Q_i \sin\delta_i h_i]}{\sum_{i=1}^{n} [b_i (f_i E_i + f_{i-1} E_{i-1})]} \quad (21)$$

where parameter E refers to the inter-slice forces on the vertical sides of slices which is determined as follows:

$$E_i = \frac{[(\sin\alpha_i - \lambda f_{i-1} \cos\alpha_i)\tan\phi_i' + (\cos\alpha_i + \lambda f_{i-1} \sin\alpha_i) FS] E_{i-1} + FST_i + R_i)}{(\sin\alpha_i - \lambda f_i \cos\alpha_i)\tan\phi_i' + (\cos\alpha_i + \lambda f_i \sin\alpha_i) FS} \quad (22)$$

It is important to note that at the lower and upper bounds of the slope, E_0 and E_n respectively, the inter-slice forces are neglected, (E_0=E_n=0).

The complete iterative procedure for the factor of safety calculation is illustrated in Figure 10. As shown, once the value of R_i and T_i are determined, it is then required

to define the type of inter-slice function *f(x)*, a constant function (*f*(x) = 1) is adopted in this study, as well as to initialize the factor of safety and the scaling factor. Zhu et al. (2005) proposed initial values of 1 and 0 for F_s and λ, respectively. Next step is to calculate the value of FS using Equation (15), followed by evaluation of λ for which the Equation (21) is utilized. These updated values are then substituted for the prescribed FS and λ values, and an iterative procedure is continued until the absolute differences in FS value as well as the value of λ in successive iterations is less than predefined parameters ε_1 and ε_2; a value of 0.0001 is proposed for both of these limits.

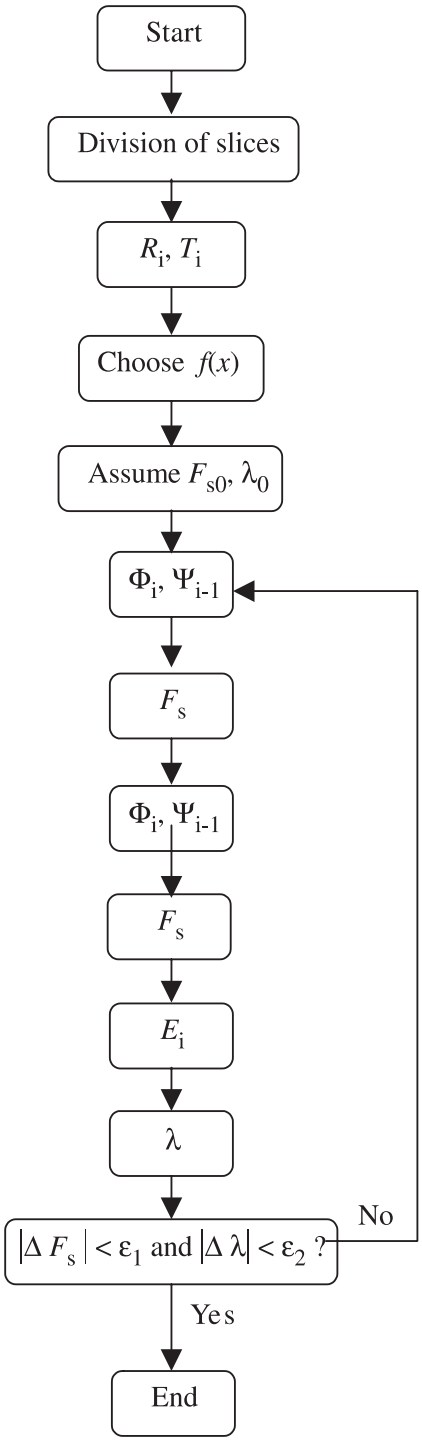

Figure 10 - Flowchart of FS Algorithm (D. Y. Zhu et al., 2005)

3.3 Optimization Methods

As has been pointed out in the previous sections, the main goal of a slope stability assessment is to evaluate the minimum safety factor corresponding to a geological surface along which the soil is more prone to slide down the slope. This objective can be reliably achieved by an optimization process formulated as follows:

$$\text{Find} \qquad V = (x_1, x_{end}, \beta_1, \beta_{end}, \delta_5, ..., \delta_{2n}) \tag{23}$$

$$\text{To minimize} \qquad FS(V) \tag{24}$$

$$\text{Subjected to} \qquad x_{i\min} \le x_i \le x_{i\max}, \quad i = 1, nVar \tag{25}$$

$$-0.5 \le \delta_j \le 0.5, \quad j = 5, 6, ..., nVar \tag{26}$$

where V is a trial solution vector containing control variables of the sliding surface and $FS(V)$ is the safety factor of the generated failure surface. $x_{i\min}$ and $x_{i\max}$ denote the boundary limitations of the starting and end points of the surface and $nVar$ indicates the number of control variables within the solution vector. The minimization procedure starts with the construction of a population of randomly generated solution vectors followed by evaluation of the corresponding objective function values, factors of safety, by using the method proposed in the previous section. The search for solutions with huge potential for further improvement in the objective value is continued through updating the variables of solution vectors over the successive iterations. Once the predefined termination criteria are met, the optimum objective value of the problem, pertaining to the best candidate solution is finally achieved. Detailed information about the implementation process of the proposed optimization methods is given in the following subsections.

3.3.1 Improved harmony search algorithm (LHS)

Review of the available evidence on the application of the harmony search method establishes its limitations in exploring the optimum solution, particularly in the case of complicated optimization problems and demonstrates the need for further refinements in its algorithm. In this regard, Ouyang et al. (2017) proposed an improved harmony search algorithm (LHS) which enhances the ability of HS algorithm both in exploring the search space thoroughly in order to discover a region of better candidate solutions, along with locating new promising solutions in the neighborhood of the current optimum solution. Three major alteration to the harmony search algorithm is made which includes the incorporation of (1) local opposition-based learning, (2) self-adaptation global pitch adjusting, and (3) competition-selection strategies into the original HS method. The implementation procedure of LHS is outlined and a brief overview of the selection of appropriate parameters for this method is given, as follows:

3.3.1.1 Definition of the Algorithm

In opposition-based learning scheme, a candidate solution and its opposing solution are generated simultaneously in order to explore the search space more comprehensively. Exploitation ability in harmony search method, however, is mainly influenced by the pitch adjusting operation. Consequently, employing a self-adapting pitch adjustment concept can improve the efficacy of the harmony search method in problem solving. Adoption of the competition-selection approach helps the algorithm update the existing harmony memory over the successive iterations. The implementation procedure of the LHS is summarized as follows:

3.3.1.1.1 Initializing algorithm and problem parameters

In this step, harmony memory size (HMS), harmony memory consideration rate (HMCR), the maximum dimension of candidate solutions D, lower and upper bounds for the control variables and maximum generation number G, are required to be specified.

3.3.1.1.2 Initializing harmony memory

To construct an initial population of randomly generated candidate solutions, the same procedure, as explained in the initialization step of the HS method, is followed in this subsection.

3.3.1.1.3 Improvisation

Unlike harmony search, LHS improvises two new harmonies in the course of memory consideration process as illustrated in Equations (27) and (28):

$$x_{new,j} = \begin{cases} x_{r,j}, & \text{with probability of } HMCR \\ x_{j,L} + rand().(x_{j,U} - x_{j,,L}), & \text{without probability of } 1-HMCR \end{cases} \quad (27)$$

$$\tilde{x}_{new,j} = \begin{cases} x_{j,U} + x_{j,L} - x_{new,j}, & \text{without probability of } HMCR \\ x_{j,L} + rand().(x_{j,U} - x_{j,,L}), & \text{without probability of } 1-HMCR \end{cases} \quad (28)$$

where x_{new} is a newly generated candidate solution and $\tilde{x}_{new}$ is its opposite estimate. The subscript r is a member of the set $\{1,2,\ldots,HMS\}$ denoting the index number of a randomly selected harmony in the memory. HMCR represents the probability of deriving j^{th} decision variable in the new solution vector from the corresponding component of the r^{th} individual in the memory, while the remaining components are determined randomly, as in Equation (27). In opposition solution vector, however, HMCR refers to the probability of selecting j^{th} component within the opposite estimate of the new candidate solution to fill the corresponding element in the new opposite candidate solution and $(1-HMCR)$ demonstrates the probability of assigning random values to the remaining components of the solution. A self-adaptation pitch adjustment is subsequently made to the new candidate solutions, as in Equation (29):

$$x_{new,j} = \begin{cases} x_{r,j} + rand \times (x_{best,j} - x_{r,j}), & if\ rand \le \eta \\ x_{r,j} - rand \times (x_{worst,j} - x_{r,j}), & otherwise \end{cases} \quad (29)$$

where $x_{best,j}$ and $x_{worst,j}$ represent the index number of selected components within the best and worst individuals in the memory, respectively. Incorporation of the best and worst individuals helps the algorithm approach the global optimum over the successive generations. The parameter η represents a dynamic factor where its value is dependent on the number of the current iteration along with the maximum iterations number, as expressed in Equation (30):

$$\eta = \begin{cases} \sqrt{1-1.5k/K}, & k < K/2 \\ 0.5, & K/2 \le k \le 3K/4 \\ \exp\left(-\left(\sqrt{14.53-14.04k/K}\right)\right), & otherwise \end{cases} \quad (30)$$

where k denotes the current iteration's number, and the maximum iterations number is depicted with K .

3.3.1.1.4 Updating

In this step, fitness value for both the new solution and its opposite estimate is compared and the better solution is substituted for the worst individual in the population.

3.3.1.1.5 Termination

The procedure will be continued until the maximum number of iterations is reached and the best solution will be reported. Figure 11 and Figure 12, illustrate the implementation process of the proposed method.

.

3.3.1.2 Parameter Selection

Appropriate determination of the key parameters involved in any optimization method requires an extensive research effort. In this regard, Ouyang et al. (2017) carried out a number of investigations into the impacts of the values assigned to HMS and HMCR on the performance of LHS; according to their study, selection of a small value for HMS would yield much promising results while, in contrast, a large value is recommended for the HMCR (HMCR > 0.90) for a better performance.

In an effort to determine the appropriate parameter values in this study, slope stability analysis using LHS method is repeated several times, with varied values assumed for the HMS and the HMCR. Based on the results obtained, the selected values for these parameters are as follows: HMCR= 0.99 and HMS = 40.

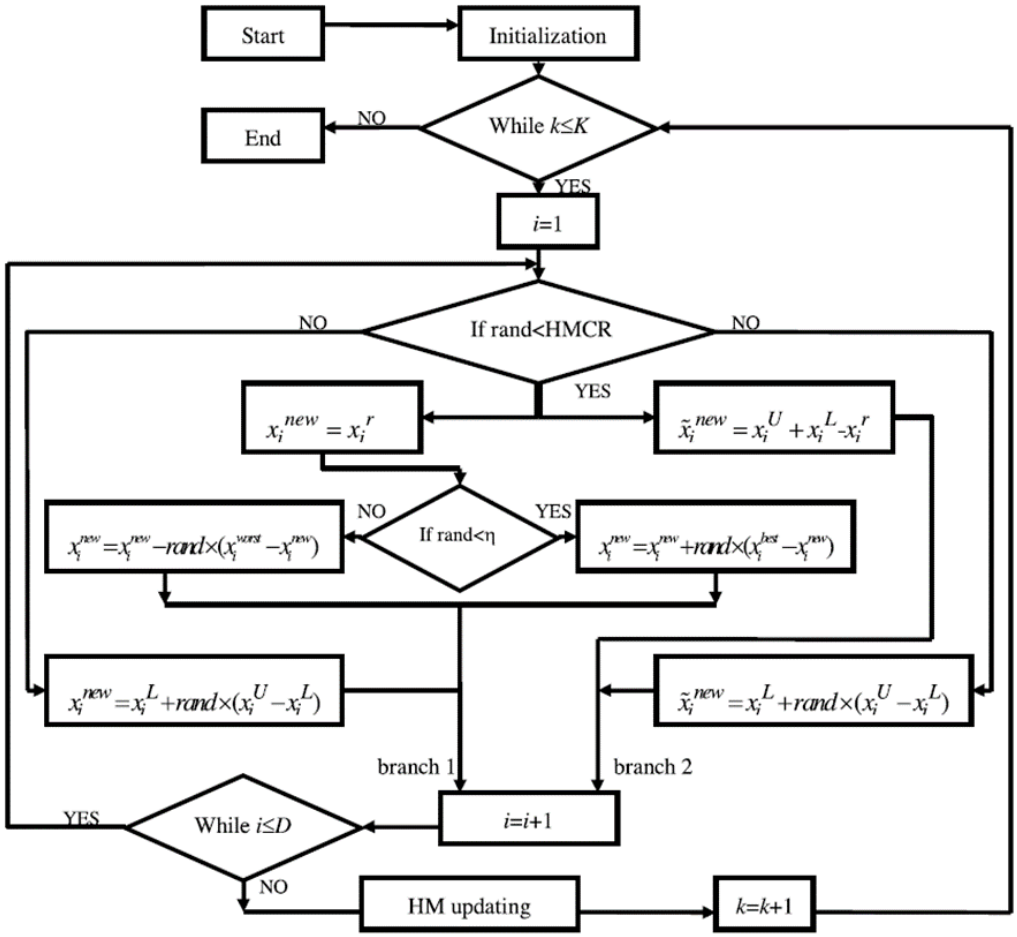

Figure 11 - Two main branches about the improvisation process (Ouyang et al., 2017)

1. Initializing algorithm and problem parameters.
   Harmony memory size HMS, maximum dimension D, maximum generation G, $PAR_{\min}$ and $PAR_{\max}$

2. Initializing harmony memory
   For i=1 to HMS **do**
      For j=1 to D
      $x_{i,j} = x_{j,L} + rand.(x_{j,U} - x_{j,L})$;
      End For
   Calculate $f(x_i)$
   End For

3. Improvisation
   g=0, **while** the stopping criteria is not adequate (g<G) **do**
   For j=1 to D **do**
   If rand () ≤ *HMCR*
      $x_{new,j} = x_{r,j}\ (r \in 1,2,3,\ldots HMS)$ % memory consideration
      $\tilde{x}_{new,j} = x_{j,U} + x_{j,L} - x_{new,j}$
      Calculate the parameter η

      If rand () ≤ η **then** % pitch adjustment
         $x_{new,j} = x_{new,j} + rand.(x_{best,j} - x_{new,j})$
         Else
         $x_{new,j} = x_{new,j} - rand.(x_{worst,j} - x_{new,j})$
      End If
   Else
      $x_{new,j} = x_{j,L} + rand.(x_{j,U} - x_{j,L})$ % random selection
      $\tilde{x}_{new,j} = x_{j,L} + rand.(x_{j,U} - x_{j,L})$
   End If
   End For

4. Updating
   Select the worst harmony vector x_{worst} in the current harmony memory and calculate $f(x_{new})$ and $f(\tilde{x}_{new})$
   If $f(x_{new}) < f(\tilde{x}_{new})$
      $x_{worst} = x_{new}$
      $f(x_{worst}) = f(x_{new})$
   Else
      $x_{worst} = \tilde{x}_{new}$
      $f(x_{worst}) = f(\tilde{x}_{new})$
   End If
   g=g+1
End While

5. Algorithm stops and the best solution is obtained

Figure 12 - LHS Algorithm (Ouyang et al., 2017)

3.3.2 Grasshopper optimization algorithm (GOA)

Grasshopper optimization algorithm (GOA) is a recent nature-inspired stochastic optimization method proposed by Saremi et al. (2017). Mathematical theorem of the GOA is thoroughly formed on the basis of the natural behavior of grasshopper swarm in foraging the farms for adequate sources of food. Each grasshopper in this method relocates from its current position according to the location of the best forager, a grasshopper possessing the optimal objective value, and remaining agents' position. Simulation of the social interaction, i.e. repulsion and attraction forces, between the grasshoppers which is balanced with a decreasing coefficient help GOA thoroughly explore the design space in order to discover the most adequate food source, i.e. the optimum value of the objective function. Successful application of the proposed method on several test functions of various complexities as well as design optimization of multiple real problems has demonstrated the accuracy and applicability of GOA in obtaining the optimum solutions. The implementation process of the GOA is summarized as follows:

3.3.2.1 Definition of the Algorithm

The initial position of N number of potential solutions (grasshoppers) in the search space is randomly determined prior to the formation of the foraging swarm. Control parameters of GOA, including C_{max}, $C_{\min}$ as well as the number of maximum iterations are also required to be specified in this phase. Objective value of each candidate solution is then evaluated and the one owning the optimum objective value – best candidate solution – is subsequently determined. A successful optimization process, however, requires the entire search space to be comprehensively explored. In this regard, Equation (31) is introduced in GOA which helps the grasshoppers update their current position, and thus discover new regions in the neighborhood. It also can be inferred from the Equation (31) that in addition to the position of both the current grasshopper and the best individual thus far, the remaining members of the swarm play a considerable role in updating the current positions.

$$X_i^d = c\left(\sum_{\substack{j=1 \\ j\neq i}}^{N} c\frac{ub_d - lb_d}{2} s\left(\left|x_j^d - x_i^d\right|\right)\frac{x_j - x_i}{d_{ij}}\right) + T_d \qquad (31)$$

where X_i^d indicates the updated position of the i^{th} individual in the d^{th} dimension, N refers to the number of individuals, lb_d and ub_d define the boundary limits in dimension d, $\left(\left|x_j^d - x_i^d\right|\right)$ represents the distance separating the individuals i and j. In addition, $(x_j - x_i)/d_{ij}$ indicates a vector of magnitude 1, from individual i to individual j. T_d is the d^{th} component of the best candidate solution in the swarm, and subscripts i and j refer to the i^{th} and j^{th} grasshopper, respectively. In Equation (31), c is a coefficient balancing the attraction and repulsion forces between the search agents, which contributes to the improvement of the results through guiding the search agents towards the best solution within the swarm. Value of the coefficient c varies over the successive iterations and it can be determined by using Equation (32) as follows:

$$c = c_{\max} - l\frac{c_{\max} - c_{\min}}{L} \qquad (32)$$

where c_{max} and c_{min} refer to the boundary limitations for the coefficient c, parameter l denotes the current iteration, and L is the maximum iterations number. In addition, s in the Equation (31) is a function which measures the interactive forces between the grasshoppers. Equation (33) is proposed for this purpose, as follows:

$$s(r) = f\,e^{\frac{-r}{l}} - e^{-r} \qquad (33)$$

where parameter f denotes the attraction intensity and l refers to the scale of the attractive length.

The search for regions with huge potential for further improvement in the objective value is continued through updating the position of search agents over the successive iterations. Once the predefined termination criteria are met, the optimum fitness value of the problem, corresponding to the best target is finally achieved. Figure 13, illustrates the pseudo codes of the proposed method.

3.3.2.2 Parameter Selection

In an effort to determine appropriate values for the key parameters of the GOA, Saremi et al. (2017) carried out a number of investigations into the impacts of the values assigned to *f* and *l* on the performance of function *s.* According to their study, the function s would yield much promising results when assuming *l=1.5* and *f=0.5*. In addition, as for the parameters $c_{max}$and c_{min}, the values 1 and 0.00001 are recommended, respectively,

In an effort to determine the appropriate parameter values in this study, slope stability analysis using GOA method is repeated several times, with varied values assumed for the boundary limitations of the parameter c – c_{max} and c_{max}. Based on the results obtained, the selected values for these parameters are as follows: c_{max}= 2 and c_{min} = 0.001. It is worth mentioning that the values proposed in the original study are used for the parameters *l* and *f*.

Initialize the swarm X_i, (i= 1,2,…,n)

Initialize c_{max}, c_{min} and maximum number of iterations

Calculate the fitness of each search agent

T= the best search agent

While (l < Max number of iterations)

Update c using Equation (32)

For each search agent

Normalize the distances between grassoppers in [1,4]

Update the position of the current search agent by the Equation (31)

Bring the current search agent back if it goes outside the boundaries

End for

Update T if there is a better solution

l= l+1

End while

Return T

Figure 13 - GOA Algorithm (Saremi et al., 2017)

3.3.3 Hybrid Artificial Bee Colony with Differential Evolution (HABCDE)

Recent studies have consistently shown that basic ABC, as mentioned earlier, lacks the ability to exploit better solutions as it lacks the capability of taking advantage of the information collected by the forager bees swarm. So far, however, there has been made considerable attempts to get around the above-mentioned drawbacks.

Jadon et al. (2017) hybridized Artificial Bee Colony and Differential Evolution methods to develop a new algorithm, namely HABCDE, which benefits both from the advantages of ABC, such as (1) straightforward implementation and (2) few parameter adjustment requirements, and from the fast-converging feature of the differential evolution algorithm. Various modifications are carried out on each phase of ABC to enhance its efficiency and convergence speed as well as to obtain results of high accuracy. In HABCDE, employed bees utilize an updated equation

while exploring food sources. Besides, onlooker bees in HABCDE exploit the current solutions by the means of DE's evolutionary operations, and the entire scout bees in this method are required to look for new alternative food sources to replace exhausted ones.

3.3.3.1 Definition of the Algorithm

In the following subsections, the implementation process of the proposed HABCDE method is outlined in three phases. Also, a brief overview of the parameter selection for this method is provided, as follows:

3.3.3.1.1 Initialization

First, a population of potential solutions containing *SN* randomly initialized individuals is generated using Equation (34). Each individual $X_i (i = 1, 2, ..., SN)$ can be generated as follows:

$$X_{id} = X_{\min d} + \text{rand}[0.1](X_{\max d} - X_{\min d}) \quad (34)$$

where X_{id} is the d^{th} design parameter of the i^{th} solution in the population, $X_{\min d}$ and $X_{\max d}$ denote the boundary limitations for the d^{th} variable of X_i, and rand [0,1] is a random number selected from a uniform distribution between [0,1].

3.3.3.1.2 Employed bee phase

At this step, employed bees attempt to locate a new source of food surrounding the current sources. To accomplish this objective, a search equation similar to the one proposed in gbest-guided ABC (G. Zhu & Kwong, 2010) is adopted, which contributes to the improvement in exploitation ability of the employed method through the incorporation of the position of the best candidate solution into Equation (35), as follows:

$$v_{id} = x_{id} + \varphi_{id}(x_{id} - x_{kd}) + \psi_{id}(y_d - x_{id}) \quad (35)$$

where, the subscript *i* indicates the index number of the current solution, *k* refers to a solution selected randomly from the population and $i \neq k$, and *j* is a randomly selected index. φ_{id} is a random number in the interval [0,1], y_d is the d^{th} variable within the best individual. Ψ is a random number in the interval $(0, C)$ and *C* is a positive user-defined constant. Finally, the solutions with better fitness values are selected by using the greedy selection mechanism between updated solutions and the old ones.

3.3.3.1.3 Onlooker bee phase

Onlooker bees evaluate the information collected by employed bees to serve the purpose of selecting rich sources of food in an effort to search for better sources in their vicinity. This selection is performed on merit based on a probability $prob_i$, which is proportional to the solution's fitness value, as shown below:

$$prob_i(G) = \frac{0.9\, fitness_i}{maxfit} + 0.1 \quad (36)$$

where $fitness_i$ is the calculated fitness value associated with the i^{th} solution. To generate new candidate solutions, DE's evolutionary operations, i.e. mutation, crossover, and selection, are utilized. This process starts with generating a mutated vector according to the best food source position as well as the position of two other sources which are selected randomly from the population as presented in Equation (3) in the previous chapter. Following this, a crossover operation, as in Equation (4), is applied and current solution's design variables are merged with those of mutated vector to produce a trial vector. Finally, selection operator, Equation (5), is applied in the last phase so as to determine the solution of the optimal value.

3.3.3.1.4 Scout bee phase

Typically, available nutrients of the food sources get exhausted due to the continued exploitation by the forager bees. A candidate solution in ABC is called abandoned if its corresponding control parameter reaches a predefined value, namely limit, after a number of successive iterations. In basic ABC, a scout bee identifies an alternative source of food, by using Equation (34), to replace the exhausted one. However, in the proposed method, all the exhausted solutions update their current position to lead to an improvement in the exploration capability of HABCDE. Consequently, the optimum solution for the problem can be discovered by performing this three-step iterative procedure until a certain termination criterion is met. Figure 14 and Figure 15, illustrate the implementation process of the proposed method.

3.3.3.2 Parameter Selection

In an effort to determine the appropriate setting for the key parameters of the HABCDE, Jadon et al. (2017) carried out a number of investigations into the impacts of the values assigned to F and CR – key parameters of DE method – on the performance of proposed method. According to their study, the method would yield much promising results with the values $F=0.7$ and $CR=0.6$ assumed in the analyses.

In an effort to determine the appropriate parameter values in this study, slope stability analysis using HABCDE method is repeated several times, with varied values assumed for the parameters F and CR. Based on the results obtained, the selected values for these parameters are as follows: F = 0.7 and CR = 0.9.

Initialize the swarm and control parameters;

While !Termination criteria **do**

Employed bee phase: generate neighborhood solutions for each solution in the swarm using position update Equation (35)

Onlooker bees phase: generate neighborhood solutions for the solutions selected based on their probabilities as follows:

for (each onlooker's solution x_i) **do**

if (U (0, 1) < $prob_i$) **then**

Apply mutation (as in Equation(3)) to generate the trial solution u_i
Apply binomial crossover (as in Equation(4)) to generate an offspring x'_i

if (f (x'_i) is better than f (x_i)) **then**
$x_i = x'_i$
end if

end if

end for

Scout bee phase: randomly reinitialize all the exhausted solutions in the search space.

end while

Output the best solution.

Figure 14 - HABCDE Algorithm (Jadon et al., 2017)

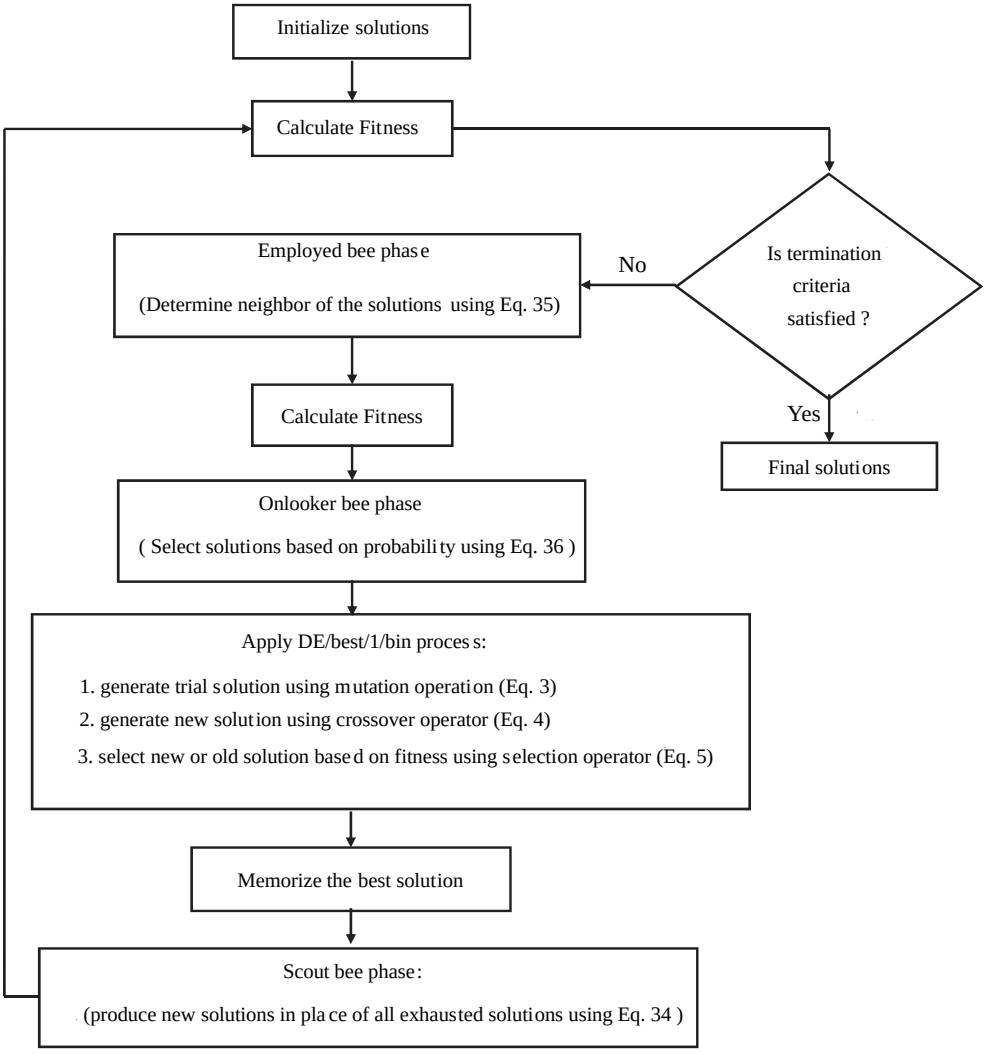

Figure 15 - Flowchart for HABCDE Algorithm (Jadon et al., 2017)

CHAPTER 4

CASE STUDIES

In this section capability and efficacy of the proposed methods in determination of the expected failure surface and the relating factor of safety are thoroughly revealed. In this regard, four case studies of varying computational complexity are considered. Selected numerical examples consist of a set of three complex layered slopes of diverse geometries and a simple homogeneous slope problem, subjected to different external loading conditions. Furthermore, computer codes developed in MATLAB software are used for the implementation of the optimization methods in the analyses. The analyses are performed with 40 randomly initialized individuals and 3000 generations. Each of the case studies is solved 30 times to reduce the possible statistical errors which may arise in association with the stochastic behavior of the optimization techniques. Also, in this study, the slice number is set equal to 20 in all the case studies.

Analyses results in this study are compared with those obtained in previous studies carried out by different researchers and summarized in tables. A comprehensive comparison of the results necessitates the use of identical assumptions and analysis methods for the same slope problem. Available results in the literature are, however, obtained by using different limit equilibrium method. This consequently might adversely affect the reliability of the comparison; however, it is believed that adequate comparisons of different metaheuristic methods can be made in terms of their accuracy as well as the overall performance. In the following sections, available information about the geometry of the case studies along with the characteristic of the soil in situ is provided in details.

4.1 Case study 1

As the first test case, a homogeneous earth slope with a simple geometry as presented in Figure 16 is considered. Information about the soil parameters of this slope is, for effective cohesion c =9.8 kN/m^3, unit weight γ =17.64 kN/m^3, residual friction angle φ =10° and the water table is not observed within the slope.

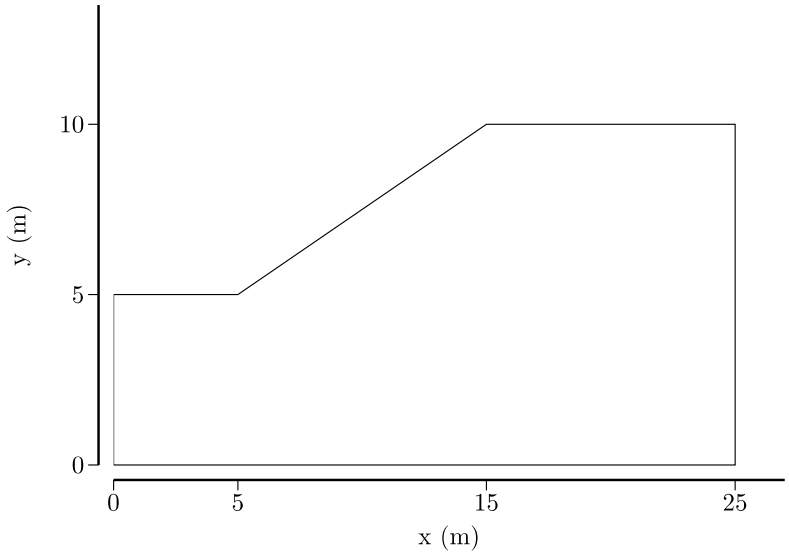

Figure 16 - Slope geometry—Example 1

Various optimization schemes are used to solve this problem, where the comparison of the results allows researchers to benchmark the performance of one optimization technique against other methods. Classical optimization methods such as the Davidon-Fletcher-Powell (DFP) method, the Broyden-Fletcher-Goldfarb-Shanno (BFGS) method, the Powell method and the simplex method, integrated with the Morgenstern-Price method (assuming interslice function, f(x)=1) are used by Yamagami and Ueta (1988) in their study to locate the noncircular failure surface in this problem. Additionally, Greco (1996) adopted the Mont-Carlo and pattern search methods to determine the minimum safety factor. This problem has also been

studied with several metaheuristic algorithms including, genetic algorithms as in Sun et al. (2008), harmony search and particle swarm techniques in Cheng et al. (2007; 2008), and ant colony optimization algorithm in the work by Kahatadeniya et al. (2009). Table 2 provides an overview of the optimum results obtained in the literature by applying different methods on this problem. It is worth mentioning that NOF in the table below refers to the overall number of evaluations performed during the analyses.

Table 2 - Result Comparison – Example 1

Study	**Method**	**Optimization Method**	**FS**	**NOF**
Yamagami (1988)	Spencer	BFGS,DFP,Powell	1.338	NA
Greco (1996)	Spencer	Monte Carlo	1.327-1.333	NA
Cheng et al. (2008)	MP	Modified HS	1.3379	10568
Cheng et al. (2006)	Spencer	PSO	1.3249	54022
Cheng et al. (2007)	Spencer	Modified PSO	1.3273	20021
Sun et al. (2008)	Spencer	GA	1.324 (line)	NA
			1.321(spline)	
Kahatadeniya et al (2009)	MP	ACO	1.311	NA
Khajezadeh et al. (2012)	MP	PSO	1.321	NA
		MPSO	1.308	NA
Kashani et al. (2014)	MP	ICA	1.3206	NA

In this study, the methods introduced in the previous chapters are properly implemented to assess the stability of this case study. While the application of the most popular optimization methods on this problem results in reasonable approximations for the factor of safety against failure, lower FS value for HABCDE proves its superiority over other techniques (Table 3). According to the Table 3, an optimum safety factor of 1.328 is obtained in 50th iteration. More critical slip surface can be located by continuing the analyses up to a higher number of iterations, say 250, in which a failure surface possessing a FS value of 1.324 is obtained.

Table 3 - Results of this study—Example 1

	Iteration			
Method	**50**	**250**	**750**	**3000**
ABC	1.364786	1.336126	1.328142	1.325433
DE	1.354253	1.339867	1.334564	1.327605
GA	1.333774	1.32692	1.326453	1.325885
GOA	1.339832	1.336682	1.32741	1.325197
HABCDE	**1.32883**	**1.324999**	**1.324212**	**1.324108**
HS	1.443136	1.391691	1.33782	1.326653
LHS	1.331135	1.327289	1.326331	1.325309
PSO	1.342849	1.338558	1.3288	1.325527

Comparison of the rates at which the implemented methods converge to their optimum values demonstrate that almost all the methods reach nearly similar values at the end of the analyses (Figure 17a). However, both the HS and the DE methods represent a relatively weaker performance resulting in higher factor of safety values for the case of study. Convergence to near-optimal values within a few successive iterations is the feature which distinguishes the best optimization method from others. For better illustration, consider the convergence rate of the PSO and LHS methods in Figure 17a; while no significant difference is observed in the obtained FS values, fast convergence of the LHS method makes it a more favorable method of analysis.

In addition, a closer look into the convergence history of the three recent optimization methods proposed in this study indicates that HABCDE outperforms the competition in terms of both convergence rate and precision, as illustrated in Figure 17b. Furthermore, GOA ranks second according to the factor of safety value, although in the earlier iterations, LHS demonstrates better performance in terms of rate of convergence considering its capability in obtaining comparatively better optimized values within less computational efforts.

In order to gain a better insight into the performance of the optimization algorithms, convergence history of each method is also illustrated in separate figures (see Appendix A).

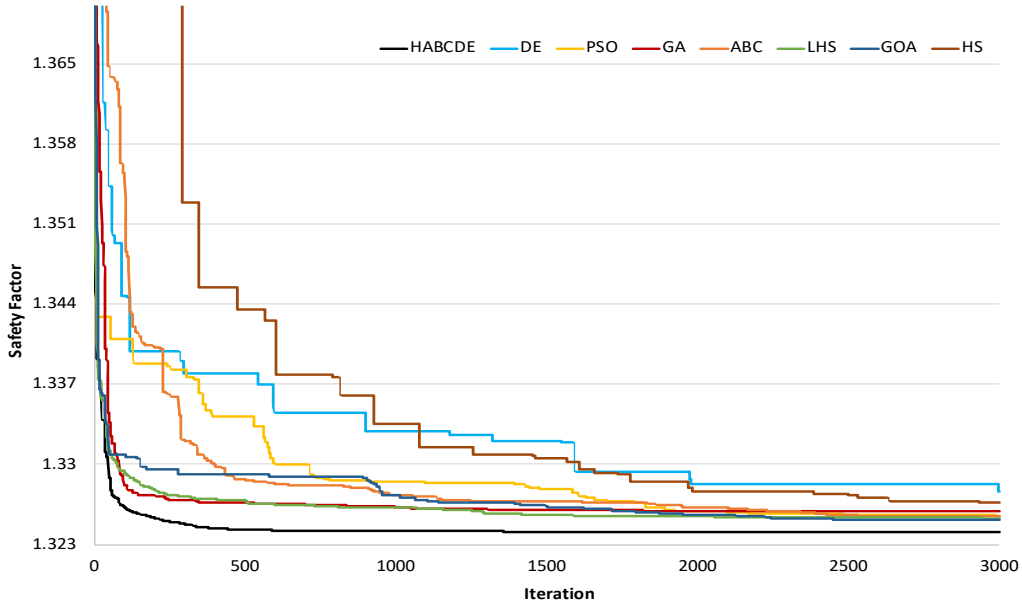

(a)

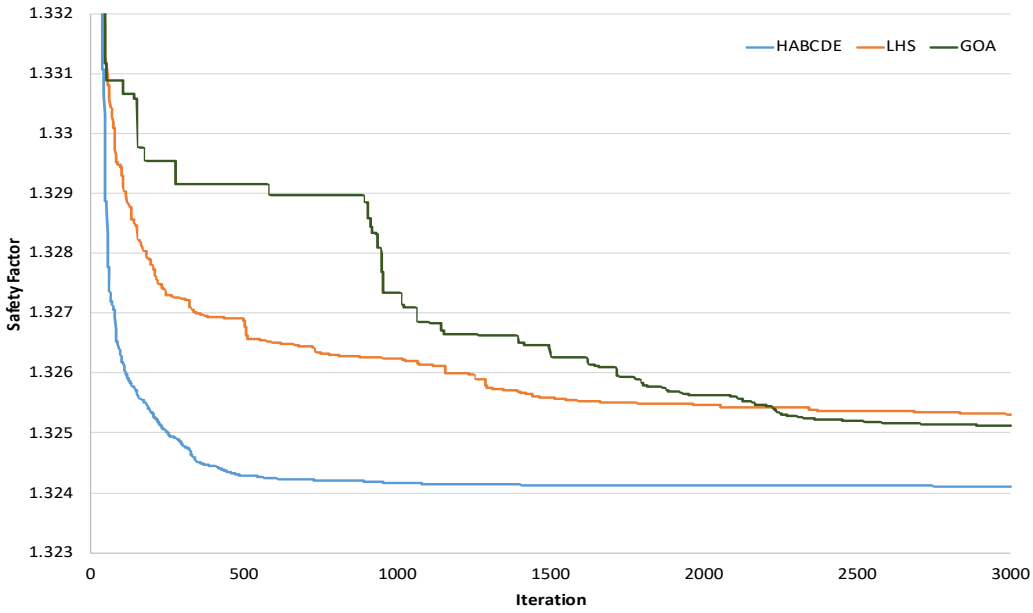

(b)

Figure 17 - Comparison of the convergence rates -- Example 1 (a) all the methods (b) proposed methods

Furthermore, in Figure 18, the critical slip surfaces associated with the implemented methods are displayed graphically. From this figure, the sensitivity of the safety factor to slight changes in the location of the failure surface can be readily inferred.

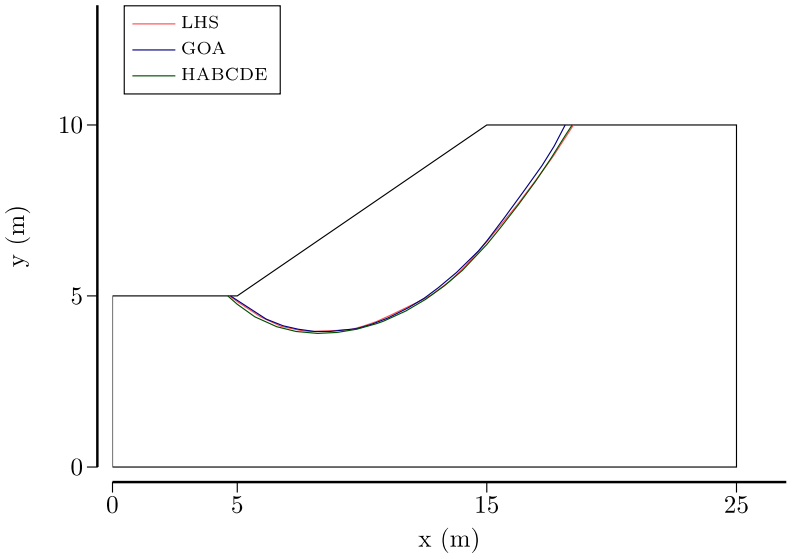

Figure 18 - Critical Slip Surfaces -- Example 1

4.2 Case study 2

In the second case, a non-homogeneous earth slope comprising four layers of different soil properties which is first proposed by Zolfaghari et al. (2005), is considered. Figure 19 illustrates the slope geometry and Table 4 indicates the soil parameters of each layer, independently. Presence of the low-resistant soil layer in the slope profile makes it a challenging optimization problem attributable to various local optimum points existing in the search space, and consequently, determination of the expected slip surface entirely depends on the ability of the optimization techniques in evading these local minima.

Table 4 - Soil Parameters – Example 2

Soil Parameters	**Layer 1**	**Layer 2**	**Layer 3**	**Layer 4**
C (kN/m^2)	14.7	16.7	4.9	34.3
φ $(degrees)$	20	21	10	28
γ (kN/m^3)	18.63	18.63	18.63	18.63

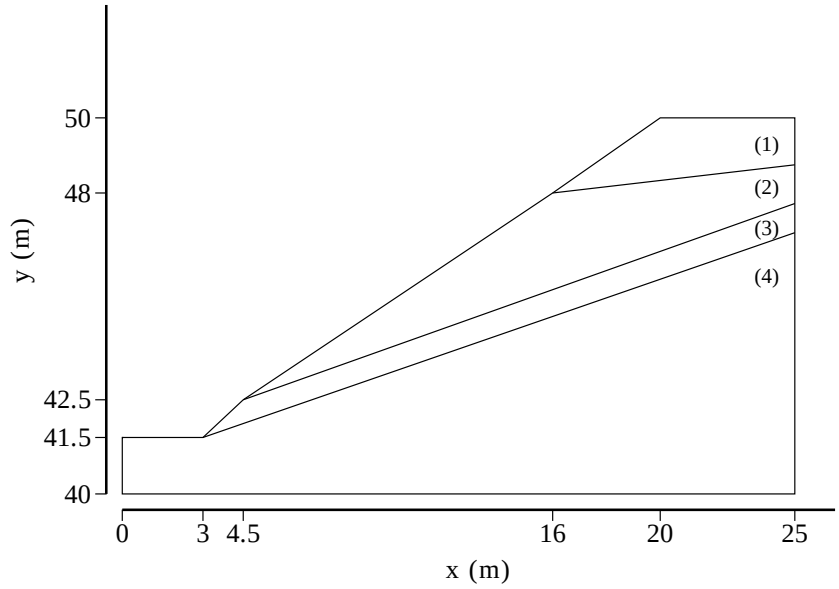

Figure 19 - Geometry of Slope – Example 2

Various optimization algorithms are employed to solve this test problem, including a simple form of genetic algorithm combined with Morgenstern-Price method in Zolfaghari et al. (2005), modified PSO and modified HS, Ant Colony Optimization method and Real-coded GA in the studies done by Cheng et al. (2007) and Cheng et al. (2008) and Kahatadeniya et al. (2009) and Li et al. (2010), respectively.

Table 5 provides an overview of the optimum results obtained in the literature by applying different methods on this problem.

Table 5 - Result comparison—Example 2

Study	Method	Optimization Method	FS	NOF
Zolfaghari et al. (2005)	MP	Simple GA	1.24	NA
Cheng et al. (2006)	Spencer	PSO	1.1095	119,940
Cheng et al. (2006)	Spencer	MPSO	1.1174	15,925
Cheng et al. (2006)	Spencer	SA	1.1789	54,326
Cheng et al. (2006)	Spencer	SHM	1.2512	29,692
Cheng et al. (2006)	Spencer	MHM	1.1509	32,418
Cheng et al. (2006)	Spencer	Tabu	1.4714	30,418
Sarma and Tan (2006)	Sarma	Sarma's(2000) Program	1.091	NA
Cheng et al. (2007b)	Spencer	Modified PSO	1.1139	24330
Cheng et al. (2008a)	MP	Modified HS	1.24	16968
Khajezadeh et al. (2014)	MP	Imperialistic competitive algorithm	1.0642	NA
Gandomi et al. (2014)	MP	Levy-flight krill herd	1.0579	150000

In this study, the methods introduced in the previous chapters are also utilized in evaluating the FS value for this slope problem. Table 6 and Figure 20 represent a summary of the obtained results and the rate of convergence corresponding to the implemented methods, respectively.

Table 6 - Results of this study—Example 2

	Iteration			
Method	**50**	**250**	**750**	**3000**
ABC	1.195945	1.143791	1.130091	1.096879
DE	1.146035	1.107374	1.099355	1.090039
GA	1.146816	1.130846	1.1037	1.098585
GOA	**1.118573**	1.100305	1.093879	1.091733
HABCDE	1.119918	**1.093996**	**1.093067**	**1.088924**
HS	1.425048	1.367045	1.166839	1.104455
LHS	1.136886	1.135185	1.120741	1.095613
PSO	1.145621	1.132767	1.100862	1.100862

Comparison of the results obtained in this optimization problem indicates that HABCDE outdoes its conventional counterparts in terms of accuracy and convergence rate. According to the Table 6, an optimum safety factor of 1.119 is obtained in 50^{th} iteration. Continuing the analyses up to a higher number of iterations, say 250 and 3000, yields failure surfaces possessing safety factors equal to 1.093 and 1.088, respectively.

Comparison of the rates at which the implemented methods converge to their optimum values demonstrate that not all the implemented methods are capable of determining the lowest factor of safety (most critical slip surface) for this case of study (Figure 20a). Investigation of the results indicate that the HS and the PSO methods represent a relatively weaker performance resulting in higher factor of safety values for this case of study. The LHS, the ABC and the GA methods yield nearly similar values at the end of the analyses. Although fast convergence of the GA method makes it a more favorable method, optimized factor of safety value obtained by using LHS method proves its superior performance in a reliable slope stability analysis.

In addition, a closer look into the convergence history of the three recent optimization methods proposed in this study indicates that HABCDE outperforms the competition in terms of both convergence rate and precision, as illustrated in Figure 20b. In this comparison, GOA ranks second according to the factor of safety value, and the LHS method demonstrates the worst performance in terms of both convergence rate and the factor of safety value.

In order to gain a better insight into the performance of the optimization algorithms, convergence history of each method is also illustrated in separate figures (see Appendix A).

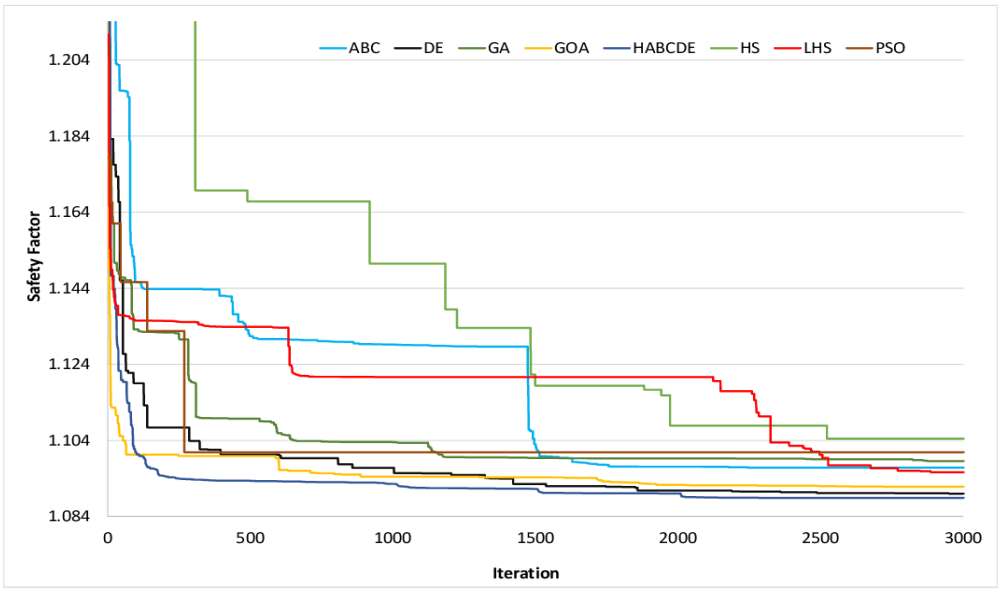

(a)

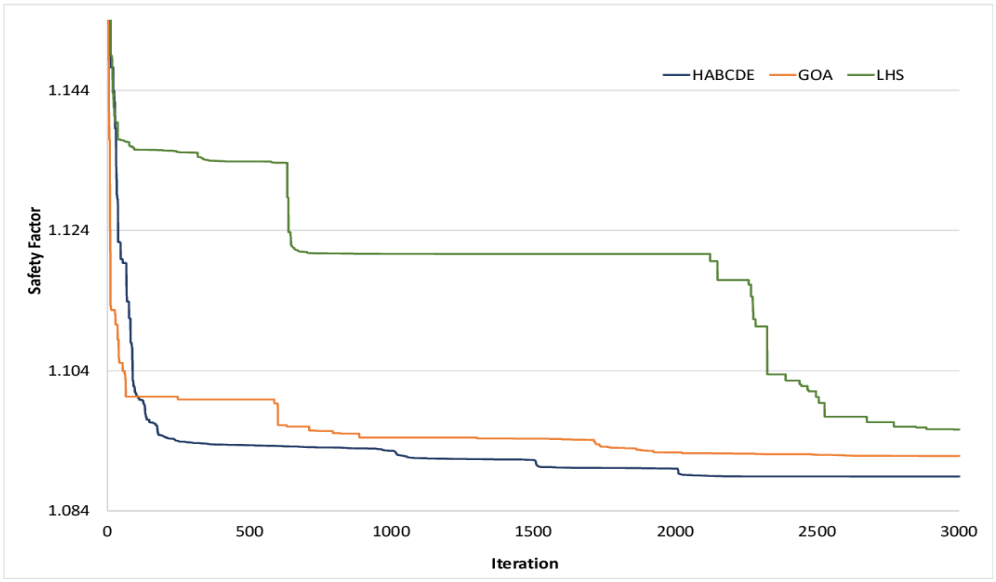

(b)

Figure 20 - Comparison of the convergence rates -- Example 2 (a) all the methods (b) proposed methods

Additionally, the critical slip surfaces associated with the implemented methods are depicted graphically in Figure 21. From this figure, it can be observed that the failure surface extends to a surface at the weakest layer in the soil profile.

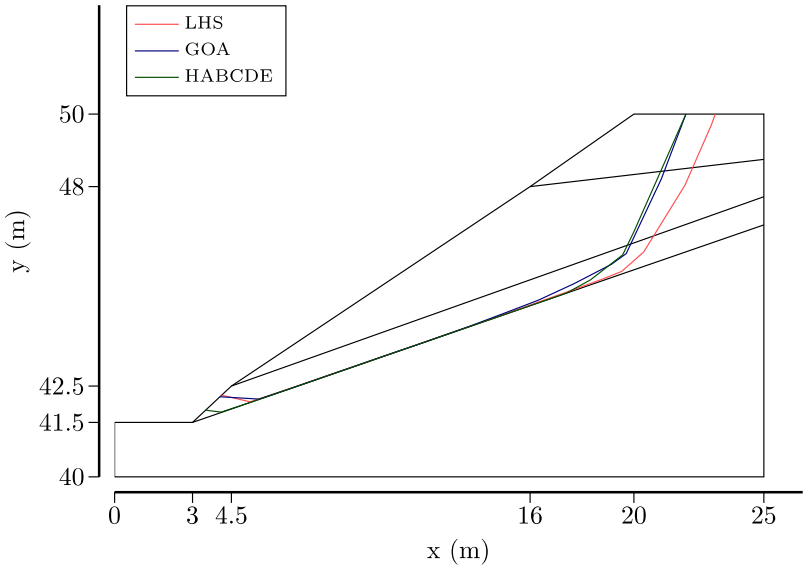

Figure 21 - Critical Slip Surfaces -- Example 2

4.3 Case study 3

The third test problem concerns a three-layered heterogeneous earth slope with a non-horizontal stratification, which is first introduced in ACADS (Donald & Giam, 1989) study. The slope profile consists of soils with different properties which are detailed in Table 7 below. This problem is analyzed with and without considering the destructive effect of earthquake (case (1) and case (2), respectively) on the stability in two separate cases. In this regard, a value of 0.1 is considered for the horizontal seismic coefficient of the earthquake loading acting on the soil mass.

Table 7 - Soil parameters—Example 3

Soil Parameters	**Layer 1**	**Layer 2**	**Layer 3**
C $(\boldsymbol{kN/m^2})$	0.0	5.3	7.2
$\boldsymbol{\varphi}$ $(\boldsymbol{degrees})$	38	23	20
$\boldsymbol{\gamma}$ $(\boldsymbol{kN/m^3})$	19.5	19.5	19.5

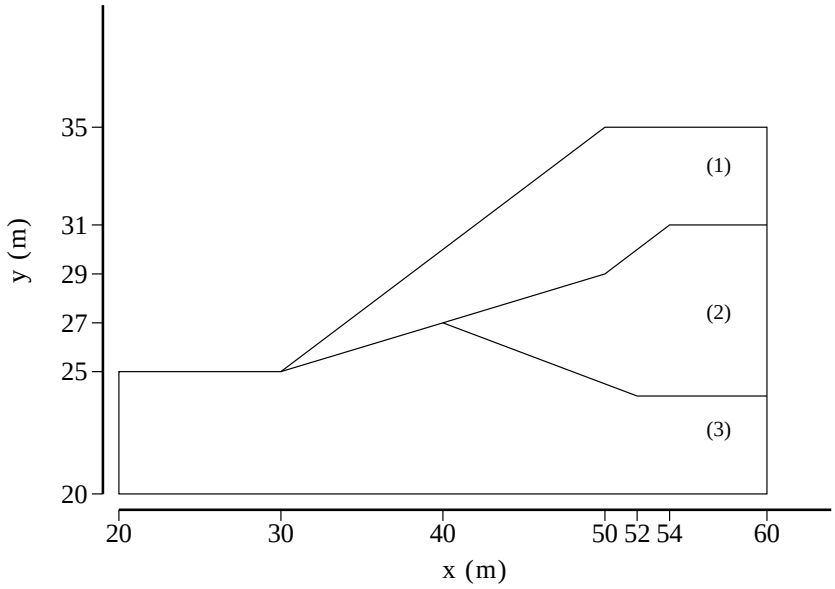

Figure 22 - Geometry of Slope—Example 3

Multiple optimization methods have been confidently applied to this problem, which includes GAs as in the study by Goh (2000) and the Leap-Frog method which was employed by Bolton et al. (2003) to the same problem. Later, several well-applied techniques including Simple Harmony Search algorithm (SHM), Modified Harmony Search algorithm (MHM), Tabu Search method, Simulated Annealing algorithm (SA), Genetic Algorithms, Particle Swarm Optimization algorithm (PSO) and Ant-Colony algorithm were tested in the study by Cheng et al. (2007).

Table 8 provides an overview of the optimum results obtained in the literature by applying different methods on this problem.

Table 8 - Result comparison—Example 3

Study	**Method**	**Optimization Method**	**FS**	**NOF**
Cheng et al. (2006)	Spencer	SA	1.3569	74120
Cheng et al. (2006)	Spencer	GA	1.3582	39088
Cheng et al. (2006)	Spencer	PSO	1.3591	60000
Cheng et al. (2006)	Spencer	SHM	1.3596	106237
Cheng et al. (2006)	Spencer	MHM	1.3587	41059
Cheng et al. (2006)	Spencer	Tabu search	1.3762	44168
Cheng et al. (2006)	Spencer	Ant-Colony	1.3931	76200
Bolton et al. (2002)	Spencer	Leap-frog	1.359	Unknown
Goh (2000)	Spencer	GA	1.387	Unknown
Wei Gao (2015)	Spencer	Meeting Ant Colony	1.348	Unknown

Besides, the results in Table 9 and Table 10 represent the safety factors obtained by applying the proposed methods of optimization on cases (1) and (2), respectively. Rate of the convergence corresponding to the implemented methods are also represented graphically in separate figures (see Appendix A). For both of the cases, amongst the methods used in both cases, HABCDE proved very powerful in terms of overall performance, i.e. rate of convergence and precision.

Table 9 - Results of this study—Example 3, Case (1)

	Iteration			
Methods	**50**	**250**	**750**	**3000**
ABC	1.380262	1.366905	1.362523	1.359061
DE	1.381753	1.372657	1.365299	1.35807
GA	1.365557	1.359677	1.358434	1.358153
GOA	1.392262	1.369703	1.365632	1.358615
HABCDE	**1.363444**	**1.358358**	**1.357979**	**1.357765**
HS	1.487626	1.443304	1.370094	1.361191
LHS	1.365658	1.359866	1.359753	1.359157
PSO	1.404648	1.393505	1.375095	1.375095

According to Table 9, an optimum safety factor of 1.363 is obtained in 50^{th} iteration. In successive iterations, the value of safety factor decreases continuously, where performing 250 and 750 iterations of this process yields failure surfaces possessing safety factors equal to 1.358 and 1.357, respectively.

Comparison of the rates at which the implemented methods converge to their optimum values demonstrate that for both the case (1) and case (2), all the methods

except the PSO and the HS reach nearly similar values at the end of the analyses (Figure 23a and Figure 25a). The PSO method for both of the cases fails to obtain an appropriate value. Similarly, HS method represent a relatively weaker performance resulting in higher factor of safety values, particularly in the case (2) where relatively high computational efforts is required to reach a reasonable result for the case of study.

For the remaining methods, however, no significant difference is observed in the obtained FS values and therefore, performance of the methods can be evaluated in terms of their rate of convergence. For better illustration, consider the convergence rate of the ABC and the DE methods in Figure 25a. Lower FS values obtained over the same number of iterations proves the superiority of the ABC method over the DE algorithm.

In addition, a closer look into the convergence history of the three recent optimization methods proposed in this study indicates that HABCDE outperforms the competition in terms of both convergence rate and precision for both of the cases, as illustrated in Figure 23b and Figure 25b. Similarly, for both of the cases, GOA ranks second according to the factor of safety value, and the LHS method demonstrates the worst performance. In terms of convergence rate, however, LHS performs better in the case (1) while for the case (2) GOA proves successful.

In order to gain a better insight into the performance of the optimization algorithms, convergence history of each method is also illustrated in separate figures (see Appendix A).

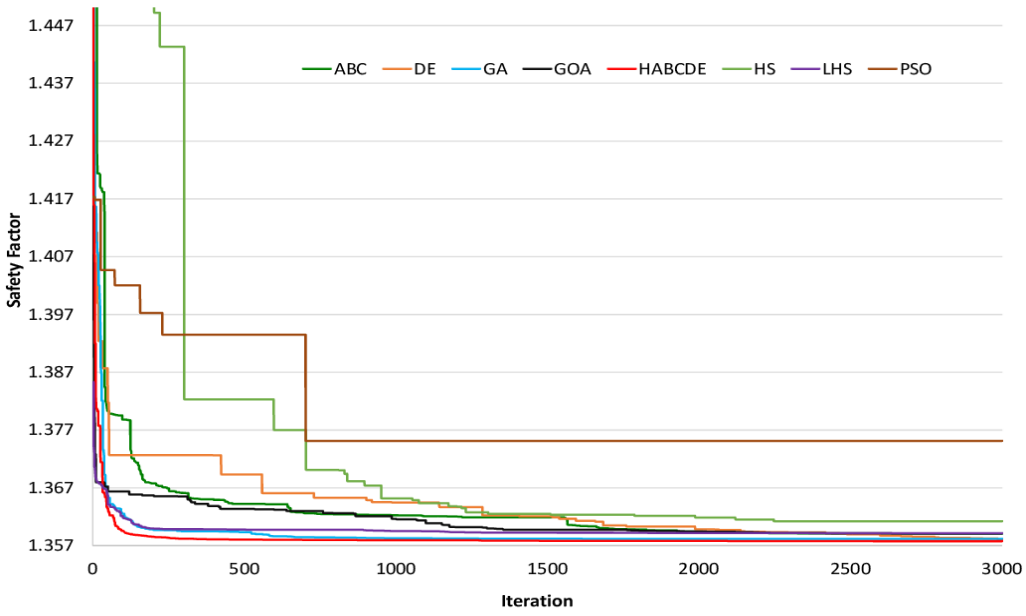

(a)

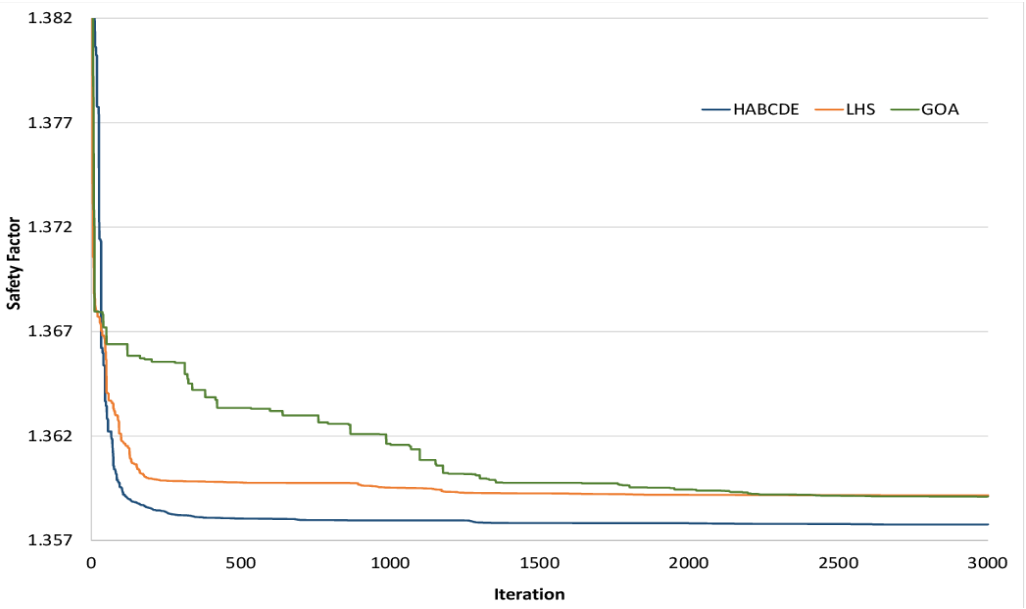

(b)

Figure 23 - Comparison of the convergence rates -- Example 3, Case (1)

(a) all the methods (b) proposed methods

Additionally, the critical slip surfaces associated with the implemented methods are depicted graphically in Figure 24. From this figure, it can be observed that the critical failure surfaces determined by using LHS and GOA methods are almost identical.

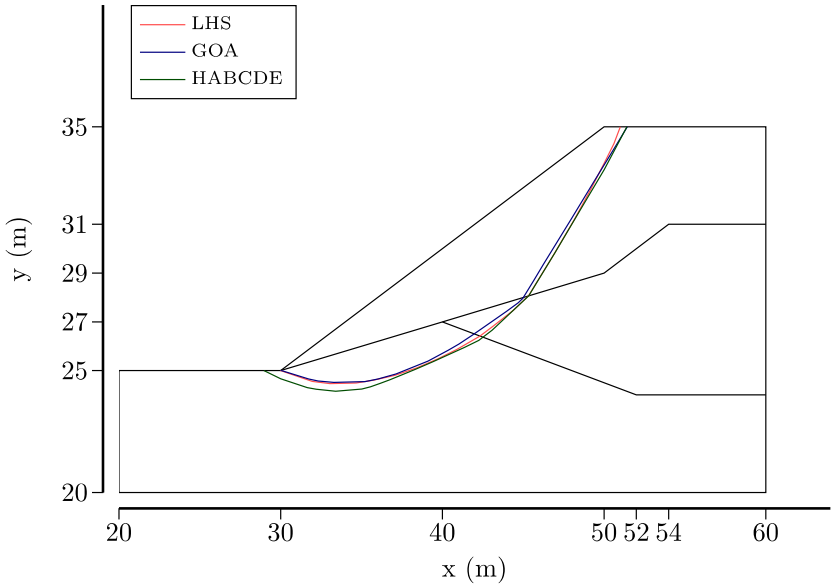

Figure 24 - Critical Slip Surfaces —Example 3, Case (1)

Likewise, Table 10 represents the safety factors obtained by applying the proposed methods of optimization on case (2). As with the case (1), HABCDE method yields more optimal results for this problem. According to Table 10, an optimum safety factor of 1.002 is obtained in 50^{th} iteration. In successive iterations, the value of safety factor decreases continuously, where performing 750 and 3000 iterations of this process yields failure surfaces possessing safety factors equal to 0.977 and 0.976, respectively.

Table 10 - Results of this study—Example 3, Case (2)

	Iteration			
Methods	**50**	**250**	**750**	**3000**
ABC	0.99717	0.980165	0.979288	0.979288
DE	1.020548	0.991459	0.98603	0.979214
GA	1.011537	0.983481	0.978353	0.977911
GOA	0.995375	**0.978401**	0.977525	0.977525
HABCDE	**1.002134**	0.978964	**0.977046**	**0.976773**
HS	1.05532	1.047549	1.010335	0.984624
LHS	1.043134	1.02188	1.02188	0.981427
PSO	1.023048	1.00648	1.003268	0.992467

Furthermore, visual comparison of the critical failure surfaces from applied methods is also represented in Figure 26. As can be inferred from this figure the failure surface passes through the weakest soil layer in the slope profile.

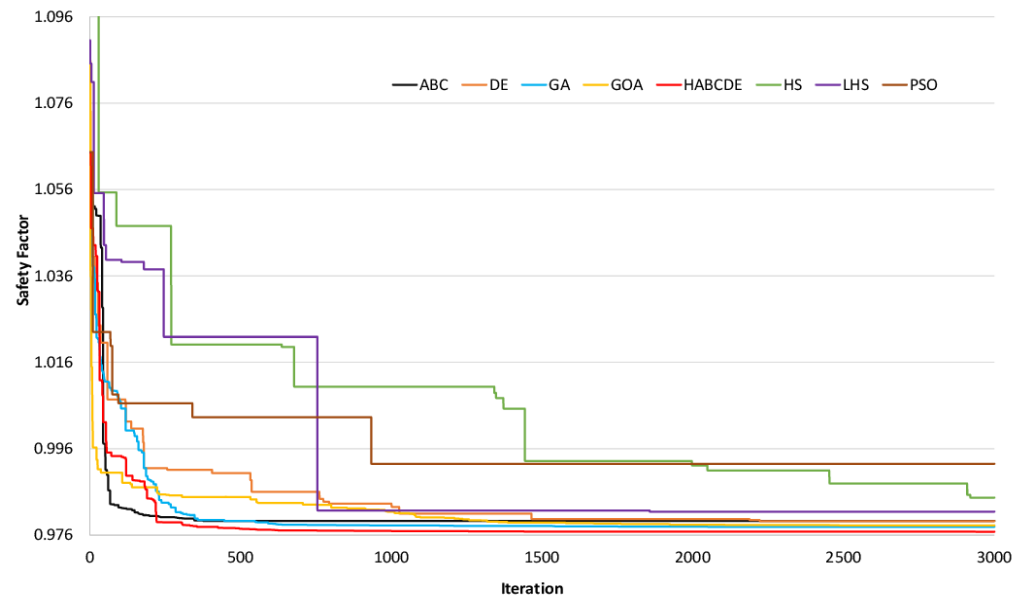

(a)

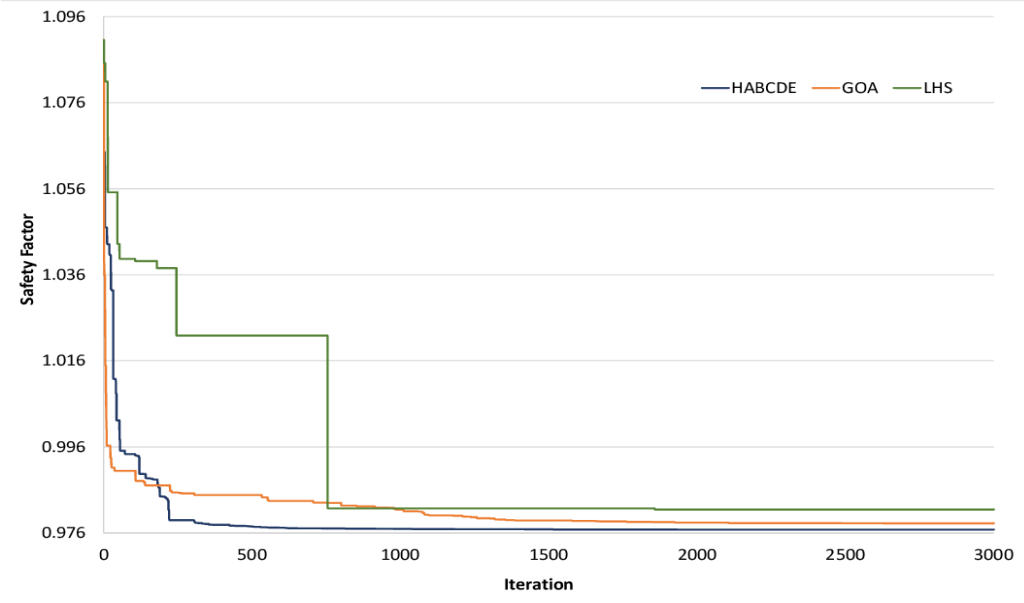

(b)

Figure 25 - Comparison of the convergence rates -- Example 3, Case (2)
(a) all the methods (b) proposed methods

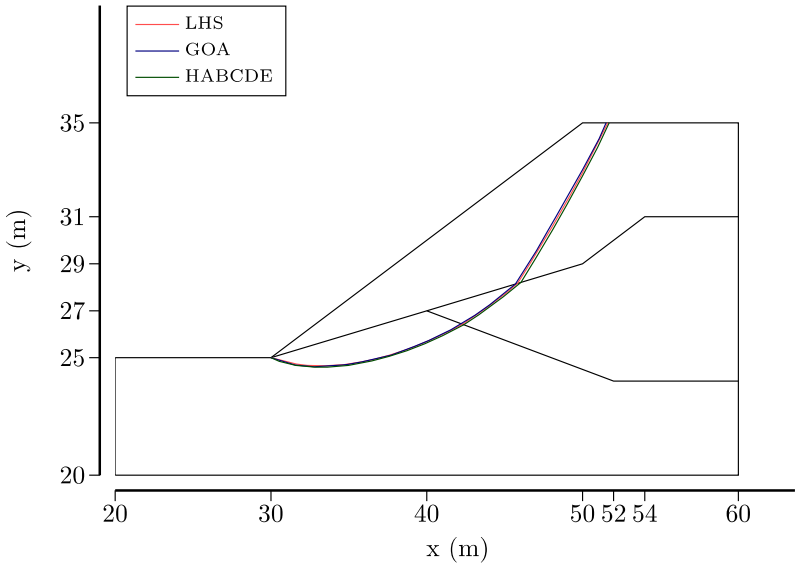

Figure 26 - Critical Slip Surfaces —Example 3, Case (2)

4.4 Case Study 4

Details of the cross-section of a multilayered earth slope is given in the Figure 27. Stability of this slope against sliding was primarily investigated by Zolfaghari et al. (2008) using Morgenstern-Price method integrated with GA optimization technique, given the soil strength parameters outlined in Table 11. In this regard, four different loading conditions involving water table and earthquake forces were considered:

- Case (1): No water pressure, No earthquake
- Case (2): Water pressure, No earthquake
- Case (3): No water pressure, Earthquake
- Case (4): Water pressure, Earthquake

In addition, a value of 0.1 is considered for the horizontal seismic coefficient of the earthquake loading acting on the soil mass.

In an effort to enhance the accuracy of stability assessment various optimization methods have been acceptably applied to this problem; in a study which set out to

identify the critical slip surface in the slope, Cheng et al. (2006) used particle swarm optimization (PSO) method in the analyses.

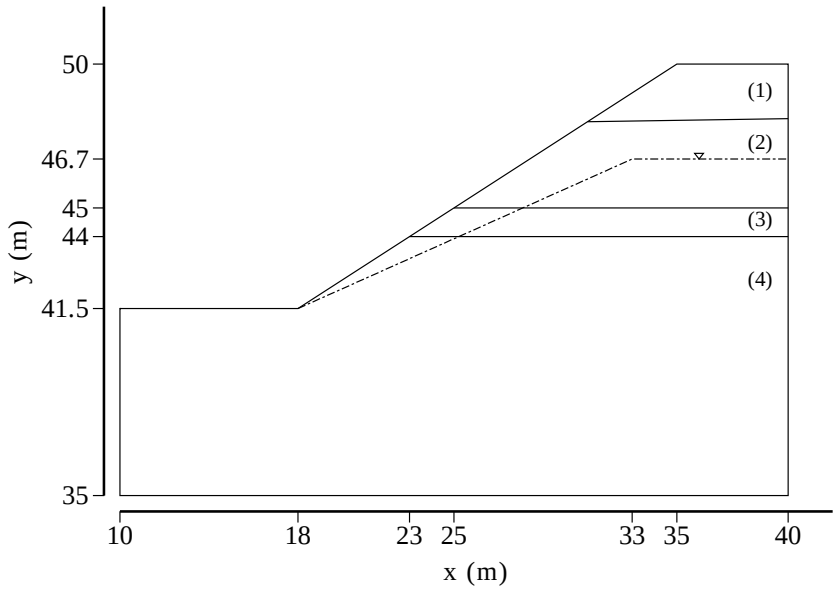

Figure 27 - Geometry of the slope – Example 4

Table 11 - Soil Parameters – Example 4

Soil Parameters	**Layer 1**	**Layer 2**	**Layer 3**	**Layer 4**
C $(\boldsymbol{kN/m^2})$	14.7	16.7	4.9	34.3
$\boldsymbol{\varphi}$ $(\boldsymbol{degrees})$	20	21	10	28
$\boldsymbol{\gamma}$ $(\boldsymbol{kN/m^3})$	18.63	18.63	18.63	18.63

In another major study, Cheng et al. (2007) adopted six different global optimization approaches to evaluate their performance in locating the surface with the smallest safety factor. Likewise, Kahatadenya et al. (2009) and Khajezadeh et al. (2012) applied the ant colony optimization (ACO) and a modified particle swarm

optimization method (MPSO) to this case problem, respectively. Table 12 provides an overview of the optimum results obtained in the literature by applying different methods to this problem.

Table 12 - Result Comparison – Example 4

Study	**Method**	**Optimization Method**	**Case (1)**	**Case (2)**	**Case (3)**	**Case (4)**	
Zolfaghari et al. (2005)	Spencer	GA	1.48	1.36	1.37	0.98	FS
			---	---	---	---	NOF
Cheng et al. (2006)	Spencer	SA	1.3961	1.2837	1.1333	1.0081	FS
			135560	106742	108542	111386	NOF
		GA	1.3733	1.2324	1.0675	0.9631	FS
			63562	77178	98332	84272	NOF
		PSO	1.3372	1.2100	1.0474	0.9451	FS
			62800	83400	69600	68600	NOF
		SHM	1.3729	1.2326	1.0733	0.9570	FS
			172464	126445	99831	212160	NOF
		MHM	1.3501	1.2247	1.0578	0.9411	FS
			32510	40697	40476	33236	NOF
		Tabu search	1.4802	1.3426	1.1858	1.0848	FS
			58588	59790	63796	65398	NOF
		Ant-colony	1.5749	1.4488	1.3028	1.1372	FS
			100200	102600	109800	112200	NOF
Cheng et al. (2007)	Spencer	Modified PSO	1.3490	1.2203	1.0592	0.9441	FS
			14874	20722	14227	16835	NOF
		PSO	1.3323	1.1985	1.0465	0.9225	FS
			143919	114865	122744	160060	NOF
Kahatadeniya et al. (2009)	MP	ACO	1.501	1.377	1.091	0.846	FS
			---	---	---	---	NOF

Table 12 (Continued)

Khajezadeh et al. (2012)	MP	PSO	1.334	1.203	1.065	0.932	FS
			---	---	---	---	NOF
		MPSO	1.331	1.171	1.051	0.897	FS
			---	---	---	---	NOF

In this study, the methods introduced in the previous chapters are also utilized in evaluating the FS value for this slope problem. Table 13 and Figure 28 to Figure 31 represent a summary of the obtained results and the rate of convergence corresponding to the implemented methods, respectively.

Table 13 - Results of this study—Example 4

Optimization Method	**Factor of Safety**				**Iteration**
	Case (1)	**Case (2)**	**Case (3)**	**Case (4)**	
ABC	1.410720429	1.681255441	1.364932736	1.389854816	**50**
	1.362293174	1.253603878	1.124045665	1.072036673	**250**
	1.351134965	1.234987359	1.064676496	0.957927888	**750**
	1.339492869	1.229526378	1.047751462	0.954245906	**3000**
DE	1.403957332	1.269518087	1.124766231	0.998863957	**50**
	1.345473285	1.241309334	1.066128511	0.970215949	**250**
	1.339745834	1.23362373	1.05269343	0.95569369	**750**
	1.334658849	1.227916373	1.044939892	0.952351134	**3000**

Table 13 (Continued)

GA	1.39091611	1.295484271	1.111094569	1.131368189	**50**
	1.344271501	1.234649087	1.06342718	0.962517243	**250**
	1.338035169	1.231938028	1.049864132	0.954462111	**750**
	1.336644983	1.22971306	1.047404092	0.953760567	**3000**
GOA	1.375194098	1.269721422	1.07882198	0.98383909	**50**
	1.365378812	1.245432284	1.068523814	0.97747544	**250**
	1.344094069	1.231486596	1.058259522	0.955586733	**750**
	1.3358016	1.227739857	1.047504959	0.953976631	**3000**
HABCDE	**1.342845108**	1.345520116	**1.055651254**	**0.969561665**	**50**
	1.334481215	**1.229676026**	**1.044547922**	**0.953873421**	**250**
	1.333239328	**1.227534324**	**1.043263764**	0.95236442	**750**
	1.332841264	**1.22604568**	1.043026851	0.950764072	**3000**
HS	2.446834253	1.692717901	2.130021617	2.165308293	**50**
	1.656123408	1.572059319	1.153395619	1.757718165	**250**
	1.361398095	1.270347238	1.151045628	1.027528563	**750**
	1.339921034	1.234730702	1.056873855	0.967521291	**3000**
LHS	1.357693435	**1.239245752**	1.248068043	1.076767521	**50**
	1.351693315	1.233903188	1.065324551	0.965141849	**250**
	1.351170637	1.232030396	1.049893843	**0.951786266**	**750**
	1.336827587	1.230801909	**1.042758288**	**0.950457457**	**3000**

Table 13 (Continued)

PSO	1.365115673	1.27629403	1.101792138	1.007369006	**50**
	1.365115673	1.27629403	1.082553274	0.976929267	**250**
	1.365115673	1.274486391	1.076631359	0.973040128	**750**
	1.36168701	1.254869993	1.065205964	0.969434701	**3000**

Comparison of the results obtained in this optimization problem indicates that HABCDE and LHS outdo their conventional counterparts in terms of accuracy and convergence rate. In this regard, HABCDE method yields the best results for the cases (1) and (2). In the third and fourth case, however, the optimum solution is obtained by LHS method, although HABCDE represents more satisfactory performance over the earlier iterations.

For better illustration, let us consider the values obtained by the HABCDE method in the stability analysis of the case (1). According to the Table 13, an optimum safety factor of 1.3428 is obtained in 50^{th} iteration. Continuing the analyses up to a higher number of iterations, say 250 and 3000, yields failure surfaces possessing safety factors equal to 1.3344 and 1.3328, respectively.

In this case of study as well, comparison of the rates at which the implemented methods converge to their optimum values demonstrate that for both the case (1) and case (2), the PSO method yields the worst solution for the problem. Similarly, ABC and HS methods fail to obtain an appropriate factor of safety value, particularly in the case (1) where relatively high computational efforts are required to reach a reasonable result for the case of study. Nevertheless, ABC shows a better performance in the case (2) resulting in a value close to the optimum solution.

For the remaining methods, however, no significant difference is observed in the obtained FS values and therefore, performance of the methods can be evaluated in

terms of their rate of convergence. For better illustration, let us consider the convergence rate of the ABC and the GA methods in the case (2). As represented in Figure 29a, for both ABC and GA the ultimate factor of safety values are of similar quantity, while obtaining lower values at the earlier iterations of the GA method proves its superiority over the ABC algorithm.

In addition, a closer look into the convergence history of the three recent optimization methods proposed in this study indicates that HABCDE outperforms the competition in terms of both convergence rate and precision for both case (1) and (2), as illustrated in Figure 28b and Figure 29b. Additionally, GOA ranks second according to the overall performance of the methods, i.e. accuracy of the factor of safety value and the rate of convergence, although LHS performs more favorably during the initial assessments.

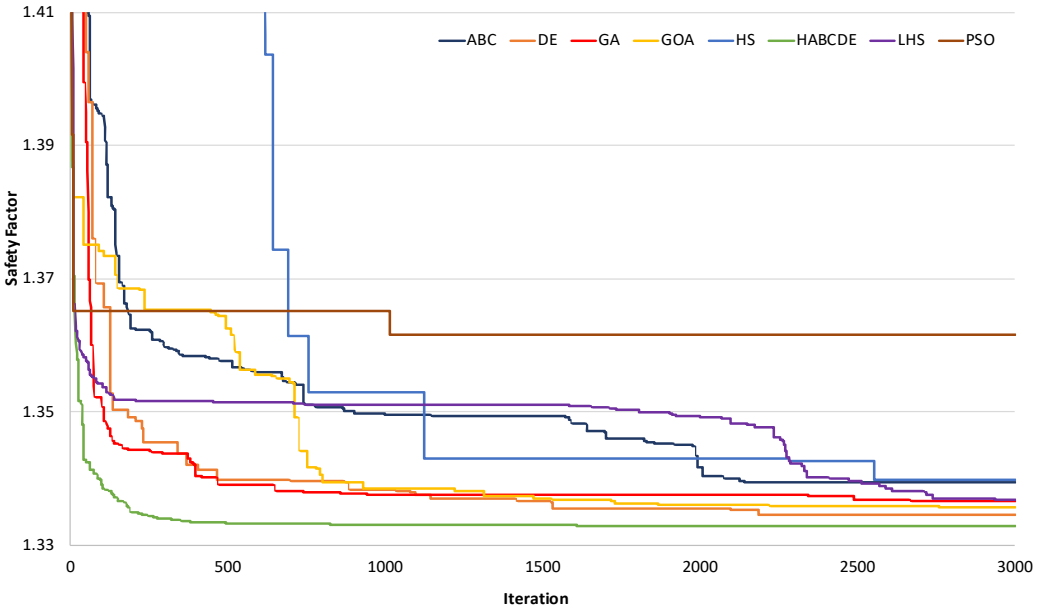

(a)

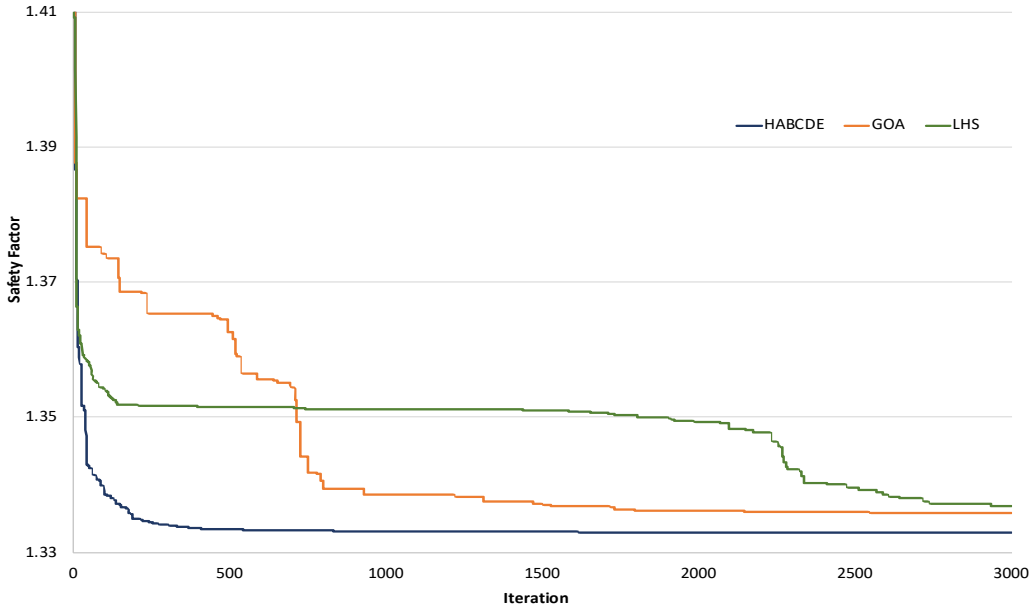

(b)

Figure 28 Comparison of the convergence rates -- Example 4, Case (1)
(a) all the methods (b) proposed methods

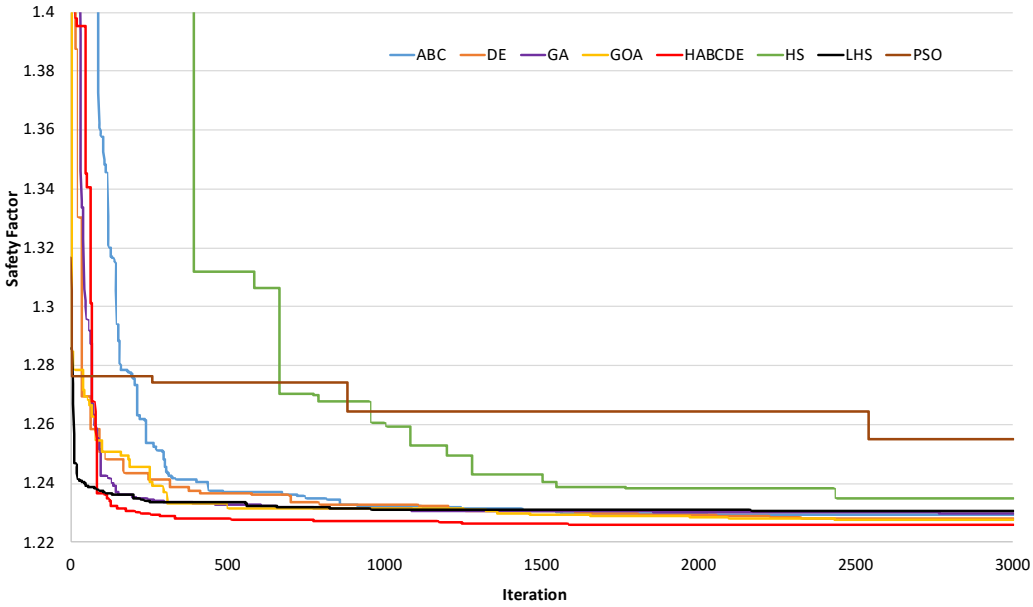

(a)

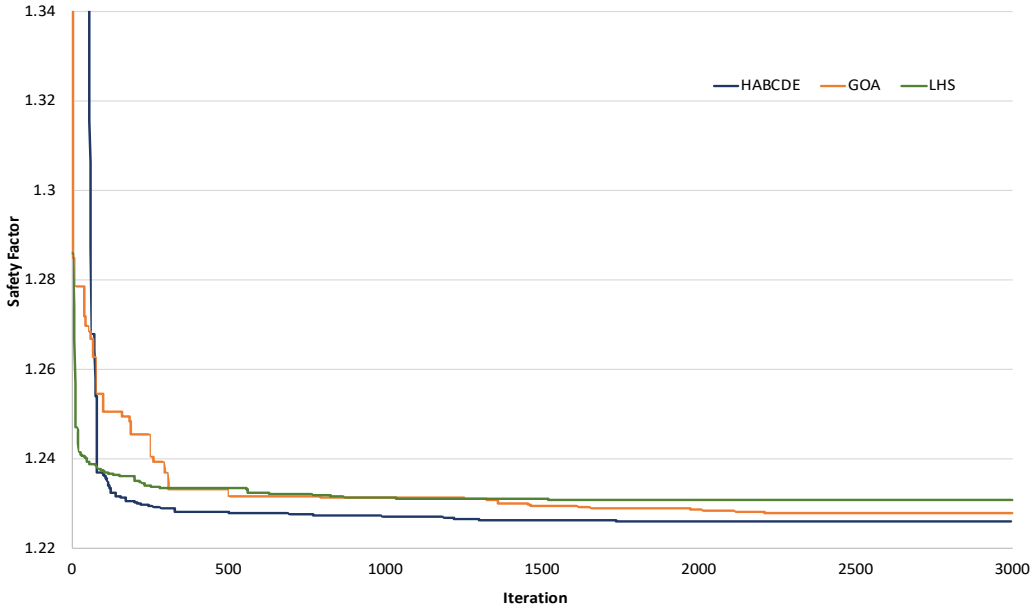

(b)

Figure 29 - Comparison of the convergence rates -- Example 4, Case (2)

(a) all the methods (b) proposed methods

In the case (3) and (4), likewise, comparison of the rates at which the implemented methods converge to their optimum values demonstrate that the PSO method yields the worst solution for the problem. Similarly, HS method fails to obtain an appropriate factor of safety value, particularly in the case (3) where relatively high computational efforts are required to reach a reasonable result for the case of study.

For the remaining methods, however, no significant difference is observed in the obtained FS values and therefore, performance of the methods can be evaluated in terms of their rate of convergence. For better illustration, let us consider the convergence rate of the ABC and the GA methods in the case (4). As represented in Figure 31a, for both ABC and GA the ultimate factor of safety values are of similar quantity, while obtaining lower values at the earlier iterations of the GA method proves its superiority over the ABC algorithm.

In addition, a closer look into the convergence history of the three recent optimization methods proposed in this study indicates that LHS outperforms the competition in terms of the accuracy, as illustrated in Figure 30b and Figure 31b. Even though LHS yields a relatively better optimized solution at the end of the analyses, overall HABCDE represents more satisfactory performance as far as the convergence rate of the methods is considered. Additionally, GOA method results in relatively higher objective values and thus cannot function appropriately for both case (3) and (4).

In order to gain a better insight into the performance of the optimization algorithms, convergence history of each method is also illustrated in separate figures (see Appendix A).

Additionally, for each case study the critical slip surfaces associated with the implemented methods are depicted graphically in Figure 32. From this figure it can be observed that the failure surface extends to a surface at the weakest layer in the soil profile.

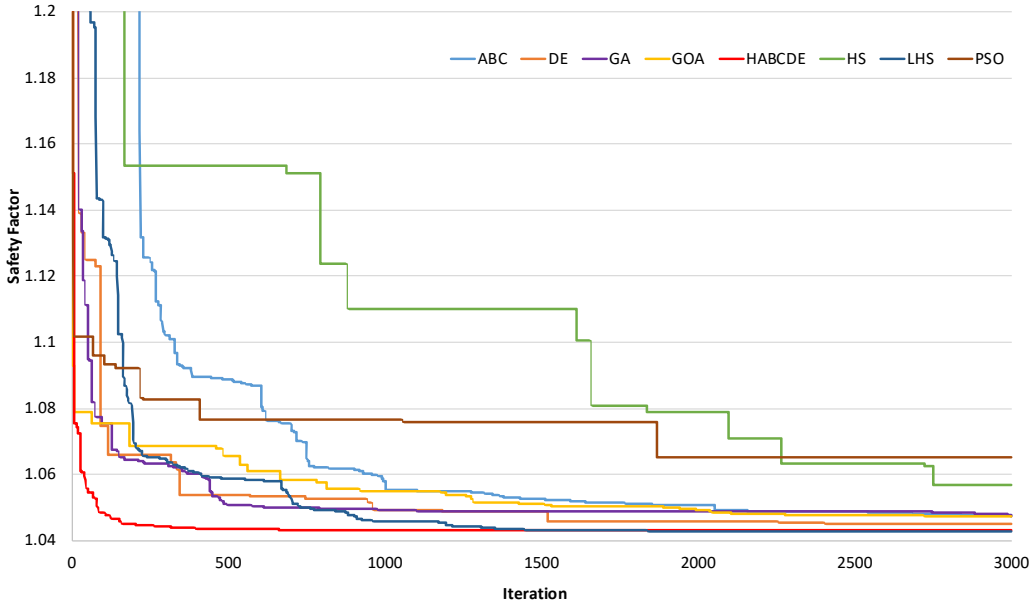

(a)

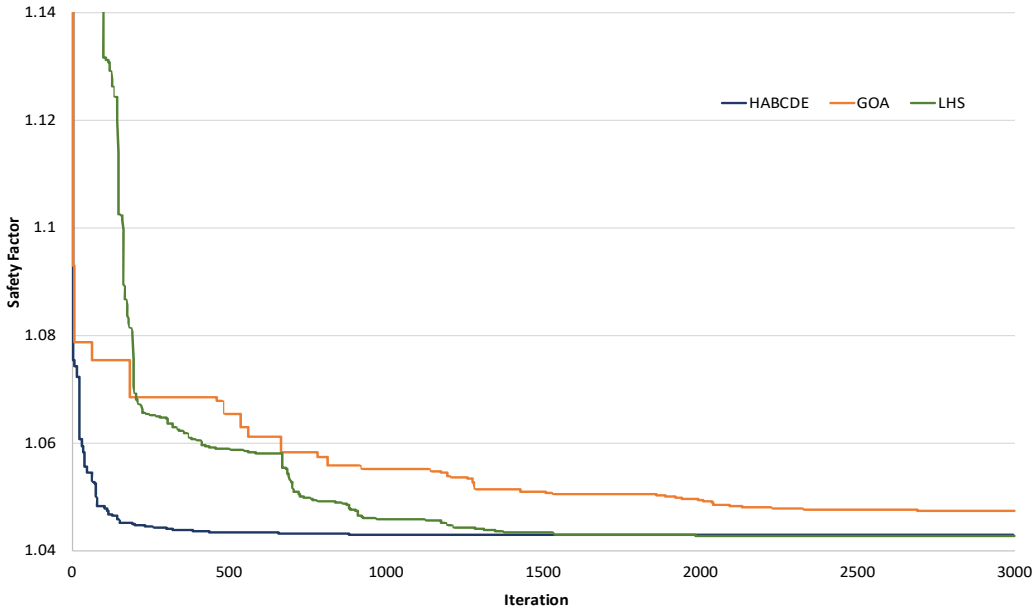

(b)

Figure 30 - Comparison of the convergence rates -- Example 4, Case (3)
(a) all the methods (b) proposed methods

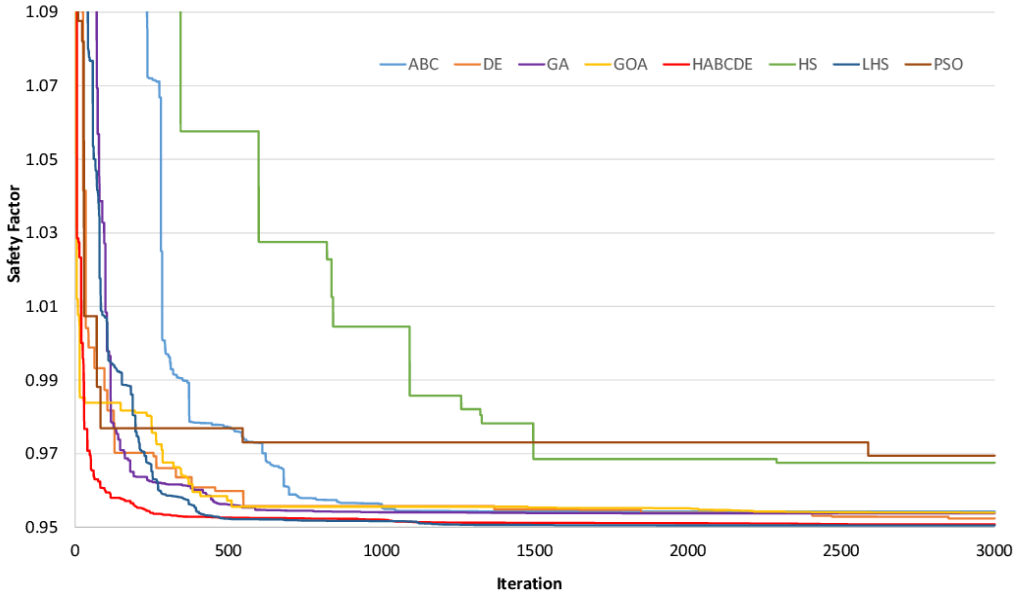

(a)

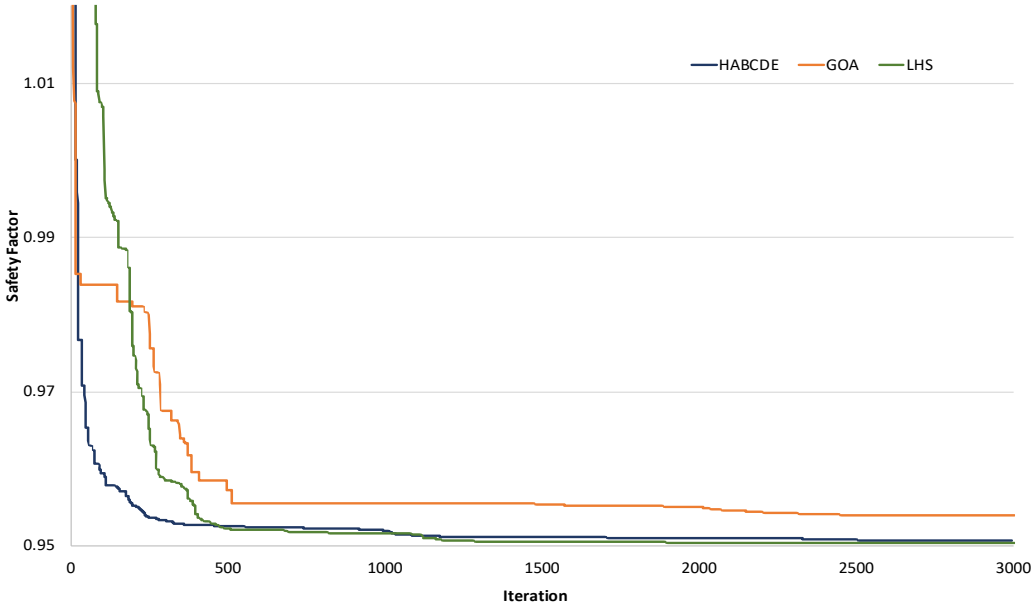

(b)

Figure 31 - Comparison of the convergence rates -- Example 4, Case (4)
(a) all the methods (b) proposed methods

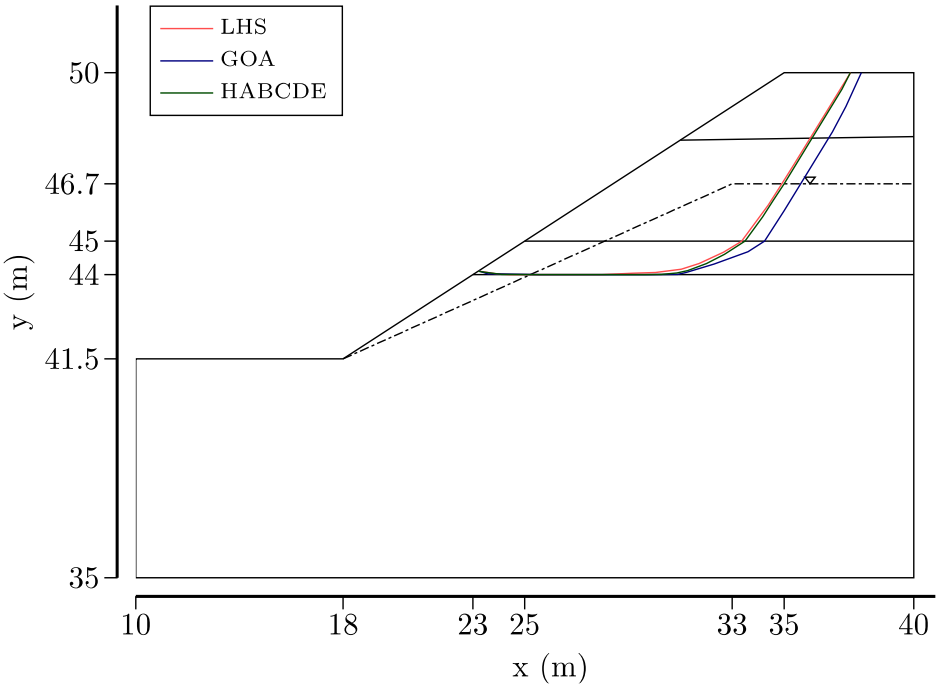

(a) Case (1)

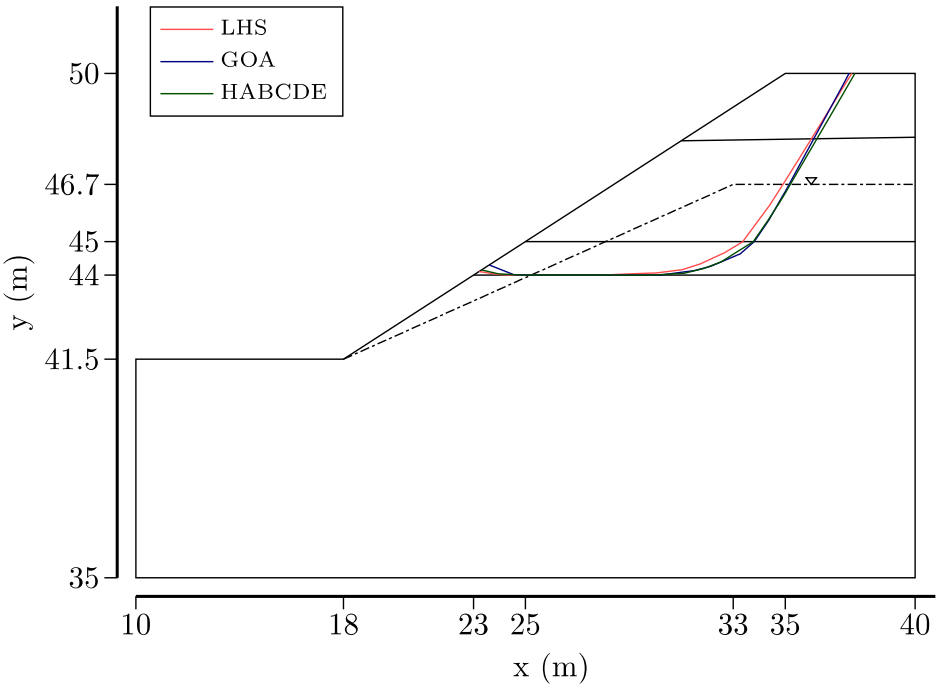

(b) Case (2)

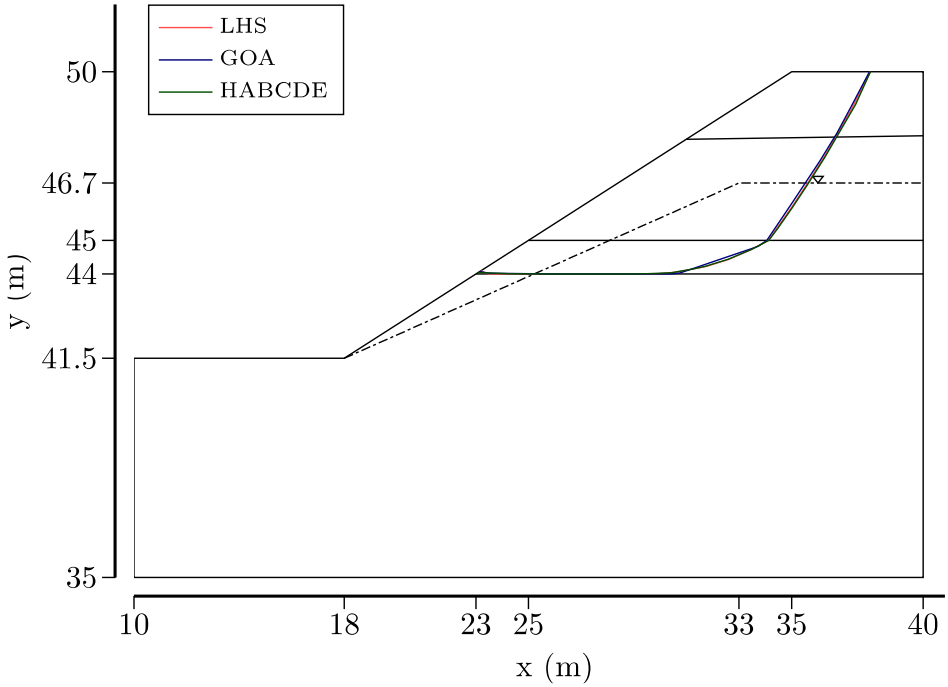

(c) Case (3)

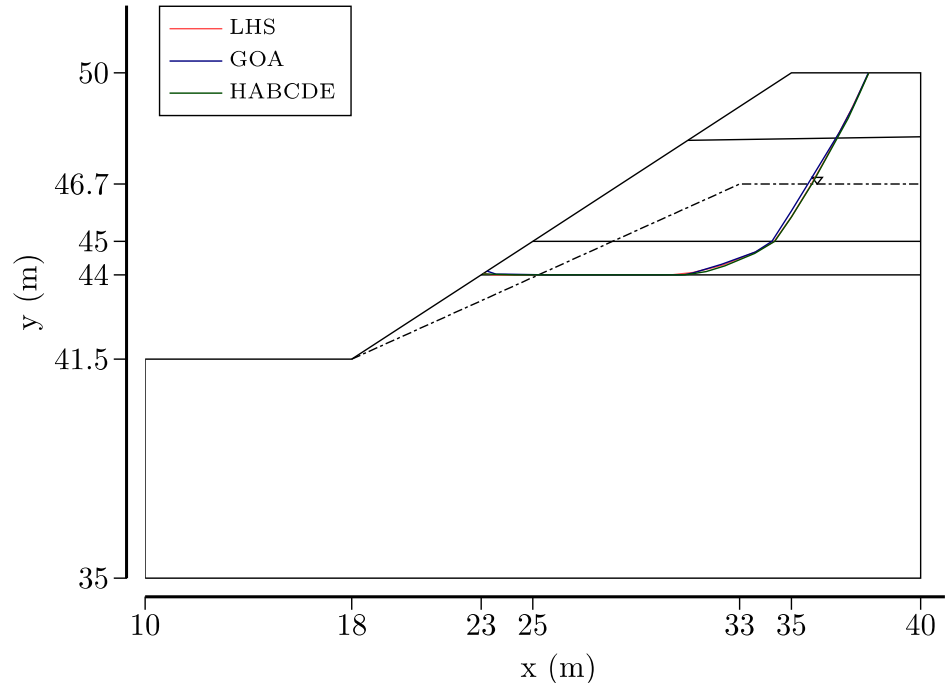

(d) Case (4)

Figure 32 – Critical Slip Surfaces – Example 4

CHAPTER 5

SUMMARY AND CONCLUSION

5.1 Summary

Investigating the safety of infrastructures against instabilities is a continuing concern in civil engineering, which necessitates comprehensive slope stability analyses to be conducted prior to major construction activities. This helps the engineers identify the vulnerable zone within the slope profile, providing crucial insights into the earth condition in the construction site. As a result, realistic quantification of the safety of the structure against potential failures is of great importance in the slope stability analysis.

In this study, an effective analysis framework is developed to evaluate the factor of safety of earth slopes on the basis of limit equilibrium methods. Stability analyses in this framework are performed in three main steps, which include (1) generating a number of trial slip surfaces, (2) evaluating safety factors corresponding to the generated surfaces and lastly, (3) looking for the most critical failure surface possessing the minimum safety factor. A non-circular surface generation technique that is capable of forming admissible slip surfaces, i.e. concave upward surfaces, is efficiently adopted for this purpose. In addition, Among the methods developed for the slope stability analysis a simplified form of Morgenstern-Price approach that has found widespread application in practice is implemented in evaluating the corresponding safety factors along each failure surface. However, the most challenging step in a complete slope stability analysis is the fast and accurate localization of the potential failure surface within the slope concurrent with the determination of the relating FS value, which reflects the minimum factor of safety of the case study. This objective is too challenging to accomplish considering the broad diversity of slope problems in geometry, geotechnical parameters of the soil,

the depth of the groundwater table, and condition of the external loadings. Robust optimization techniques, however, have recently performed well in tackling such difficulties. In this regard, the factor of safety equation is generally considered as the objective function of the optimization problem and a thorough minimization process is performed to explore the optimum solution in the search space. In this study, three recently developed metaheuristic methods that has shown satisfactory performance on various real-world optimization problems in terms of both reliability and validity, are implemented.

The applicability of the proposed analysis framework for the slope stability assessments is subsequently investigated considering several widely-used numerical examples. Furthermore, in order to gain a better understanding of the impact of variations in ground conditions on the overall stability of slopes, four case studies, from simple homogeneous to multi-layered heterogeneous earth slopes with varied geometries and stratifications, are thoroughly analyzed.

5.2 Findings of the Study

The significance of the quantitative stability analysis of earth slopes as well as the determination of the surface along which failure is expected has been widely acknowledged. To date, optimization techniques of different kinds have helped researchers evaluate how stable is the case of study through completing a fast and relatively simple procedure. In this study, three recent optimization algorithms, namely hybrid artificial bee colony with differential evolution, (HABCDE), grasshopper optimization algorithm (GOA) and improved harmony search algorithm (LHS) are implemented so as to calculate the lowest FS value pertaining to the surface of high failure probability. This objective is achieved by minimizing an objective function (factor of safety) which is defined based on a concise form of Morgenstern-Price algorithm. Slip surface of the slope is considered to be of non-circular geometry to provide a better approximation to the actual failure. A set of three numerical examples with varying geometry and loading conditions are studied to measure the computational performance of the proposed methods, as well as to

benchmark the results against their competitors, as illustrated in the respective tables. Besides, several illustrative figures for each case study are provided to give a deeper understanding of the accuracy and convergence rate of the methods along with a schematic visualization of the expected sliding surfaces, respectively. The obtained results indicated acceptable and comparable performance for the proposed method relative to common optimization techniques already used in the analysis of the same problems. However, when accuracy and convergence rate are used to evaluate performance, HABCDE outperformed its counterparts, yielding more optimal results with less computational effort. Consequently, HABCDE proved to be a suitable scheme in assessing the stability of slopes. Furthermore, it offers researchers the chance to discover new solutions, hopefully, improved ones, to a number of challenging optimization problems in their field of study.

5.3 Future Works

The framework proposed in this study proved successful for the stability evaluation of various slope problems. However, the following key recommendations are proposed to improve the functionality of the method:

Results indicate that the methods used for generating trial slip surfaces have a direct influence on the factor of safety evaluations and thus, different results might be obtained for the same slope problem in this regard. Furthermore, development of alternative techniques can offer researchers the opportunity to explore new solutions, hopefully, improved ones.

The efficiency of the framework developed in this study depends heavily on the rigorousness of the limit equilibrium method and the robustness of the optimization methods. In future studies, finite element methods can be used in the analyses which eliminate the need for preliminary assumptions, e.g. consideration of initial trial slip surfaces and the inter-slice forces in each slice. In addition, certain modifications can be made to the algorithms of the optimization methods in order to enhance their performance in acquiring superior results for each benchmark problem.

The reliability of slope stability assessments relies entirely on the validity of the values assumed for the soil parameters. In this study, key parameters of the soil medium, namely friction angle, the coefficient of cohesion, unit weight, and pore water pressure ratio are considered to be constant throughout the soil mass and therefore, a deterministic analysis is conducted. However, inherent variabilities and the errors resulting from improper site investigations can also be taken into account to quantify the probability of slope failures.

Two-dimensional models are adopted in this study for investigating the failure mechanism of the slopes. However, available evidence demonstrates that all slope instabilities in nature are virtually in three-dimensional forms. Consequently, in order to obtain more realistic and accurate results in the analysis, three-dimensional models can be adopted. This, however, requires huge computational efforts compared to conventional two-dimensional assessments.

REFERENCES

Abramson, Lee, Sharma, & Boyce. (2002). *Slope stability and stabilization methods*. John Wiley & Sons.

Arai, & Tagyo. (1985). Determination of noncircular slip surface giving the minimum factor of safety in slope stability analysis. *Soils and Foundations*, *25*(1), 43–51.

Baker. (1980). Determination of the Critical Slip Surface. *Geomechanics*, *4*(October 1979), 333–359. https://doi.org/10.1002/nag.1610040405

Baker, & Garber. (1978). Theoretical analysis of the stability of slopes. *Geotechnique*, (4). https://doi.org/10.1680/geot.1978.28.4.395

Bolton, Heymann, & Groenwold. (2003). Global search for critical failure surface in slope stability analysis. *Engineering Optimization*, *35*(1), 51–65. https://doi.org/10.1080/0305215031000064749

Celestino, & Duncan. (1981). Simplified search for non-circular slip surface. In *Proceedings of the 10th international conference on soil mechanics and foundation engineering, Stockholm, Sweden* (pp. 391–394).

Chen, L.-K., Chen, & Ke. (2015). Investigation of the Freeway No. 3 Landslide in Taiwan. In *Engineering Geology for Society and Territory-Volume 2* (pp. 2093–2096). Springer.

Chen, Z., & Shao. (1988). Evaluation of minimum factor of safety in slope stability analysis. *Canadian Geotechnical Journal*, *25*(November 1988), 735–748. https://doi.org/doi:10.1139/t88-084

Cheng, Y. M., Li, & Chi. (2007). Performance studies on six heuristic global optimization methods in the location of critical slip surface. *Computers and Geotechnics*, *34*(6), 462–484. https://doi.org/10.1016/j.compgeo.2007.01.004

Cheng, Y. M., Li, Chi, & Wei. (2007). Particle swarm optimization algorithm for the location of the critical non-circular failure surface in two-dimensional slope stability analysis. *Computers and Geotechnics*, *34*(2), 92–103. https://doi.org/10.1016/j.compgeo.2006.10.012

Cheng, Y. M., Liang, Chi, & Wei. (2008). Determination of the Critical Slip Surface Using Artificial Fish Swarms Algorithm. *Journal of Geotechnical and Geoenvironmental Engineering*, *134*(2), 244–251. https://doi.org/10.1061/(ASCE)1090-0241(2008)134:2(244)

Cheng, Y. M, & Lau. (2008). *Slope Stability Analysis and Stabilization: New Methods and Insight*.

Cheng, Y.M., Li, Lansivaara, Chi, & Sun. (2008). An improved harmony search minimization algorithm using different slip surface generation methods for slope stability analysis. *Engineering Optimization*, *40*(2), 95–115. https://doi.org/10.1080/03052150701618153

Cheng, Y, & Lau. (2014). *Slope Stability Analysis and Stabilization*. https://doi.org/10.1201/b17015

Cheng, YM, Li, & Lansivaara. (2008). An improved harmony search minimization algorithm using different slip surface generation methods for slope stability analysis. *Engineering Optimization*, *40*(2), 95–115. https://doi.org/10.1080/03052150701618153

Cheng, Yung Ming, Li, Sun, & Au. (2012). A coupled particle swarm and harmony search optimization algorithm for difficult geotechnical problems. *Structural and Multidisciplinary Optimization*, *45*(4), 489–501. https://doi.org/10.1007/s00158-011-0694-z

Das. (2005). Slope stability analysis using genetic algorithm. *Electron J Geotech Eng*, *10*, 429–439.

Donald, & Giam. (1989). *Soil slope stability programs review*. Association for Computer Aided Design (Australia).

Duncan, Wright, & Brandon. (2014). *Soil strength and slope stability*. John Wiley & Sons.

Fredlund, & Krahn. (1977). Comparison of slope stability methods of analysis. *Canadian Geotechnical Journal*, *14*(3), 429–439. https://doi.org/10.1139/t77-045

Gandomi, Kashani, Mousavi, & Jalalvandi. (2015). Slope stability analyzing using recent swarm intelligence techniques. *International Journal for Numerical*

and Analytical Methods in Geomechanics, *39*(3), 295–309.

Gao. (2015). Slope stability analysis based on immunised evolutionary programming. *Environmental Earth Sciences*, *74*(4), 3357–3369. https://doi.org/10.1007/s12665-015-4372-0

Gao. (2016). Premium-penalty ant colony optimization and its application in slope stability analysis. *Applied Soft Computing*, *43*, 480–488. https://doi.org/10.1016/j.asoc.2016.03.001

Geem, Kim, & Loganathan. (2001). A new heuristic optimization algorithm: harmony search. *Simulation*, *76*(2), 60–68.

GOH. (2000). Search for Critical Slip Circle Using Genetic Algorithms. *Civil Engineering and Environmental Systems*, *17*(3), 181–211. https://doi.org/10.1080/02630250008970282

Greco. (1996). Efficient Monte Carlo Technique for Locating Critical Slip Surface. *Journal of Geotechnical Engineering*, *122*(7), 517–525. https://doi.org/10.1061/(ASCE)0733-9410(1996)122:7(517)

Griffiths, & Lane. (1999). Slope stability analysis by finite elements. *Geotechnique*, *49*(3), 387–403.

Hart. (1995). An introduction to distinct element modeling for rock engineering. In *Analysis and Design Methods* (pp. 245–261). Elsevier.

Hu, Jimenez, Li, & Li. (2013). Determination of critical slip surfaces using mutative scale chaos optimization. *Journal of Computing in Civil Engineering*, *29*(5), 131204001730002. https://doi.org/10.1061/(ASCE)CP.1943-5487.0000373

Jadon, Tiwari, Sharma, & Bansal. (2017). Hybrid Artificial Bee Colony algorithm with Differential Evolution. *Applied Soft Computing*, *58*, 11–24. https://doi.org/10.1016/j.asoc.2017.04.018

Janbu. (1975). Slope stability computations: In Embankment-dam Engineering. Textbook. Eds. RC Hirschfeld and SJ Poulos. JOHN WILEY AND SONS INC., PUB., NY, 1973, 40P. In *International Journal of Rock Mechanics and Mining Sciences & Geomechanics Abstracts* (Vol. 12, p. 67). Pergamon.

Jurado-Piña, & Jimenez. (2015). A genetic algorithm for slope stability analyses with concave slip surfaces using custom operators. *Engineering Optimization*,

47(4), 453–472.

Kahatadeniya, Nanakorn, & Neaupane. (2009). Determination of the critical failure surface for slope stability analysis using ant colony optimization. *Engineering Geology*, *108*(1–2), 133–141. https://doi.org/10.1016/j.enggeo.2009.06.010

Kang, Li, & Ma. (2013). An artificial bee colony algorithm for locating the critical slip surface in slope stability analysis. *Engineering Optimization*, *45*(2), 207–223.

Karaboga. (2005). *An idea based on honey bee swarm for numerical optimization*. Technical report-tr06, Erciyes university, engineering faculty, computer engineering department.

Kashani, Gandomi, & Mousavi. (2016). Imperialistic Competitive Algorithm: A metaheuristic algorithm for locating the critical slip surface in 2-Dimensional soil slopes. *Geoscience Frontiers*, *7*(1), 83–89. https://doi.org/10.1016/j.gsf.2014.11.005

Khajehzadeh, Raihan Taha, El-Shafie, & Eslami. (2012). Locating the general failure surface of earth slope using particle swarm optimisation. *Civil Engineering and Environmental Systems*, *29*(1), 41–57. https://doi.org/10.1080/10286608.2012.663356

Khajehzadeh, Taha, El-Shafie, & Eslami. (2012). A modified gravitational search algorithm for slope stability analysis. *Engineering Applications of Artificial Intelligence*, *25*(8), 1589–1597. https://doi.org/10.1016/j.engappai.2012.01.011

Li, K. S., & White. (1987). Rapid evaluation of the critical slip surface in slope stability problems. *International Journal for Numerical and Analytical Methods in Geomechanics*, *11*(5), 449–473.

Li, Y.-C., Chen, Zhan, Ling, & Cleall. (2010). An efficient approach for locating the critical slip surface in slope stability analyses using a real-coded genetic algorithm. *Canadian Geotechnical Journal*, *47*(7), 806–820.

Malkawi, Hassan, & Sarma. (2001). Global Search Method for Locating General Slip Surface using Monte Carlo Techniques. *Journal of Geotechnical and Geoenvironmental Engineering*, *127*(8), 688–698. Retrieved from

http://cedb.asce.org/cgi/WWWdisplay.cgi?127215

Mccombie, & Wilkinson. (2002). The use of the simple genetic algorithm in finding the critical factor of safety in slope stability analysis. *Computers and Geotechnics*, *29*(8), 699–714. https://doi.org/10.1016/S0266-352X(02)00027-7

Morgenstern, & Price. (1965). The analysis of the stability of general slip surfaces.

Nguyen. (1985). Determination of critical slope failure surfaces. *Journal of Geotechnical Engineering*, *111*(2), 238–250.

Note, & Gao. (2016). Determination of the Noncircular Critical Slip Surface in Slope Stability Analysis by Meeting Ant Colony Optimization, *30*(2). https://doi.org/10.1061/(ASCE)CP.1943-5487.0000475.

Nur. (2014). vosizneias.com, Last Visited on May 2018.

Ouyang, Gao, Li, Kong, Wang, & Zou. (2017). Improved Harmony Search Algorithm: LHS. *Applied Soft Computing Journal*, *53*, 133–167. https://doi.org/10.1016/j.asoc.2016.12.042

Pockoski, & Duncan. (2000). *Comparison of computer programs for analysis of reinforced slopes*. Center for Geotechnical Practice and Research.

Saremi, Mirjalili, & Lewis. (2017). Grasshopper Optimisation Algorithm: Theory and application. *Advances in Engineering Software*, *105*, 30–47. https://doi.org/10.1016/j.advengsoft.2017.01.004

Sarma. (1973). Stability analysis of embankments and slopes. *Geotechnique*, *23*(3), 423–433.

Sengupta, & Upadhyay. (2009). Locating the critical failure surface in a slope stability analysis by genetic algorithm. *Applied Soft Computing Journal*, *9*(1), 387–392. https://doi.org/10.1016/j.asoc.2008.04.015

Stead, Eberhardt, Coggan, & Benko. (2001). Advanced numerical techniques in rock slope stability analysis—applications and limitations. In *International conference on landslides-causes, impacts and countermeasures* (pp. 615–624).

Storn, & Price. (1995). Differential evolution–a simple and efficient adaptive scheme for global optimization over continuous spaces: technical report TR-

95-012. *International Computer Science, Berkeley, California*.

Sun, Li, & Liu. (2008). Search for critical slip surface in slope stability analysis by spline-based GA method. *Journal of Geotechnical and Geoenvironmental Engineering*, *134*(2), 252–256. https://doi.org/10.1061/(ASCE)1090-0241(2008)134:2(252)

Wolpert, & Macready. (1997). No free lunch theorems for optimization. *IEEE Transactions on Evolutionary Computation*, *1*(1), 67–82.

Yamagami. (1988). Search for noncircular slip surfaces by the Morgenstern-Price method. In *Proc. 6th Int. Conf. Numer. Methods in Geomech.* (pp. 1335–1340).

YAMAGAMI, & JIANG. (1997). A search for the critical slip surface in three-dimensional slope stability analysis. *Soils and Foundations*, *37*(3), 1–16.

Zhu, D. Y., Lee, & Jiang. (2003). Generalised framework of limit equilibrium methods for slope stability analysis. *Geotechnique*.

Zhu, D. Y., Lee, Qian, & Chen. (2005). A concise algorithm for computing the factor of safety using the Morgenstern–Price method. *Canadian Geotechnical Journal*, *42*(1), 272–278. https://doi.org/10.1139/t04-072

Zhu, G., & Kwong. (2010). Gbest-guided artificial bee colony algorithm for numerical function optimization. *Applied Mathematics and Computation*, *217*(7), 3166–3173.

Zolfaghari, Heath, & McCombie. (2005). Simple genetic algorithm search for critical non-circular failure surface in slope stability analysis. *Computers and Geotechnics*, *32*(3), 139–152. https://doi.org/10.1016/j.compgeo.2005.02.001

APPENDIX A

CONVERGENCE RATE COMPARISON

In order to gain a better insight into the performance of the optimization algorithms, convergence history of each method is illustrated in separate figures as follows. A closer look into the convergence history of the three recent optimization methods proposed in this study indicates that overall HABCDE represents more satisfactory performance in the analyses in terms of both convergence rate and accuracy.

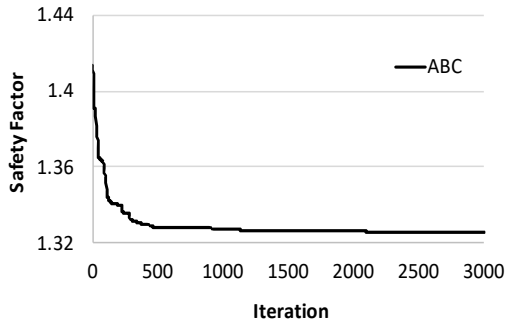

(a)

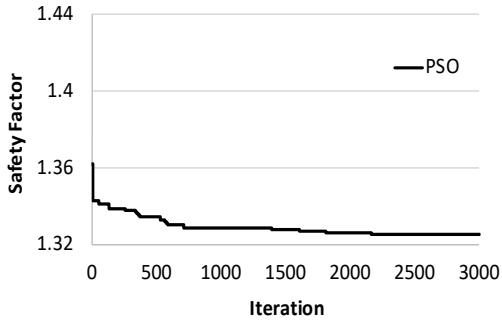

(b)

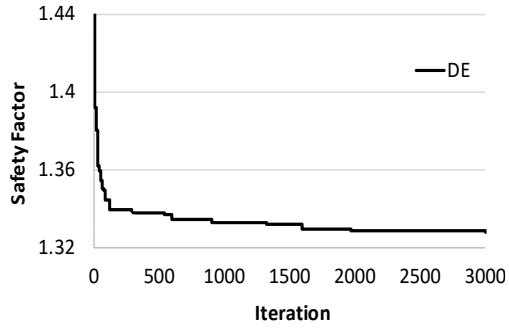

(c)

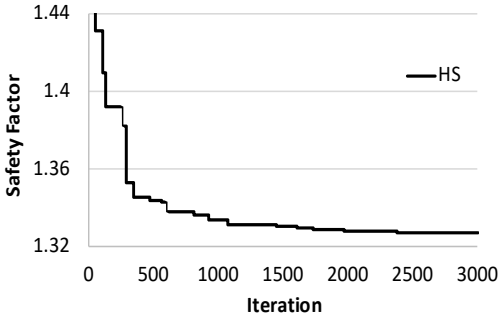

(d)

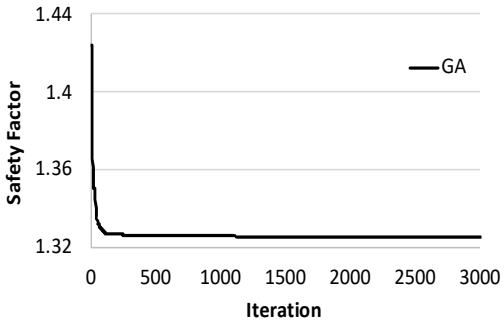

(e)

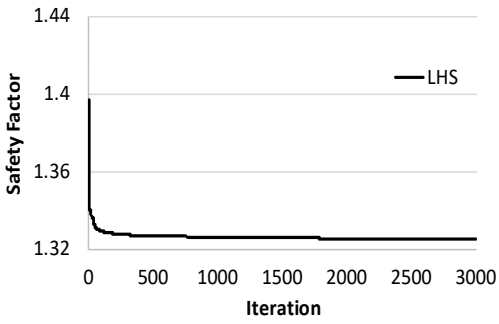

(f)

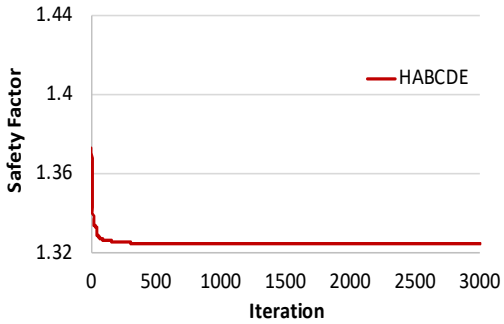

(g)

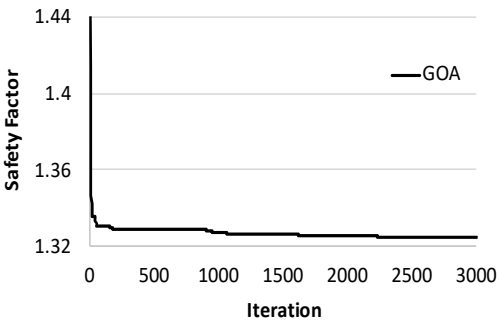

(h)

Figure 33- Convergence Rate Comparison – Example 1

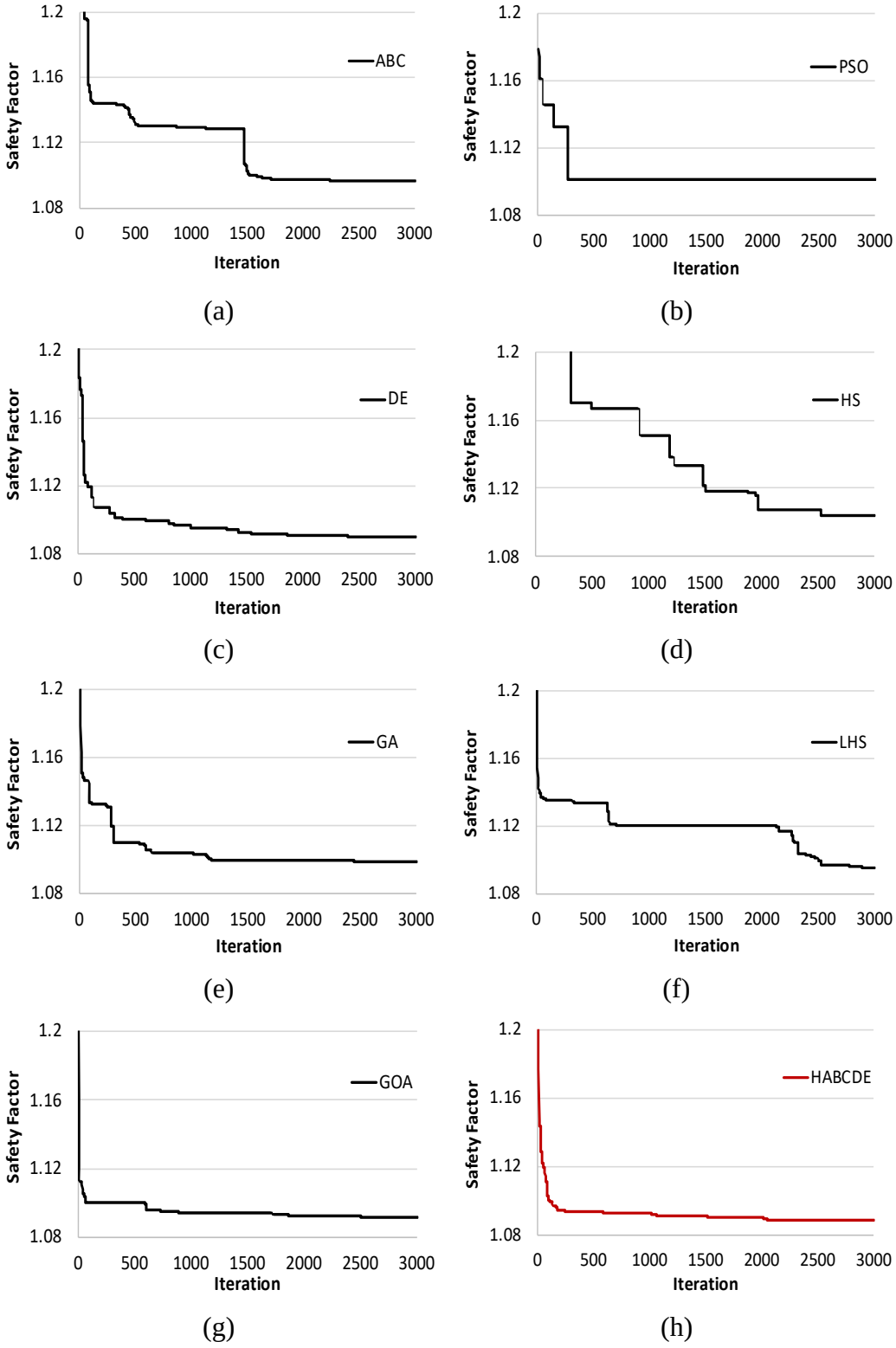

Figure 34 - Convergence Rate Comparison – Example 2

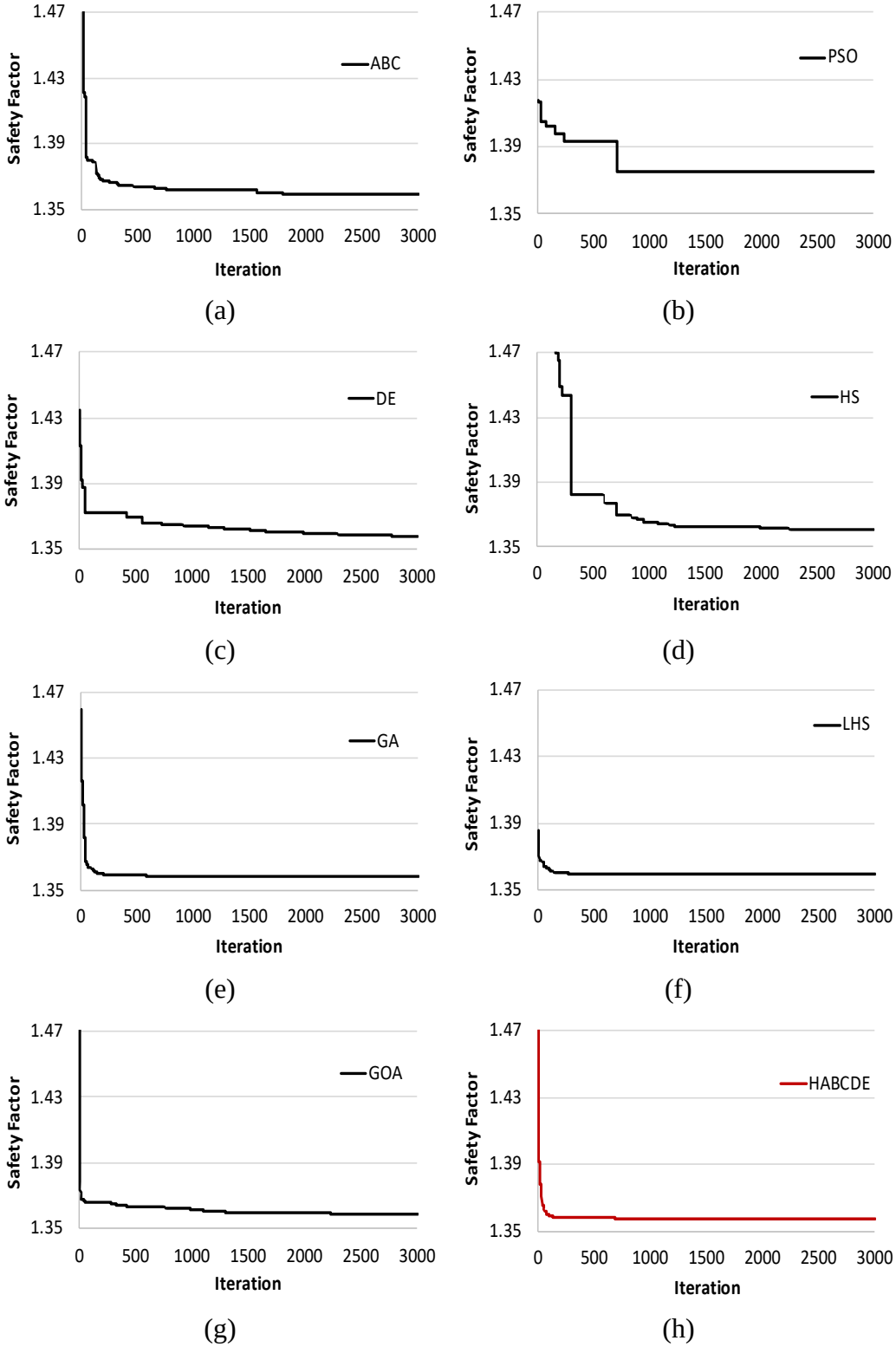

Figure 35 - Convergence Rate Comparison – Example 3, Case (1)

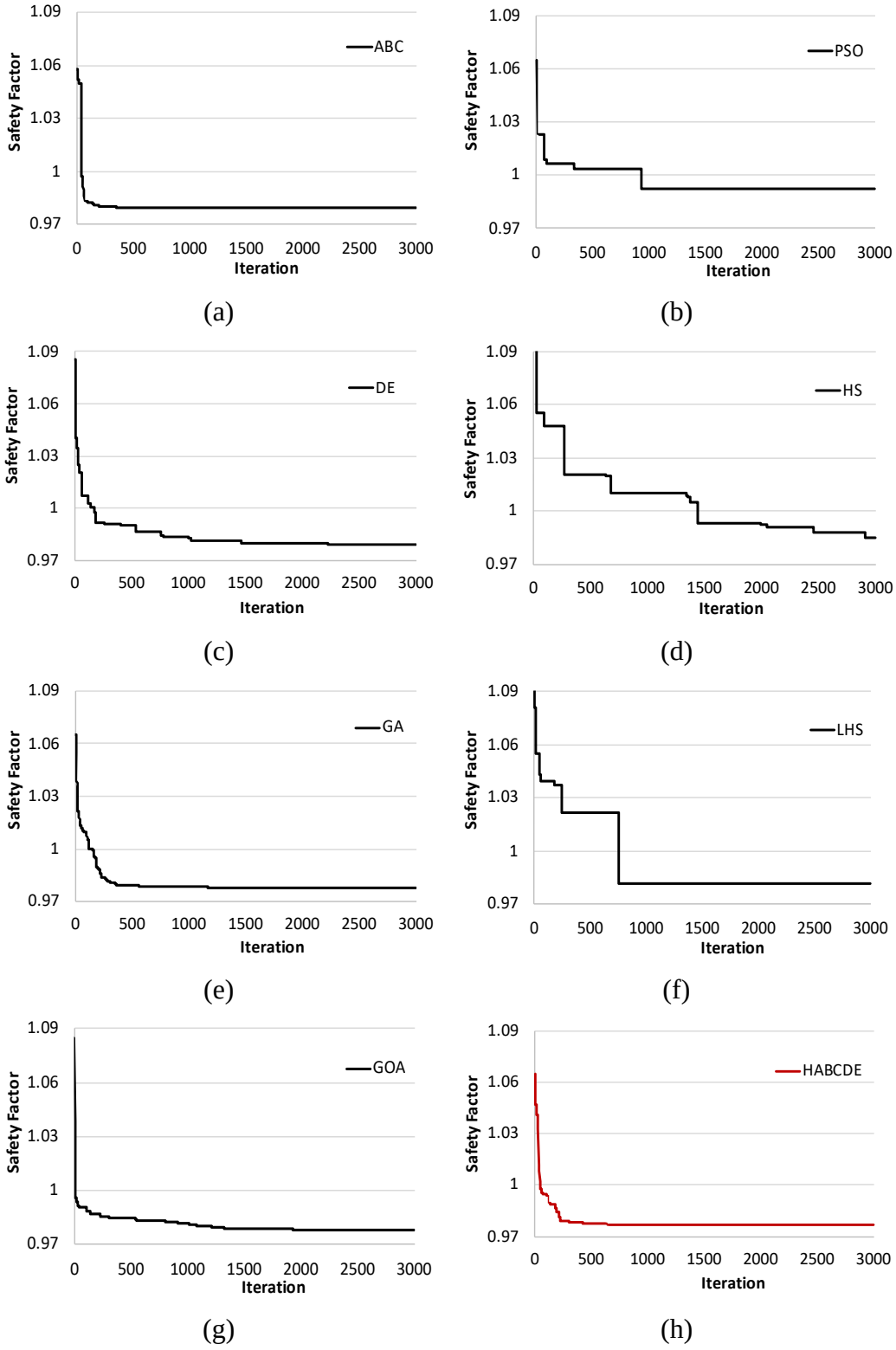

Figure 36 - Convergence Rate Comparison – Example 3, Case (2)

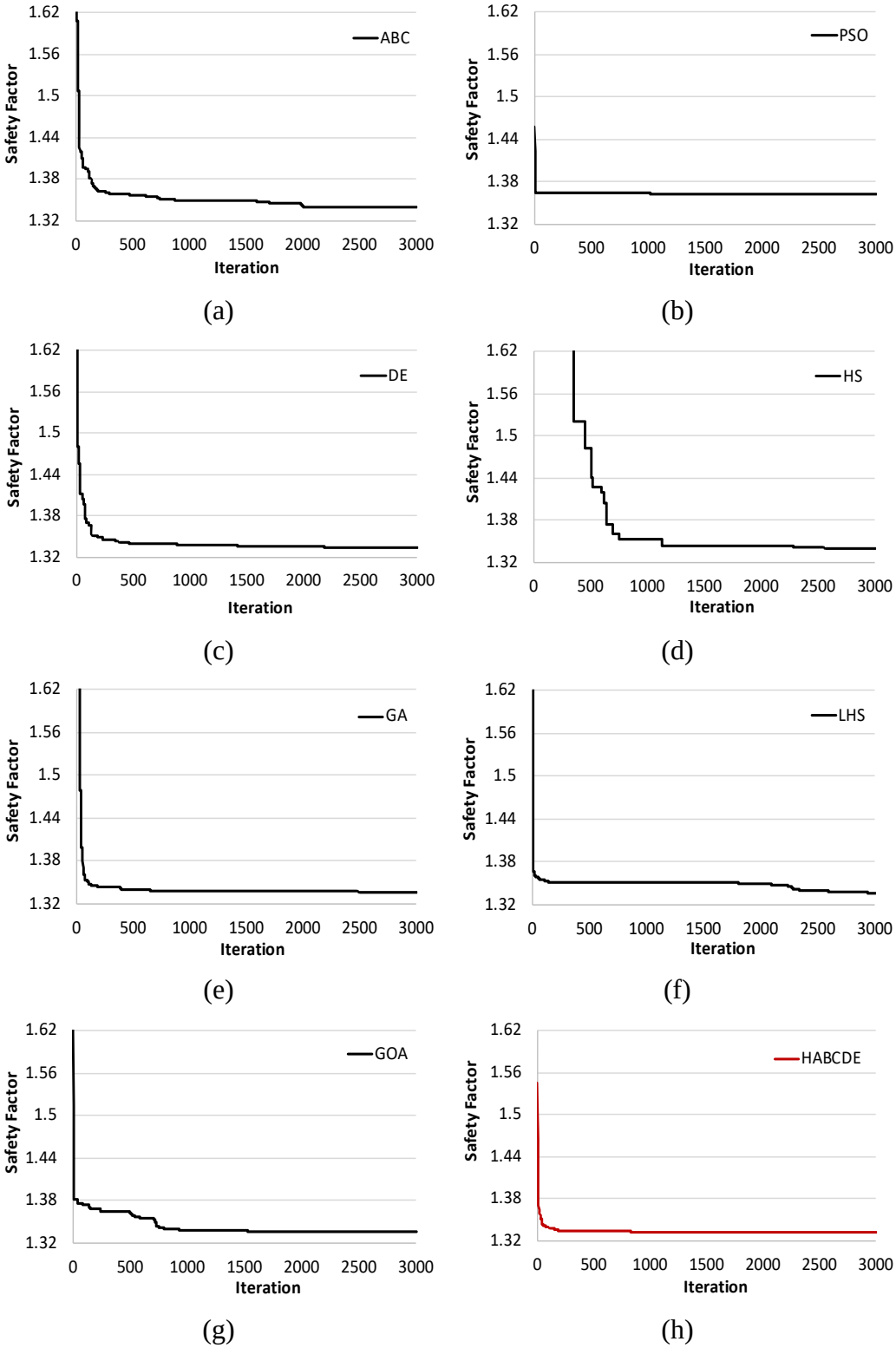

Figure 37 - Convergence Rate Comparison – Example 4, Case (1)

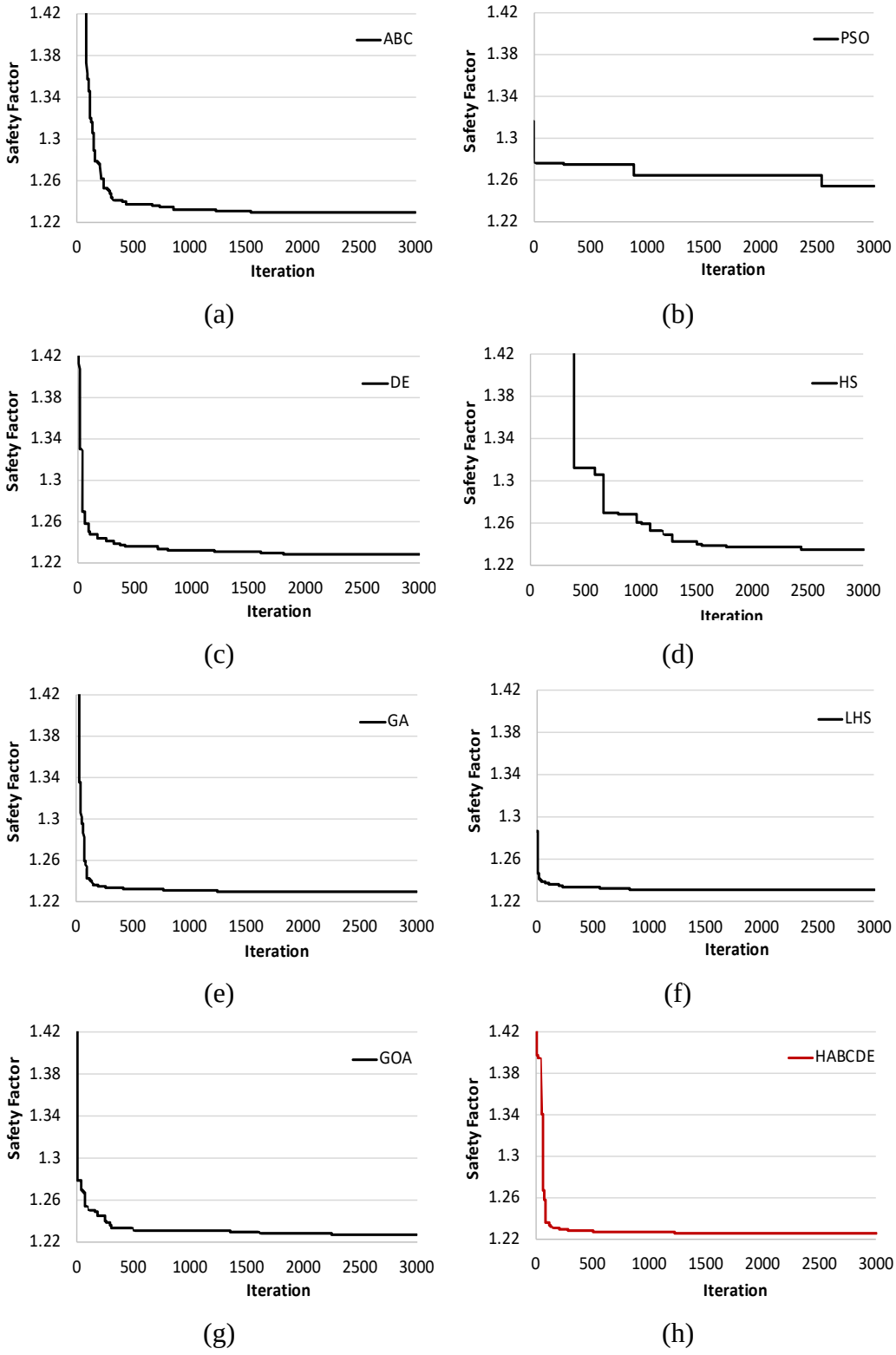

Figure 38 - Convergence Rate Comparison – Example 4, Case (2)

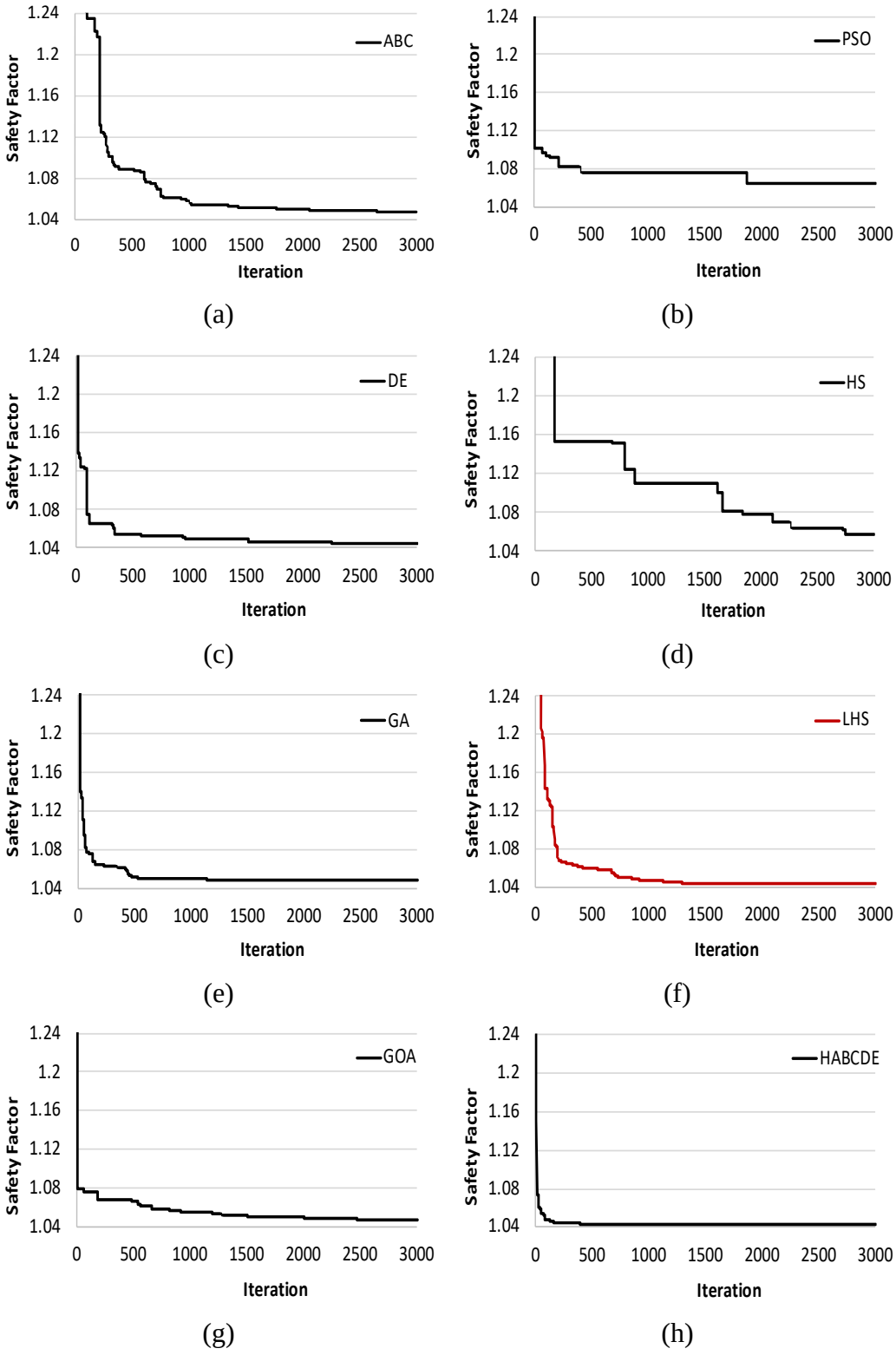

Figure 39 - Convergence Rate Comparison – Example 4, Case (3)

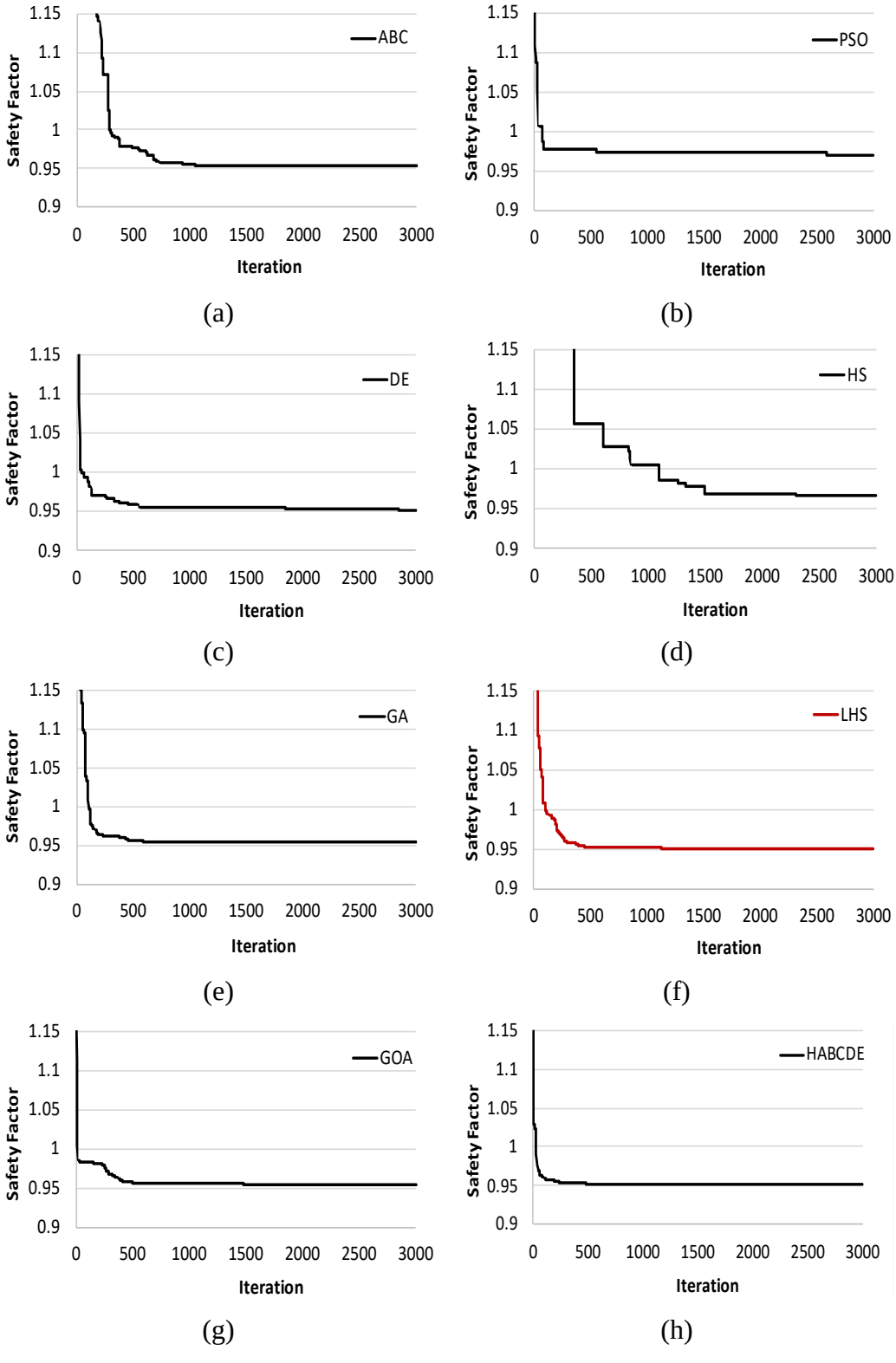

Figure 40 - Convergence Rate Comparison – Example 4, Case (4)